NASA SP-5082

NONDESTRUCTIVE TESTING: TRENDS AND TECHNIQUES

Proceedings of the
Second Technology Status and Trends Symposium
Marshall Space Flight Center

NATIONAL AERONAUTICS AND SPACE ADMINISTRATION

NONDESTRUCTIVE TESTING: TRENDS AND TECHNIQUES

Proceedings of the
Second Technology Status and Trends Symposium
Marshall Space Flight Center
October 26-27, 1966

Foreword

Few industrial functions have undergone so many significant technological changes in the last few years as has nondestructive testing. In addition to a large number of improvements in such traditional techniques as X-ray and ultrasonic testing, whole new approaches such as laminography have been proved out, and display systems have been substantially enhanced.

The activities of the National Aeronautics and Space Administration have led to a number of significant advances in nondestructive testing. Some of these advances were recently described in a symposium for industry at the NASA Marshall Space Flight Center. That symposium was an activity of the NASA Technology Utilization Program, which seeks to communicate rapidly to potential users the new knowledge generated by NASA research and development programs. Publication of the nine papers in this volume is an effort to communicate these technical advances to a broader audience.

GEORGE HOWICK, *Director,*
Technology Utilization Division
National Aeronautics and Space Administration

Contents

Nondestructive Testing Techniques for Multilayer Printed Wiring Boards

James F. Blanche

One of the basic needs in the electronics field is for a high density interconnection technique that is compact, reliable, and will eliminate the possibility of human error in wiring. Point-to-point wiring of electronic assemblies introduces the possibility for human error with every wire connected, and the assembly often becomes a rat's nest of wires. Conventional single- and double-sided printed circuit cards will not allow compact interconnection of microelectronic circuits.

One obvious solution to the problem of high density interconnections is the multilayer printed circuit board. It allows very high interconnection density, and the interconnections are identical in all assemblies using any particular circuit; thus, much of the possibility of human error is eliminated. However, the reliability of this system is questionable because multilayer printed circuit boards are generally fabricated in such a way that the internal joints formed cannot be inspected. In the most widely used multilayer system a number of copper clad sheets bonded to an insulating material are etched with the appropriate circuit pattern. The layers are laminated, and holes are drilled through the laminated assembly at the points where interlayer connections are to be made, thus exposing the edge of the copper conductors at the appropriate level. The layers are then electrically connected by plating the wall of the hole with copper or by fusing an eyelet, tublet, or post into the hole. Optimum interconnection is achieved when 100 percent of the surface of the hole is covered with a prescribed minimum thickness of the conducting material and when the cylinder, thus formed, is interconnected with 100 percent of the intersecting area of the printed conductor at each layer. The problem of reliability arises in the inspection of the joints formed at the interface of the exposed edge of the printed conductors and the plated wall.

In the past, inspection has been made in several ways. One method has been to pass a high current through the joints on the theory that any poor joints will be burned out. However, this stress testing may create new marginal joints. Another technique has been to check continuity of the circuitry. This method will detect both open and short circuits but will tell little about the quality of the joints. Some manufacturers X–ray their multilayer circuit boards to determine how closely the layers are alined. The problem with this method, par-

1

ticularly on boards with dense circuitry, is that an internal layer tends to be masked by those layers above it.

A program was initiated to develop a nondestructive technique to inspect multilayer printed circuit boards. If possible, the technique was to be rapid and accurate and lend itself to mass testing. A number of techniques were examined for relative promise in fulfilling the requirements of this program. Some of them were:

Techniques Involving Heat.—Thermographic powder is applied to the surface of the board. Under ultraviolet light, the fluorescence of this powder decreases with increasing temperature and will, therefore, detect hot spots in the board. Detection of infrared or electromagnetic radiation in the millimeter range would also detect hot spots in the board. However, these techniques lose both sensitivity and resolution as the number of layers increases.

Eddy Current Technique.—Passing an ac current through a coil placed in a plated-through or eyelet hole will cause eddy current to flow in the metal on the sides of the hole. The fields of these eddy currents will in turn affect the electrical properties of the coil. By varying the frequency of the ac current and detecting the changes in the coil caused by the behavior of the eddy currents, it is possible to determine the characteristics of the joints. One of the detection systems used with the eddy current technique was selected for more detailed study.

Intermodulation Technique.—Currents of two different frequencies are passed through the printed wiring. Currents at intermodulation frequencies are then produced by any electrical nonlinearity. These intermodulation currents can easily be filtered out to detect even small nonlinearities. Attempts to detect a defect using an intermodulation technique were successful, but difficulties were encountered in reproducing test results and in pinpointing the defective connection.

E–Field Sensors.—Faults in printed wiring boards and plated-through holes may be found by the irregularities which they cause in the equipotential surfaces of the currents flowing through the wiring. Several probing techniques to detect irregularities were examined. Although they are theoretically workable, there are a number of practical difficulties that would limit their usefulness.

Radiography.—Neutron radiography was investigated, but resolution and contrast were of insufficient quality. Autoradiography might be used if the hole-plating material could be doped; however, the film would have to be inserted into the hole which is to be inspected. Electron microscopy is primarily limited to descriptions of surface characteristics. X-ray is basically limited by the masking effect of circuit layers above the layer being inspected. The most important result of these radiographic investigations was the discovery of a technique known as axial transverse laminography. Since it appeared to meet

most of the nondestructive test requirements, this technique was chosen for detailed examination.

AXIAL TRANSVERSE LAMINOGRAPHY

Axial transverse laminography is a radiographic technique which permits examination of a thin section of a thick sample without physically sectioning the sample. The technique depends on smearing all unwanted images over a large area while the image of interest remains sharp throughout the exposure. This result is achieved by synchronously rotating the sample and the film during exposure. The system, which is shown schematically in figure 1, consists of a point X-ray source, a rotating test table which holds the sample to be inspected, and a rotating film table. The plane that will be inspected is geometrically defined by the system. This plane is located at the intersection of the main axis and rotary axis #1 and will be parallel to the film plane.

The laboratory setup is shown in figure 2. The low energy X-ray tube (25 keV silver K X-ray) is shown in the upper right-hand corner. The source diameter is approximately 0.03810 mm (0.0015 in.). The grid pattern shown on the film table is for vacuum hold-down of the film. The two tables are rim-driven by a single motor through rubber drive rings. Changing the compression of the rubber ring causes a variation in the driving ratio, allowing precise synchronism to be achieved.

The operation of the system is described in figure 3. Consider line C–B to be a through-connection in a multilayer sample at the initial point of exposure to X-ray. C–B will project $\overline{C}$–$\overline{B}$ onto the film. Now consider the same line C–B after it has rotated 180° about rotary axis #1. The line is now defined as
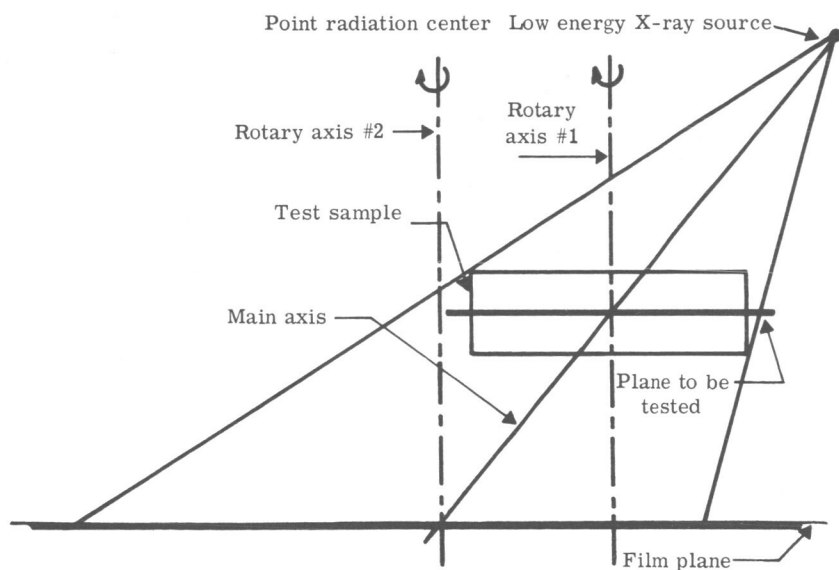

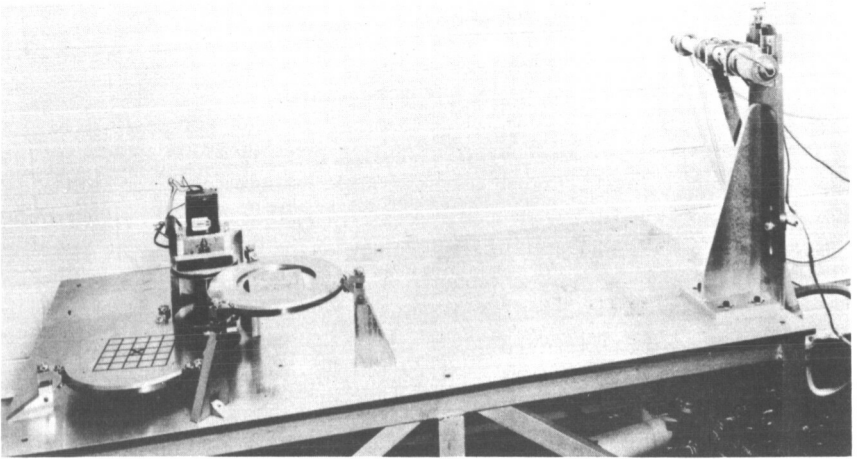FIGURE 1.—Axial transverse laminography.
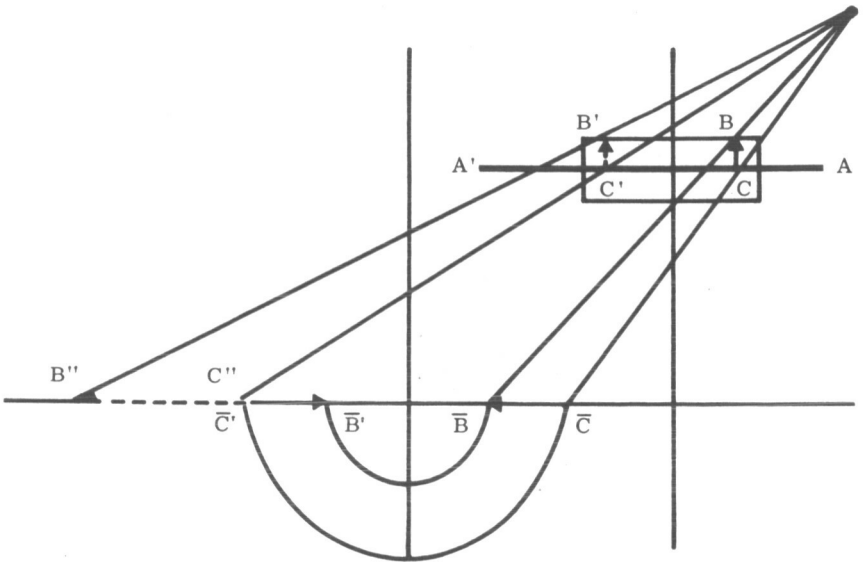
FIGURE 2.—Experimental laminograph.

FIGURE 3.—Operating principles of the axial transverse laminography technique.

C'–B'. While C–B was rotating one-half revolution, the initial image $\overline{C}$–$\overline{B}$ was also rotating one-half revolution about rotary axis #2 to position $\overline{C}'$–$\overline{B}'$. C'–B' now projects a new image C''–B'' onto the film. It will be noted that the only point at which the initial ($\overline{C}'$–$\overline{B}'$) and the new (C''–B'') image coincide or reinforce is at point C where the sample through-connection touches the geometric plane of inspection. This example considers only two positions of the line C–B. It must be recognized that C–B is in reality projecting an

image onto the film continuously throughout at least one complete revolution of the sample and film tables. Thus, it will be seen that the projected image of any point in the sample plane A–A' will reinforce itself continuously as long as the sample and film tables are rotating synchronously, while any point outside this plane will smear out or average over a larger area.

For any given vertical displacement of an object of fixed size from the plane of inspection in the sample, the area over which the object will smear is determined by the angle which the main axis makes with the horizontal plane. The angle used in the laboratory model was 20°; however, a geometric analysis was performed to determine the layering sensitivity for various angles and vertical displacements from the plane of inspection in the sample. The results are shown in figure 4. The curves assume a 76.2 cm (30 in.) horizontal displacement of the center of rotation of the sample from the X-ray source. Y is the vertical displacement above or below the plane of inspection of a spot 0.36 mm (0.014 in.) in diameter. The curve shows the ratio of the common area of projection of this spot to the projection of the same spot in the sample plane. It will be noted that for a vertical displacement of 0.10 mm (0.004 in.) and an angle of 20°, only 5 percent of the projected area of the spot is continuously reinforced or not smeared out.

One of the sample multilayer boards used in this program is shown in figure 5. It is a seven-layer board with four circuit patterns, each of which is a hole
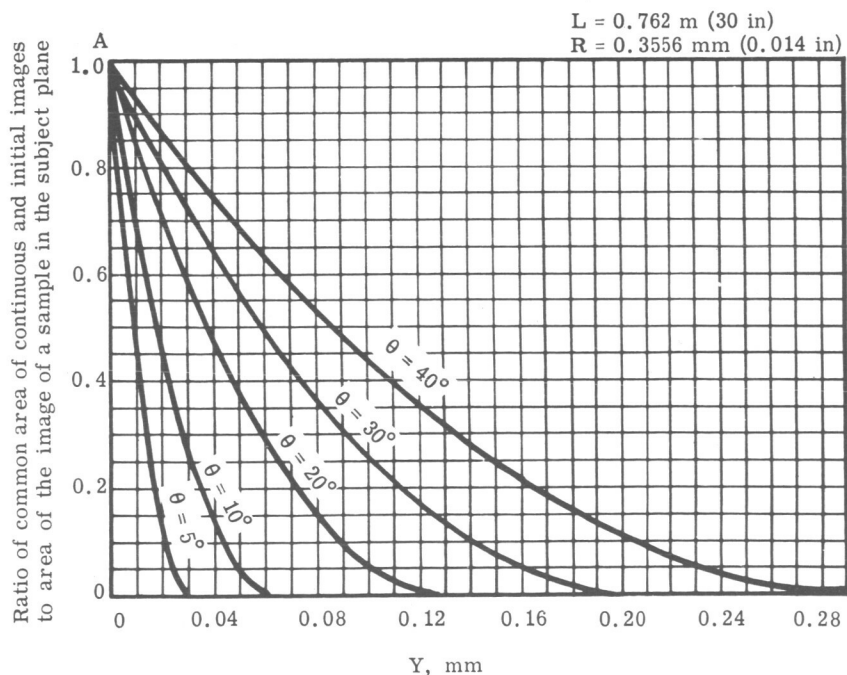

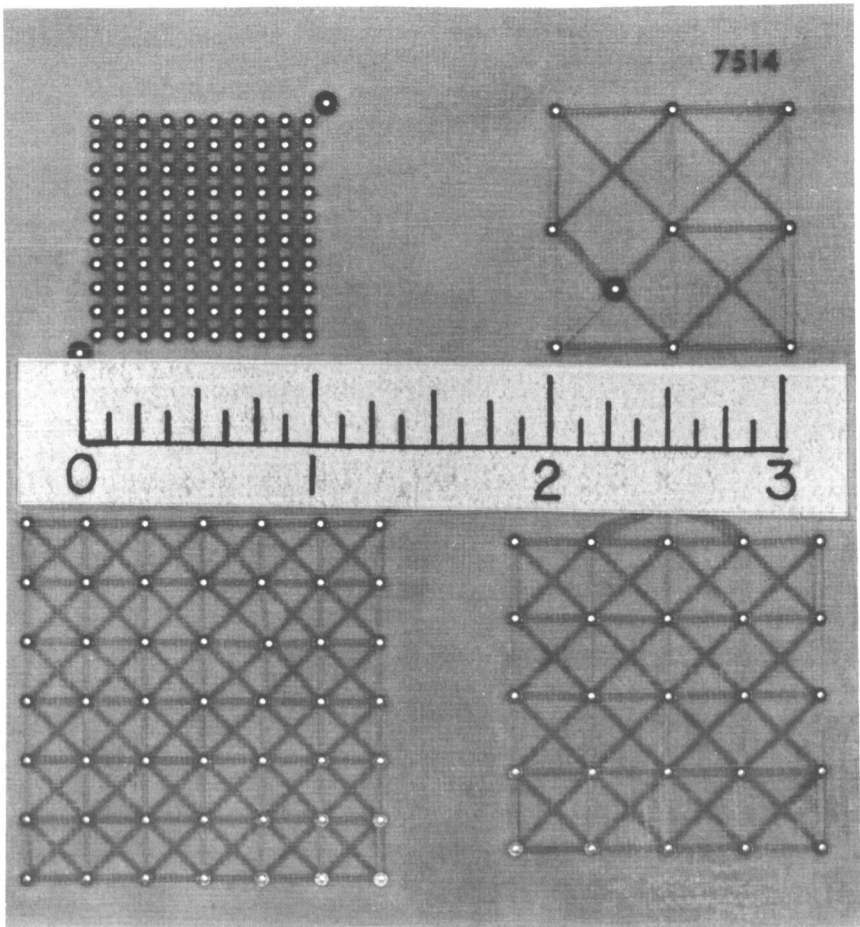FIGURE 4.—Effect of main axis angular variations.

FIGURE 5.—Sample multilayer board.

matrix with defects built into the circuit. The patterns range from widely spaced to densely spaced holes. The most dense matrix has 100 holes or 700 joints per 6.54 cm² (1 in.²). The optimum interconnection has been defined as that point at which the plated cylinder makes contact with 360° of the land to which it is joined. Some geometric deviations were introduced into the board, such as intentionally misregistering the land areas for one hole in each matrix and creating open circuits by hairline fractures. The through-connections are made by plating the holes with approximately 0.004 cm (0.0015 in.) of copper.

Figures 6 and 7 are laminographs of layers 3 and 4, respectively. The two layers are separated by 0.01 cm (0.004 in.). The cuts on the diagonal line in the upper right-hand pattern of layer 4 range from 0.06 to 0.15 mm wide. These laminographs have proven that the concept of axial transverse laminography is
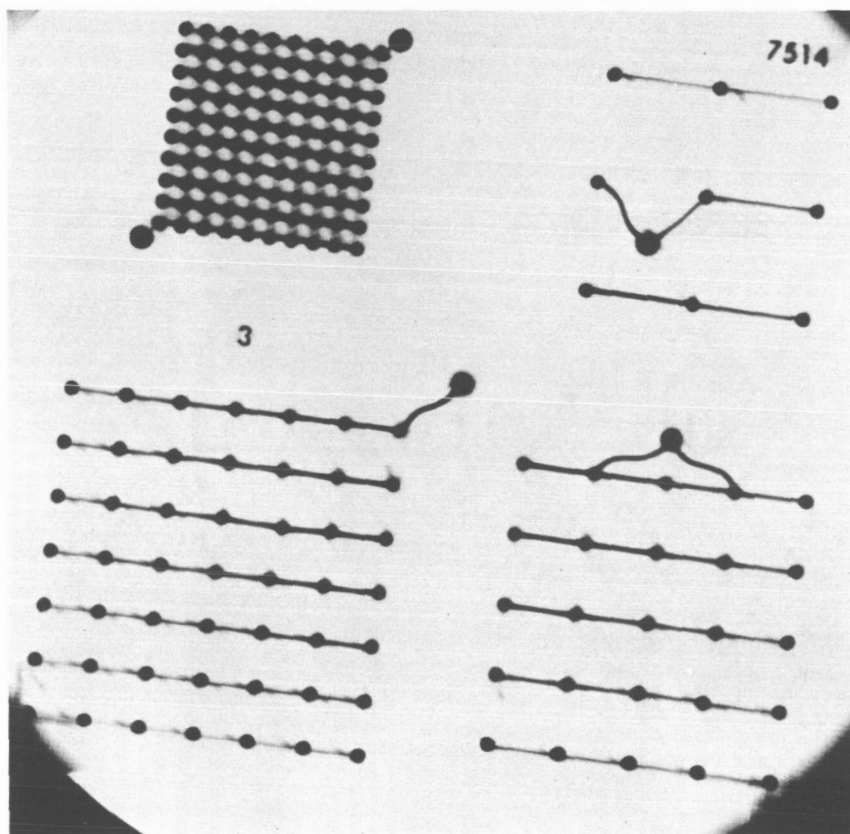
FIGURE 6.—Laminograph of layer three.

a sound one. It can separate layers which are as close together as 0.01 cm (0.004 in.) and can easily detect flaws as small as 0.03 mm (0.0007 in.).

A practical limitation is presented by the use of film. Much time is added to the inspection procedure by having to take a picture of each layer and then developing and examining the film. If the internal layers of the sample are not plane, several pictures of each layer may be required for complete inspection. To alleviate this problem, a different approach is being taken in the laminograph now being developed. The system is shown in schematic form in figure 8. The film plate has been replaced with a fluorescent screen. The visual image from the screen is focused through a lens onto a derotation prism rotating at one-half the screen speed and in the opposite direction. The stationary image from the prism is projected into a closed-circuit television system. The fluorescent screen will have the capability for vertical movement to change the plane of inspection in the sample. This design allows the operator to be at a remote station, thus permitting safe use of higher energy, higher intensity X-ray for better resolution.
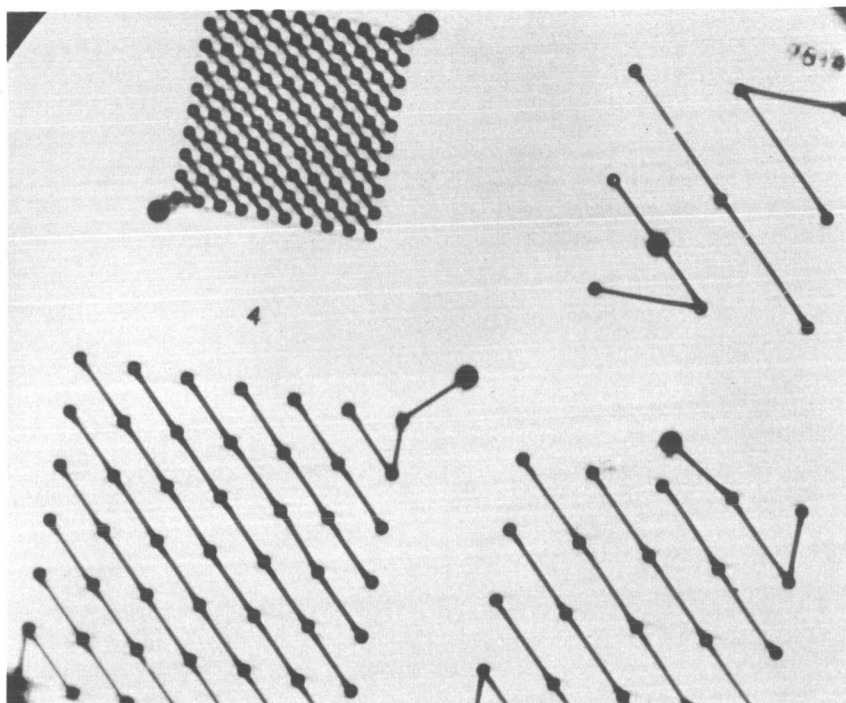
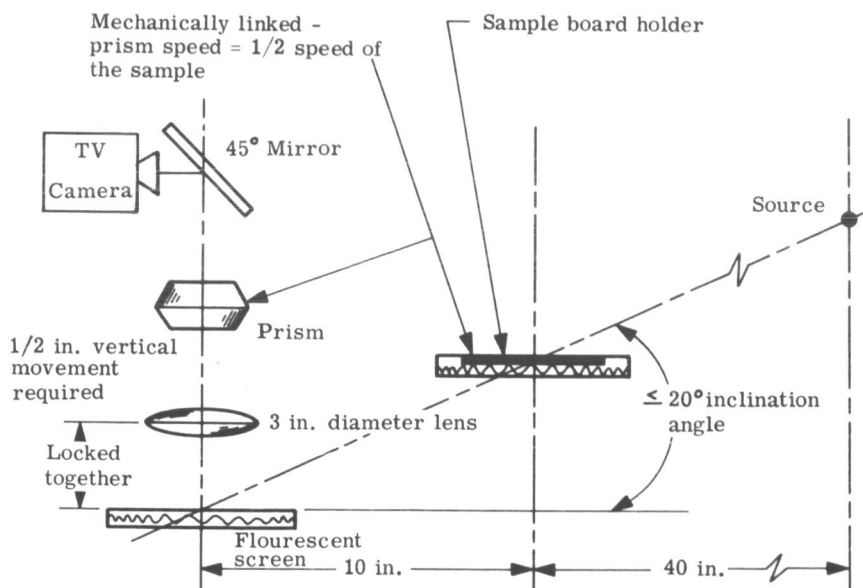FIGURE 7.—Laminograph of layer four.

FIGURE 8.—Laminograph schematic.

The conversion to an immediate visual image of the sample produces a continuous scanning device, thereby allowing the operator to scan through the complete board. A zoom attachment on the camera allows a questionable area of the sample to be magnified for more detailed inspection. Photographs of the image may be made at any time for a permanent record.

MUTUAL COUPLING

Although laminography will provide the capability to rapidly inspect multilayer printed circuit boards, the expected detail resolution of approximately 0.03 mm (0.0007 in.) may not show one serious type of defect which is an order of magnitude smaller than this. This defect is epoxy smear over the exposed surface of the internal land areas which is caused by improper drilling. The epoxy masks the internal conductors during the hole-plating process and results in either an open circuit or a joint which may have far less than the desired interconnection of 360°. To inspect for this condition, the technique of mutual coupling, which uses the presence of the gap or high resistance area of the connection to develop an output signal, has been developed.

The application of this technique is shown in figure 9. Two coils wound in the form of a figure **8** are magnetically shielded from each other and are formed into a single probe which is inserted into the through-hole. A signal generator is connected to the excitation coil. The pickup coil is shielded from the direct field of the excitation coil. When there is no gap between the plated hole and the pad, the currents that are induced in the pad circulate in the region of the pad near the excitation coil; hence, little voltage is induced in the pickup coil. However, when the probe is brought near a gap between the plated hole and the printed conductor, the magnetic field from the excitation coil induces a current in the loop formed by the edge of the gap. The magnetic field from this current which circulates around the gap induces a voltage in the pickup coil. The pickup coil is connected to a tuned voltmeter which indicates the presence of the induced voltage.

Initially a large, 1.36-cm. (0.85-in.) diameter probe was constructed to verify the concept (fig. 10). A second probe one-tenth the diameter of the initial probe was then constructed to determine the effect of miniaturization on the experimental results. When this proved successful, a further reduction of 4 : 1 was made to produce a probe with a diameter of 0.51 mm (0.020 in.). The comparative sizes of the probes are shown in figure 11. The results of the test run are tabulated in table I. In one test, a bare copper wire was wrapped around a conducting cylinder. By varying the tension on the wire, a connection having low resistance but mechanically unstable characteristics was formed. The mutual coupling probe could adequately detect this type of connection.

Tests were also conducted to determine the minimum practical gap angle that could be detected. It was found that for a reasonable ratio (5:1) of peak gap voltage to cylinder wall voltage, the minimum gap angle is approximately
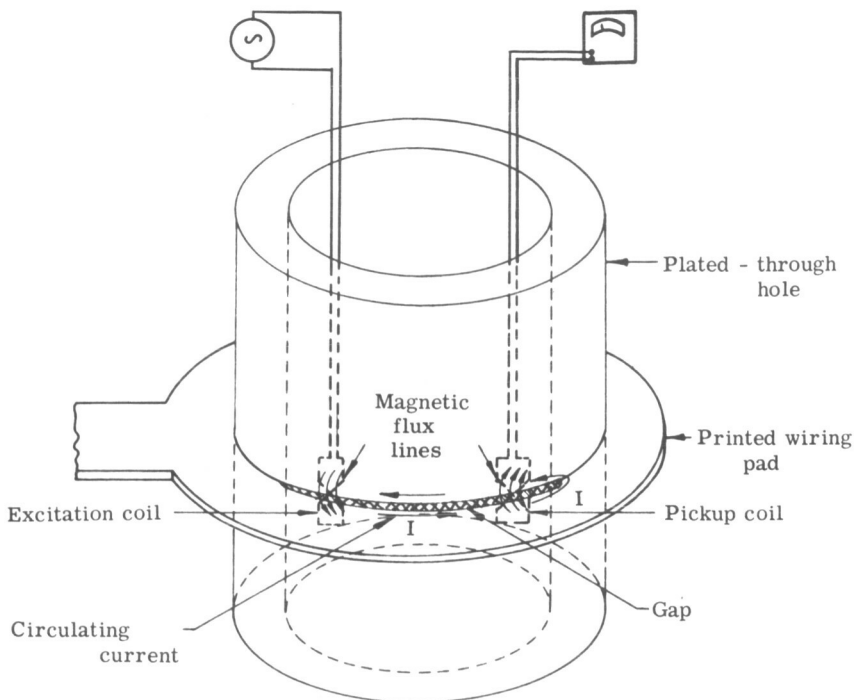
FIGURE 9.—Mutual coupling concept.

60°. This necessitates rotational as well as axial motion of the probe. The probe as designed for laboratory verification of the testing technique is very delicate and thus unsatisfactory for practical application.

A development program on the probe is presently underway. The probe will be a single piece of electrical steel with flats on it. A layer of electrical insulation will be grown on the probe, and single-turn figure **8** coils will be deposited on the flats. A number of coils will be deposited upon a single probe so that rotation within the hole will not be required for a complete profile. The same control tapes used in the automatic tape control drill to make the board could be used to program the probing of the plated-through holes.

CONCLUSIONS AND RECOMMENDATIONS

Laboratory experiments have verified the feasibility of both axial transverse laminography and mutual coupling as nondestructive testing techniques for the inspection of multilayer printed circuit boards. Laminography is well-suited for mass inspection of such boards. It will detect flaws as small as 0.03 mm (0.0007 in.) and can distinguish conductor layers separated from adjacent layers by 0.10 mm (0.004 in.). It can be used for screening the boards and for detecting gross internal defects.

TOP VIEW

Coil dimensions

0.3"

Handle

Tape insulation
(0.04")

0.3"

1.2"

Four turns on each half

Pickup coil

Excitation coil

90°

Silicon steel
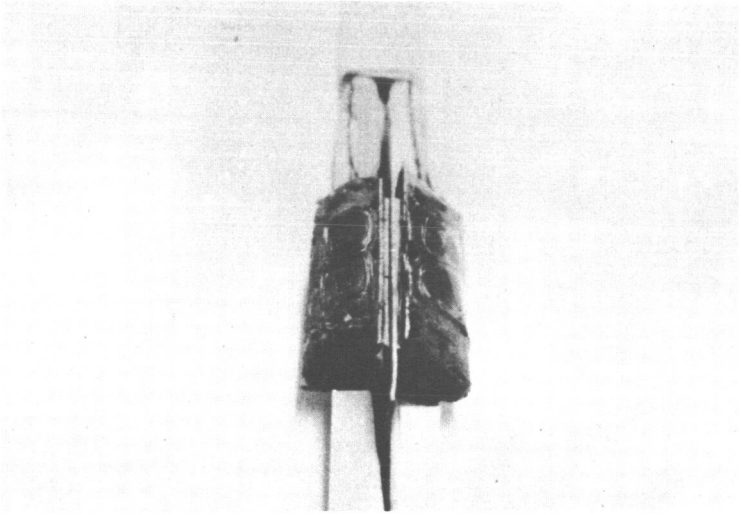laminations (0.027")

.85"

END VIEW
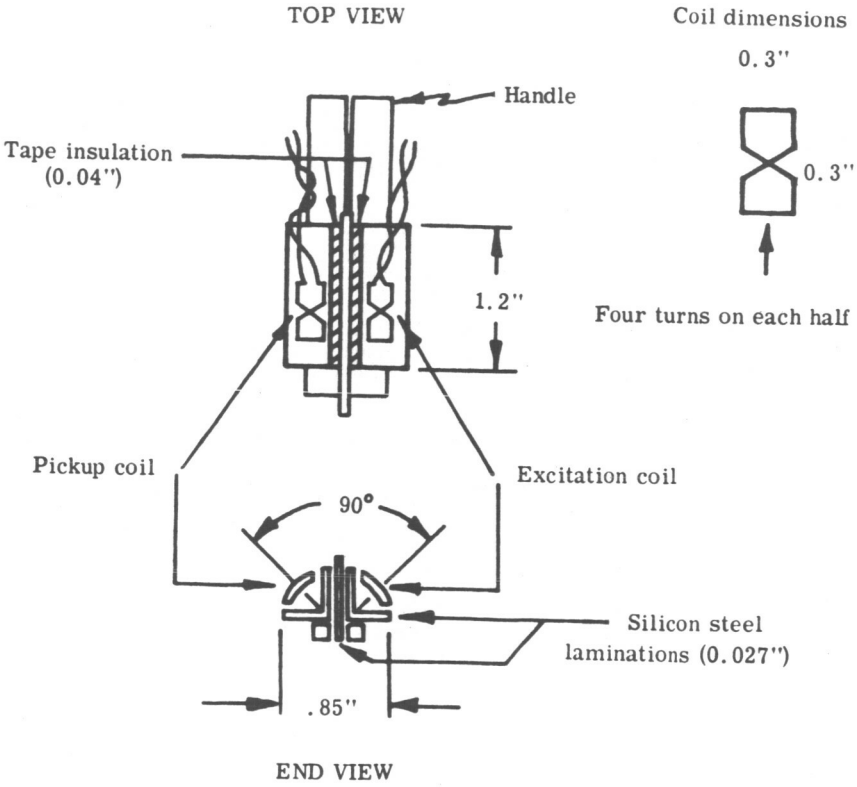
FIGURE 10.—Schematic and photograph of a large diameter probe.
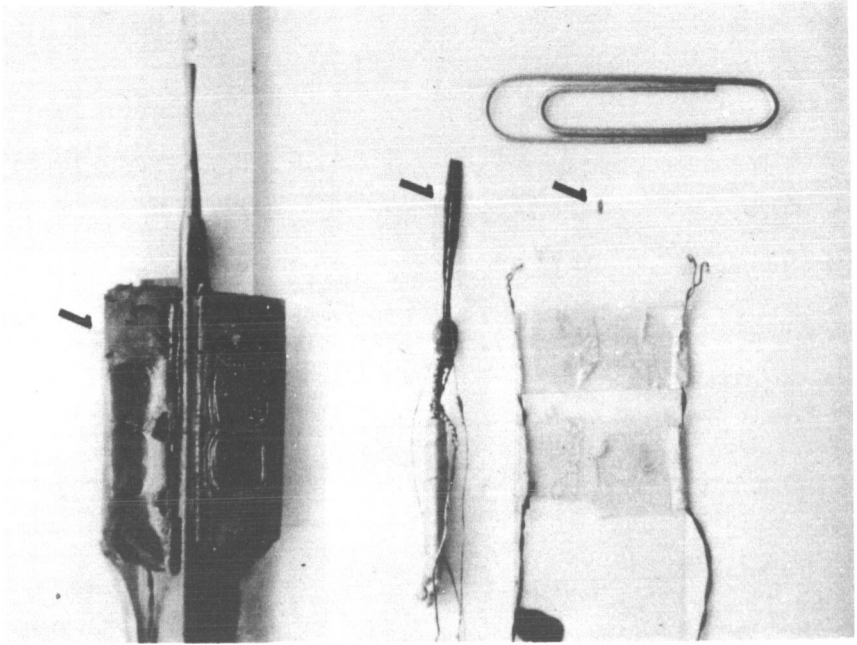
FIGURE 11.—Three mutual coupling probes with diameters of 1.36 cm (left), 2.03 mm (center), and 0.51 mm (right).

TABLE I.—*Pickup Coil Voltages for Three Mutual Coupling Probes* (*Excitation current—100 m*^{A})

	Probe 1	Probe 2	Probe 3
Probe diameter,			
mm	21.59	2.03	.51
in	.85	.080	.0015
Frequency, kHz	50	500	2000
Cylinder material	Brass	Copper	Copper
Cylinder wall thickness,			
mm	.686	.102	.038
in	.027	.004	.0015
Gap width,			
mm	.038	varied	<.0025
in	.0015		<.0001
Cylinder wall voltage, V_{cw},μv	.39	.41	.12
Soldered connection voltage, V_{sc},μv	.57	.78	....
Gap voltage, V_g,μv	15.6	4.6	1.0
Ratio, V_g/V_{sc}	27.4	5.9	8.3*

*V_g/V_{cw}.

Work is presently underway to transform the laboratory model of the laminograph into a piece of practical hardware.   The new system will make use of optical and closed-circuit television techniques in conjunction with a fluorescent screen to produce a continuous scanning laminograph with the capability to make any permanent records desired.

The application of laminography is not limited to the inspection of multilayer printed wiring boards; however, it should become a powerful nondestructive testing tool for detailed examination of the interior of solid homogeneous or nonhomogeneous bodies.

Mutual coupling can be used as an adjunct to laminography in the detection of extremely small gaps in the through-connections, but it is more limited in application because it requires probing of each through-connection to be inspected. The laboratory model of the 0.51-mm (0.020-in.) diameter probe was difficult to fabricate and too fragile to be practical.   Work is being done to deposit four to six coils on a single probe in order to simplify the probing operation, to improve the geometry of the probe, and to reduce the minimum gap angle that can be detected.   While these two complementary techniques will not answer all the questions concerning the quality of multilayer wiring boards, they will go a long way toward answering the question concerning the reliability of the interconnections.

The Nondestructive Evaluation of Adhesive Bonded Composite Materials

W. N. CLOTFELTER

The utilization of composite, honeycomb materials in the design of launch vehicles and aircraft represents a major advancement in design technology. However, to assure maximum reliability in these structures, nondestructive testing (NDT) techniques which can assure a high-quality composite material are required.

One application which illustrates the need for high quality in the composite material is the common bulkhead which separates two cryogenic propellants in Saturn launch vehicles. The upper stages (S–IV, S–IVB, and S–II) of both Saturn I and Saturn V utilize liquid hydrogen (LH$_2$) as the fuel and liquid oxygen (LOX) as the oxidizer. In all three stages, a common bulkhead design is used in the separation of LH$_2$ and LOX. These bulkheads, which are made of nonmetallic honeycomb cores bonded to thin aluminum face plates, serve both as structural members and as thermal insulators. Another type is used only for thermal insulation (figs. 1 and 2). The materials used to construct these bulkheads are rigid, good thermal insulators, and have high strength-weight ratios. Many potential applications for these or similar composite materials exist in non-aerospace industries. Specifically, composites can be used in the construction of boats, house trailers, truck bodies, portable school rooms, and in many other applications requiring thermal or acoustic insulation.

Poor adhesion at any interface degrades the strength and stiffness of these complex materials. Since they serve many purposes, typically as structural members and as thermal insulators, essentially flawless material is required.

Two major difficulties were experienced in initial attempts to test large honeycomb structures with ultrasonic through-transmission techniques: (1) transducer alinement, and (2) the determination of the exact location of debonds with respect to thickness of the material. Complex mechanical scanning equipment has reduced the alinement problem to a practical minimum; however, it usually cannot be used to evaluate common bulkheads or thermal insulation subsequent to fabrication in large tanks. Thus, the major objective of this program is to develop portable, nondestructive inspection systems which have the capability of evaluating composite materials from a single side. A second objective is to develop means of identifying the particular interface at which debonds occur.
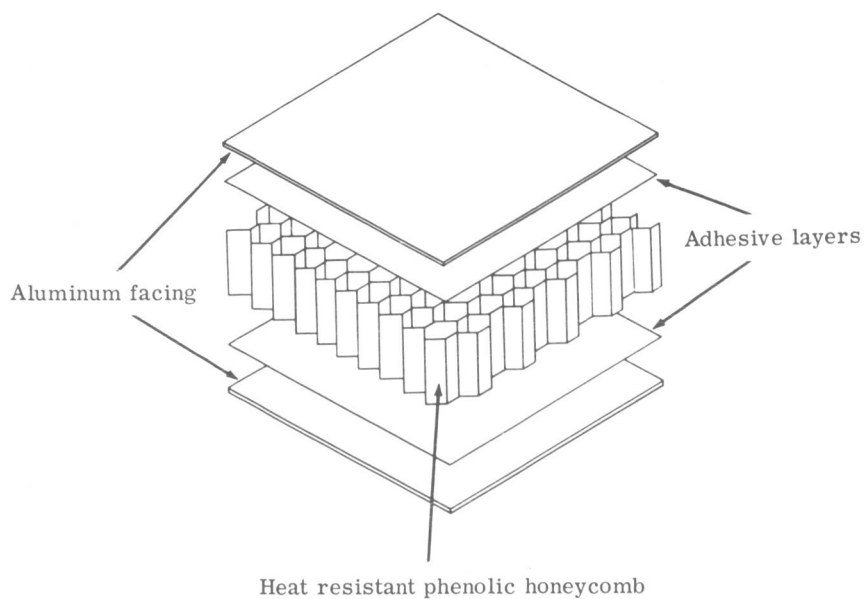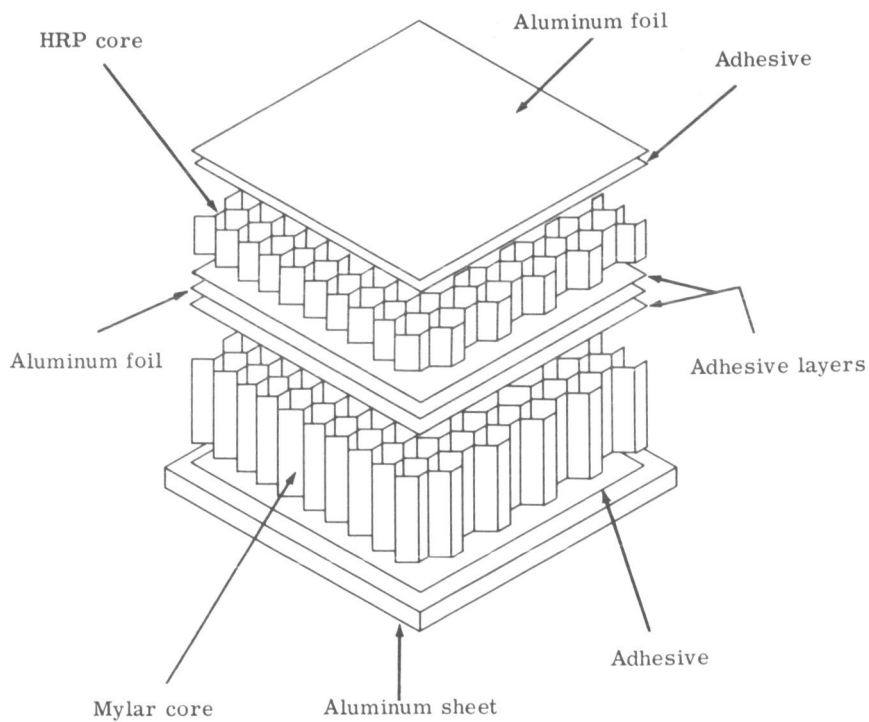
FIGURE 1.—Design of HRP insulation.

FIGURE 2.—Design of dual seal insulation.

Four complementary techniques have been developed and will be described. They are water-coupled impedance, contact impedance, through-transmission air-coupled, and eddy-sonic nondestructive techniques. Some of the methods described were developed at Marshall Space Flight Center; other methods were developed by the Los Angeles Division of North American Aviation, Inc.

THEORY

Because of the frequency sensitivity of thin sheets to sound waves, a major problem in testing honeycomb materials is getting the ultrasonic energy through the thin metallic face sheet. Thin materials are almost opaque at certain frequencies. Fortunately, the acoustic characteristics of thin sheets have been well established by both theoretical (ref. 1) and laboratory (ref. 2) work. It has been found through laboratory measurements that the relative amounts of acoustic energy reflected, transmitted, and absorbed when sound waves impinge on a thin plate are determined by the angle of incidence, the acoustic impedance of the plate, the acoustic impedance of the coupling medium, and the thickness of the plate. Material thickness loses much of its significance when the specimen is thicker than several wavelengths of the applied signal. A formula for the special case of thin plates and normal incidence of sound is:

$$R = \frac{\left(\dfrac{V_1 P_1}{V_2 P_2} - \dfrac{V_2 P_2}{V_1 P_1}\right)^2}{4 \cot^2 \dfrac{2\pi d}{\lambda} + \left(\dfrac{V_1 P_1}{V_2 P_2} + \dfrac{V_2 P_2}{V_1 P_1}\right)^2}$$

where

R ratio of reflected to incident energy
V_1 velocity of sound in first medium (or water)
V_2 velocity of sound in second medium
P_1 density of first medium
P_2 density of second medium
d thickness of plate
λ wavelength of sound in specimen

Acoustic impedance is equal to the velocity of sound in a medium times the density of the medium. This is true for any material thickness. The special acoustic characteristic of thin plates—frequency sensitivity—is explained by the expression

$$4 \cot^2 \frac{2\pi d}{\lambda}$$

in the formula above. A study of the formula shows that when plate thickness

is equal to a half wavelength of the applied acoustic signal, maximum energy will pass through the plate.   When the thickness is a quarter wavelength or an odd multiple of a quarter wavelength, maximum energy will be reflected from the surface of the plate.   Hence, we can choose the optimum frequency of the applied acoustic signal for maximum penetration.

EXPERIMENTAL TECHNIQUES

A method of evaluating honeycomb materials from a single side has been developed.   This method, which can be explained by the acoustic characteristics of thin plates described above, is based on resonance phenomena and acoustic impedance variations, although conventional pulse echo equipment is used.
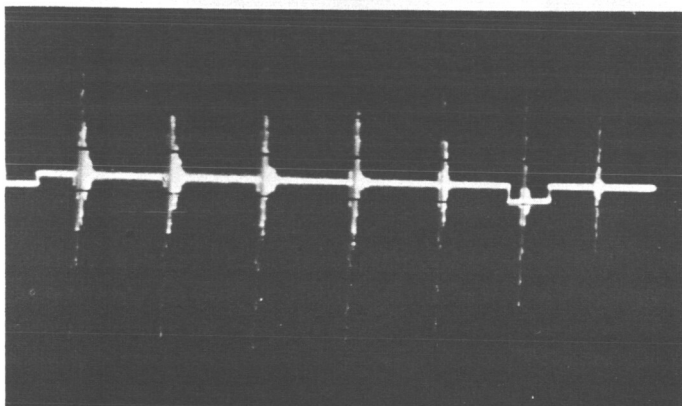
Water-Coupled Impedance Technique

A pulse of ultrasonic energy is directed at right angles to the composite through a water path.   The water may be supported by a container, or a stream may be used.   Reflected pulses are displayed on a cathode ray tube.   Details of this technique are depicted in figure 3.   The oscilloscope pattern of *a* illustrates the case of a well-bonded panel.   Two "gates" or "windows" are provided in the oscilloscope time base so that only selected reflections will be used to evaluate the composite.   The first and second gates would indicate signal changes if debonds existed at the metal-adhesive and adhesive-core interfaces, respectively. Pattern *b* shows the effect which results from a metal-adhesive debond.   Metal thickness in this case is almost exactly a half wavelength; therefore, undamped plate resonance produces a ringing effect.   An example of an adhesive-core debond is shown in the second gate of pattern *c*.   Notice that little change occurs in the first gate since a good adhesive bond dampens the ringing effect.   However, since the metal face plate is a half wavelength thick, maximum energy is available at the metal-adhesive interface to penetrate the adhesive.   This increased reflection at the second gate is due to the fact that no bond exists at the core to absorb the increased flow of energy through the face plate and adhesive; hence, the signal is reflected.   Expressed differently, the acoustic impedance of the whole panel, not just the elastic properties of the metal face plate, affects the ratio of reflected to incident energy.   The increasing difference between bond and debond conditions with each successive echo is best explained by the shift in acoustic impedance.   Since the core does not absorb energy when a debond exists, the exponential decay of reflected energy is less steep, and a greater change in reflected energy occurs between the bond and debond conditions with each successive echo.   Thus, the seventh or eighth echo is used to obtain C-scan, plan position or maplike recordings.   Figure 4 is a typical C-scan recording of simulated defects.
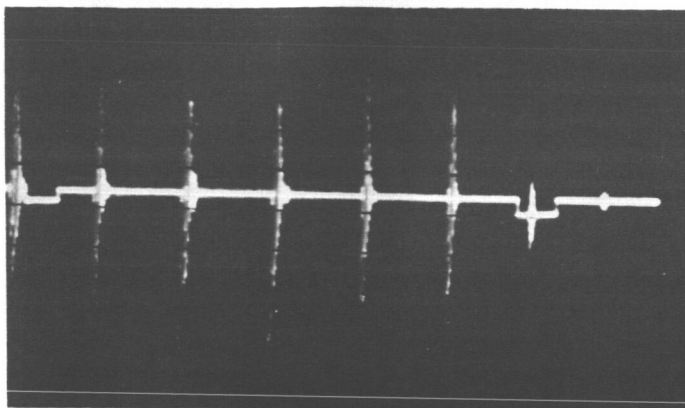
a. No defects indicated
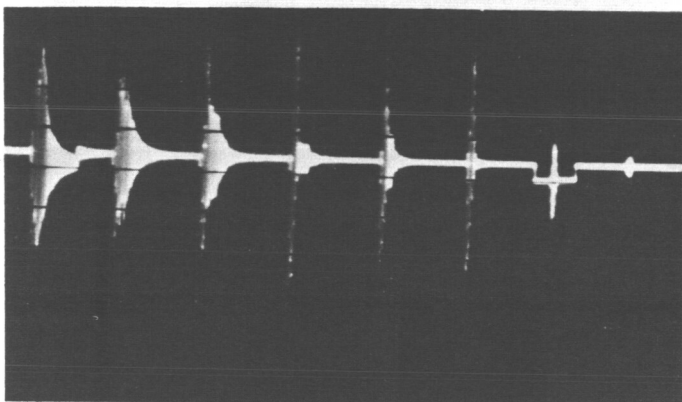
b. Metal-adhesive debond

c. Adhesive-core debond

FIGURE 3.—Water-coupled impedance technique.
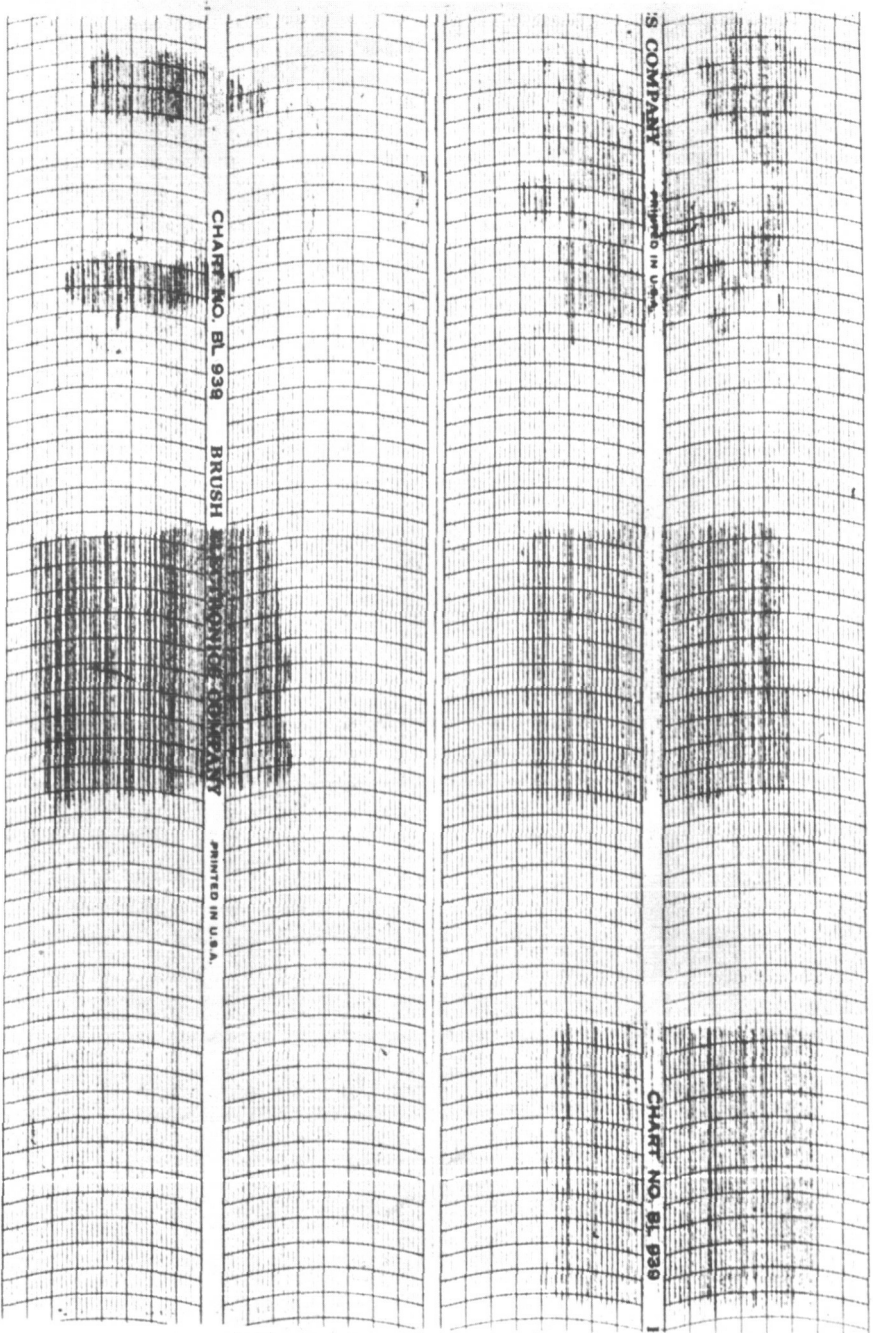
Core-adhesive debonds   Metal-adhesive debonds

FIGURE 4.—A typical C-scan recording.

Contact Impedance Method

When a vibrating crystal is placed on a composite panel, the characteristic impedance or the elastic properties of the panel determine the manner in which it is loaded. This loading will change the amplitude or phase of the crystal vibration with respect to the applied voltage. These changes are reflected from the crystal into the electronic system and are processed to obtain a readout suitable for recording. Best results are obtained when the operating frequency is near the natural resonant frequency of the panel. The entire panel behaves as a thin plate at low frequencies. A debond located at any interface within the composite can be located in this manner.

Typical transducers are shown in figure 5. These transducers require a liquid couplant for the efficient transfer of energy into the panel. With the aid of a scanning device and a recording system, a C-scan recording of a simulated defect may be obtained as shown in figure 6. Figure 7 shows the simulated defect in a honeycomb panel subsequent to removal of the aluminum face sheet. This record was obtained with the transducer on the opposite side of the panel. The scanning device and the electronic and recording systems are shown in figures 8, 9, and 10. Recent improvements in this basic technique include electronic circuit changes to increase sensitivity and the introduction of a liquid-filled wheel to couple acoustic energy into the specimen. Greater scanning speeds are obtained with the wheel transducer.

The system described is the best available for evaluating composite honeycombs with plastic core and metal face plates when access is limited to a single side.

Air-Coupled Techniques

Through-Transmission Method.—A thermal insulating material called dual seal insulation, composed of two layers of honeycomb core separated by a vapor barrier, has been developed at Marshall Space Flight Center. An exploded view of this material is shown in figure 2. This composite material is very light and has very good thermal properties; however, techniques that were developed to inspect the composites previously discussed were found to be inadequate for this insulation.

Experiments established the difficulty of penetrating this material with high frequency sound produced by conventional ultrasonic equipment. Mylar honeycomb caused most of the high frequency attenuation. Although limited penetration could be obtained with some of the lower ultrasonic frequencies, debond detection was very poor. Most of this difficulty was due to the complex structure of the panel, but part was due to the rough surface on one side of the material.

A new approach was made which involved air-coupled sound generators, such as loudspeakers. Among the receiving transducers investigated were microphones, ultrasonic leak detectors, and crystals. Initially, not enough difference
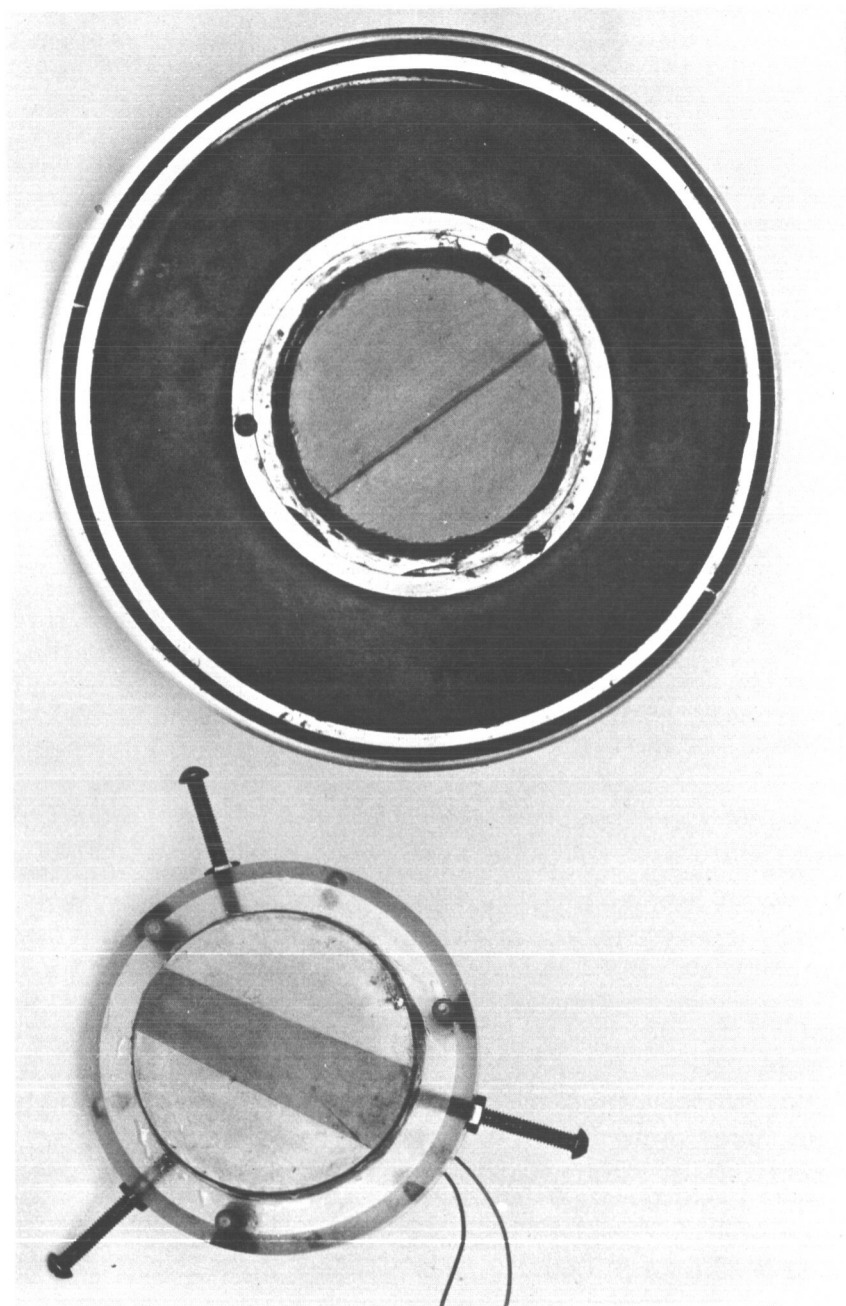
FIGURE 5.—Impedance transducers.
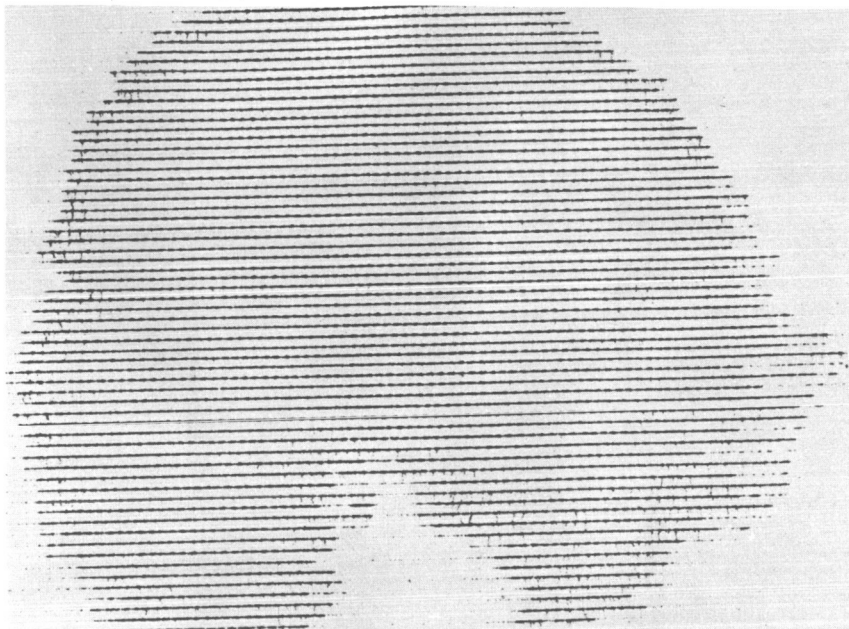
FIGURE 6.—C-scan recording of simulated defect in HRP insulation.
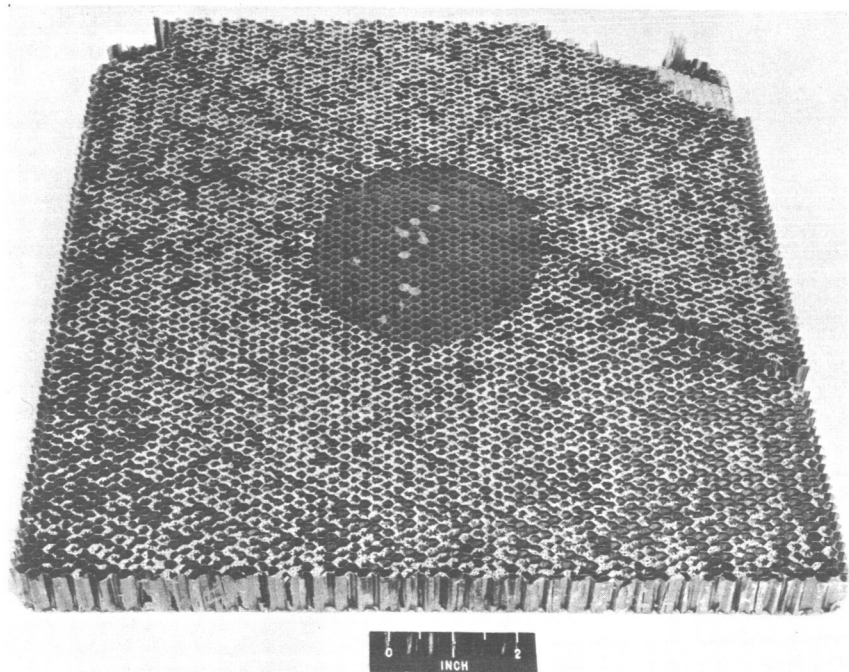
FIGURE 7.—A simulated defect.
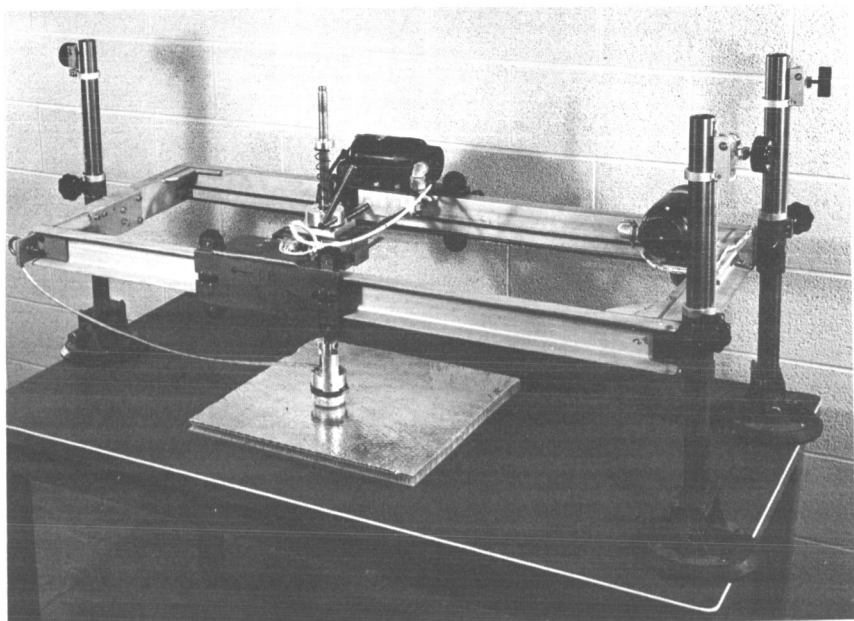
FIGURE 8.—The scanning device.
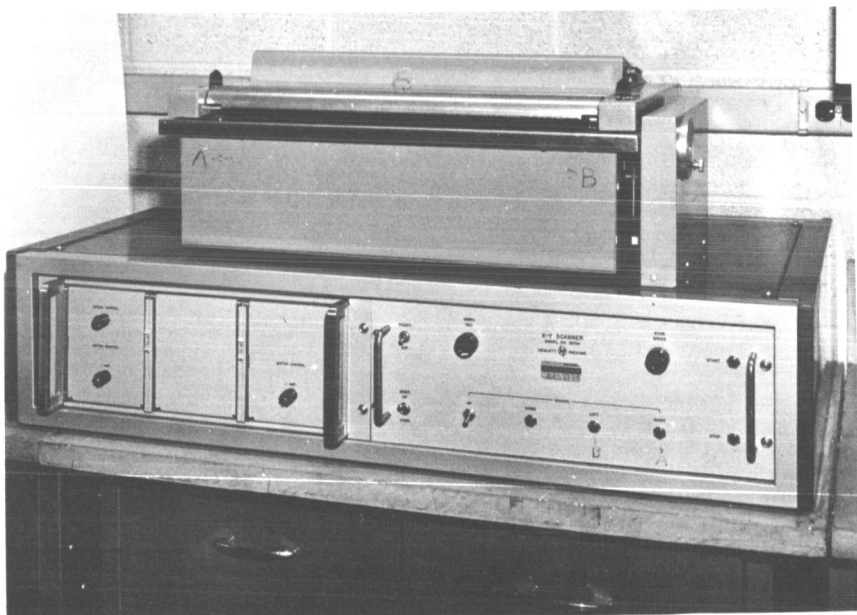
FIGURE 9.—A C-scan recorder and the scanning motor controls.
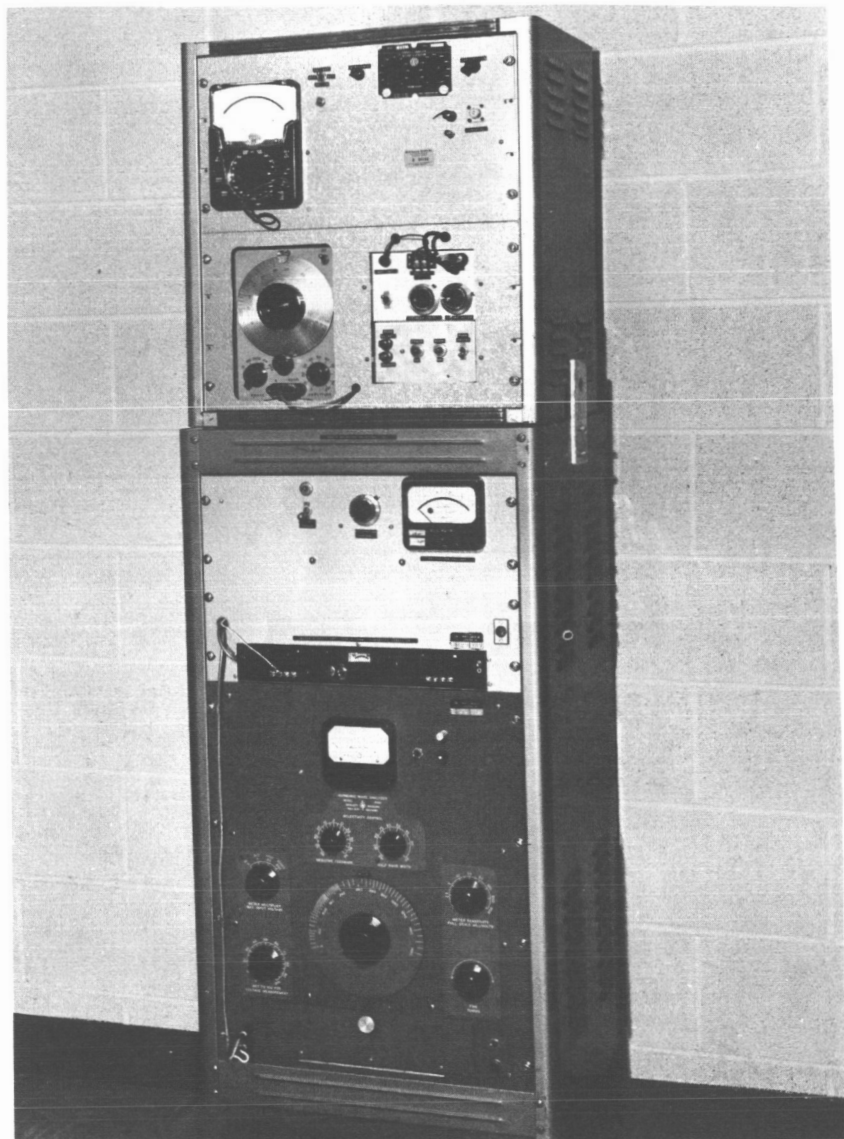
FIGURE 10.—The electronic systems.

could be obtained between the attenuation of a well-bonded specimen and a specimen containing debonds. It was theorized, and later proved, that the applied energy level of these low frequency signals was too high since low frequencies penetrated easily. When the power of the transmitters was reduced and the amplification of the receiving circuit was increased, good results were obtained. Typical oscilloscope patterns are shown in figure 11.
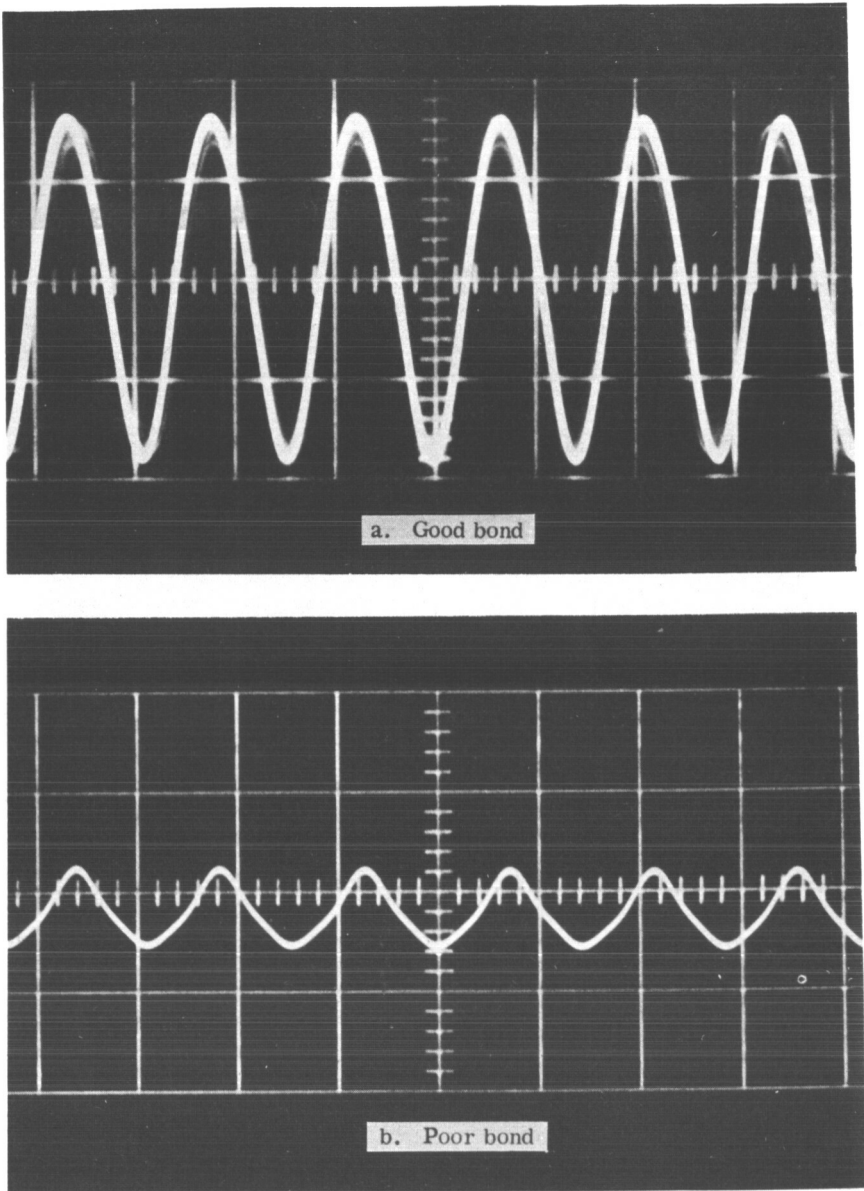
FIGURE 11.—An A-scope evaluation of dual seal insulation.

The advantages of air-coupling are numerous. Air-coupling eliminates variable contact problems as well as the handling of water, grease, or other messy couplants. Transducer alinement difficulties are eliminated since a transmitter can be placed in a fixed position in the center of a tank while receivers scan the outside.

To cathode follower

Electro voice capacitor microphone

Encapulated coil
78 Turns no. 18 wire

Ferrite cup
core Allen
Bradley
Modified
P/N C2400-
D207a

Spacing approx. 0.04 in.

FIGURE 12.—An eddy sonic transducer.

FIGURE 13.—C-scan of simulated defects in dual seal insulation.

Eddy-Sonic Method.—An electromagnetic technique has been added to these acoustic techniques to form an eddy current and sonic or "eddy-sonic" system. Vibrations are induced in the thin metallic face sheet of dual seal insulation with a coil-type transducer energized with a commercial oscillator. This transducer
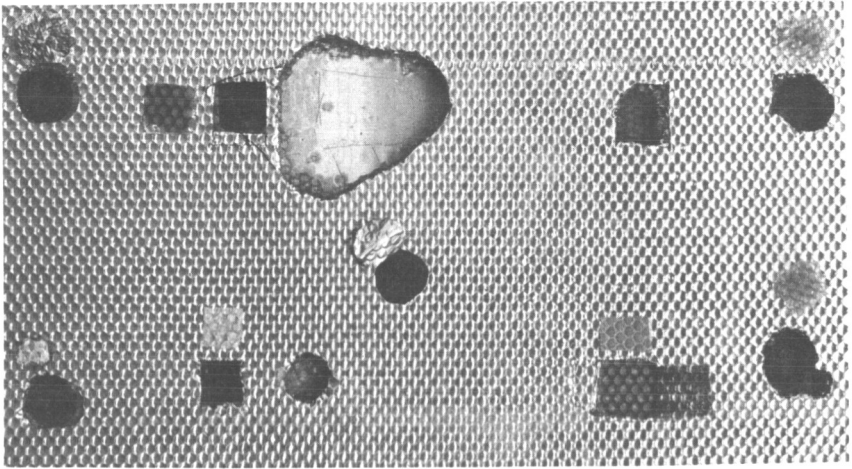
FIGURE 14.—Simulated defects in dual seal insulation.

does not have to touch the surface. The induced vibrations are transmitted to the opposite side of the honeycomb panel and are reflected to the first surface. Modifications in this reflected energy caused by defects are detected with a microphone (fig. 12). Subsequent to amplification and processing, these signals can be used to obtain a C-scan recording of simulated defects as shown in figure 13. Figure 14 shows the simulated defects in dual seal insulation. The same scanning and recording systems are used for both the eddy-sonic and the previously described contact impedance systems.

This eddy-sonic system is the best method available for the nondestructive evaluation of dual seal insulation. The interface at which debonds occur can be detected, and all debonds can be detected from a single side.
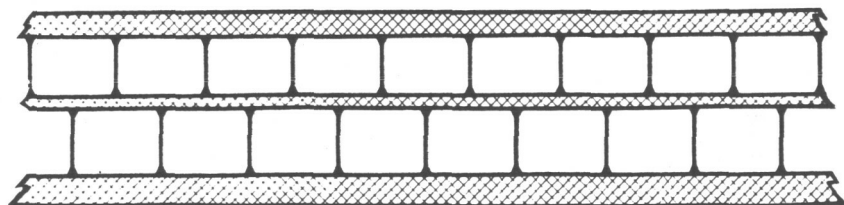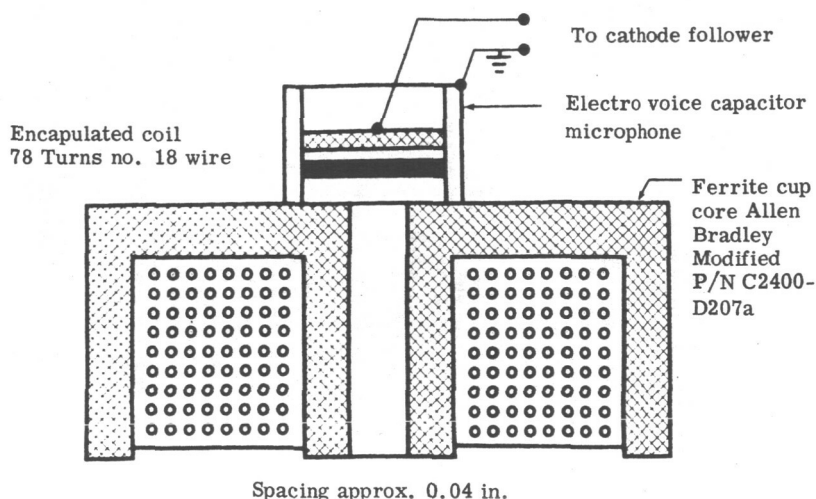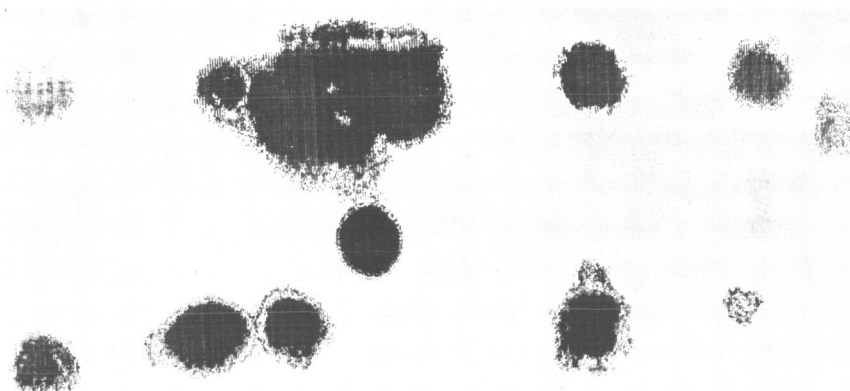
CONCLUSIONS

The ability to insure complete bonding in composite, honeycomb materials will enhance their usefulness in a wide variety of commercial applications. The water-coupled impedance, the contact impedance, and the eddy-sonic techniques have been developed to the point of making practical applications feasible. Composites of the plastic core-metal faceplate type may be tested rapidly with the low frequency contact impedance method. Any defective areas may then be examined more carefully with the high frequency water-coupled impedance method to determine the exact interface at which the debond occurs. The eddy-sonic method is rapid, all debonds can be located from a single side, and no contact is required with the surface; therefore, it is recommended for evaluating the more complex dual seal insulation.

The through-transmission air-coupled technique can, with further development, be used to increase the speed of evaluating large tanks or similar structures.

It is, for all practical purposes, a single-side method since a single source of low frequency sound may be placed at the center of a large tank while the outside is scanned for defects.

REFERENCES

1. RAYLEIGH, J. W. S.: Theory of Sound. Vol. II. Dover Publ., 1877.
2. BOYLE, R. W.; AND LEHMAN, T. F.: Passage of Acoustic Waves Through Materials. Trans. Roy. Soc. Can., 1927.
3. MOORE, J. F.; AND MARTIN, GEORGE: Development of Nondestructive Techniques for Honeycomb Heat Shields. Rep. NA–66–638, North Am. Aviation, Inc., June 1966.
4. CLOTFELTER, W. N.: Acoustic Techniques for the Nondestructive Evaluation of Adhesive Bonded Composite Materials. NASA TM X–53219, Mar. 17, 1965.

Ultrasonic Analysis of Cold-Rolled Aluminum

R. L. GAUSE

The reliability of structural systems has taken on added importance with the advent of "man-rated" spacecraft and booster vehicles. Previously, the integrity of a structure was insured by using a high factor of safety in its design; however, due to the increased emphasis on optimum structural design necessary to maximize payload and minimize redundant structural weight, this approach is not acceptable in the design of space related structures. Thus, the conflicting requirements of high reliability and minimum weight have spurred the search for more efficient structural design methods and the development of more accurate and reliable test techniques. One important area, which has recently received considerable attention and which shows promise of contributing to the solution of both the weight and reliability problems, is that of the analysis, understanding, and utilization of the residual stresses which exist in most engineering materials and structures. Of course, in order to understand and thereby be able to utilize these stresses, they must first be detected and analysed. To date, there is no technique available which provides a convenient and accurate analysis of residual stress. Of the various methods currently being investigated, those based on ultrasonics seem to show the most promise of meeting the desired requirements. One of these techniques, shear wave birefringence, will be described in this paper.

RESIDUAL STRESSES

Residual stresses, often called locked-in or internal stresses, exist in a material after all external stresses have been removed. The presence of residual stresses can greatly improve the strength of a structure; however, if the residual stresses are directed in such a way as to add to the load stresses or as to have sharp discontinuities, then they may be highly detrimental as illustrated in figure 1.

There are several basic ways in which residual stresses may be developed. In bulk materials, they may be produced by (1) cold-working, i.e., by extruding, drawing, forging, or rolling, (2) heat-treating, (3) grinding, or (4) machining processes. In engineering structures, they may be produced by welding or fitting operations. Specifically, any operation which results in a nonuniform

31
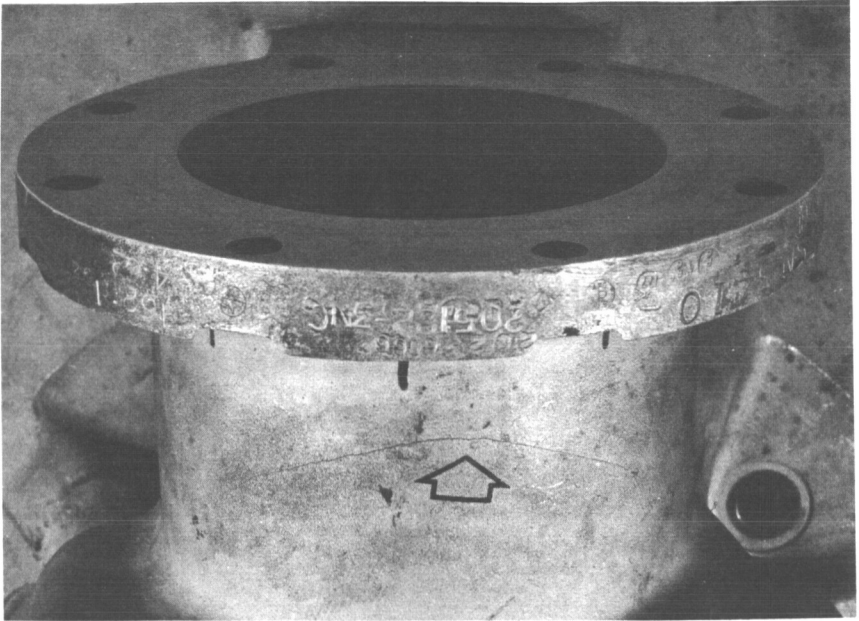
FIGURE 1.—Residual stress-induced crack in the liquid oxygen dome inlet of the H–1 engine.

change in shape or volume throughout the material will result in the creation of a residual stress distribution in that material. For example, if a material is cold-worked by cold-rolling, a residual stress distribution similar to that shown in figure 2 might be created. Notice that the area in tension is equal to that in compression. This must be true for the body to be in equilibrium.

The search for nondestructive methods of measuring residual stresses has been long and arduous. Only in the last several years when ultrasonic methods were investigated was any progress made in this important endeavor. Of the several ultrasonic techniques studied, the one based on the birefringence, or double refraction, of shear waves has received the most attention.

SHEAR WAVE BIREFRINGENCE

Before describing the shear wave birefringence technique, some background information concerning shear waves will be given. A shear wave (illustrated in fig. 3) is characterized by particle motion perpendicular to the direction in which it is moving; therefore, to completely specify a shear wave, it is necessary to designate not only the direction in which it is propagating but also the direction of particle motion. The phenomenon of birefringence, or double refraction, of a shear wave is associated with the breaking up of the wave into two components which then are transmitted through the medium on planes at right angles. This birefringence of the wave will occur only if the medium

FIGURE 2.—Representation of residual stress distribution in a cold-rolled metal.

FIGURE 3.—Illustration of a shear wave and its properties.

is anisotropic (i.e., if it possesses directional properties) and if the direction of particle motion does not coincide with a principal axis.

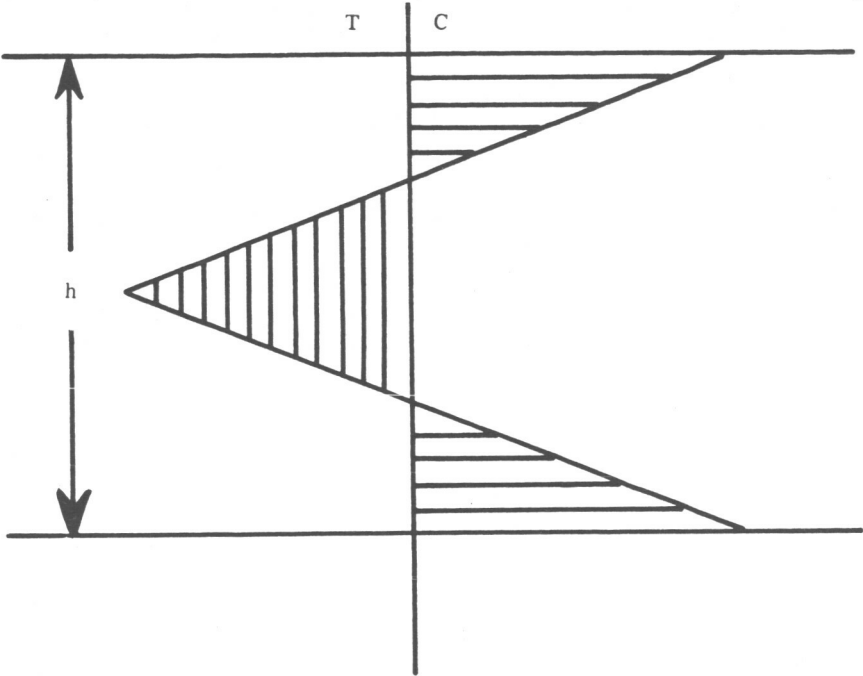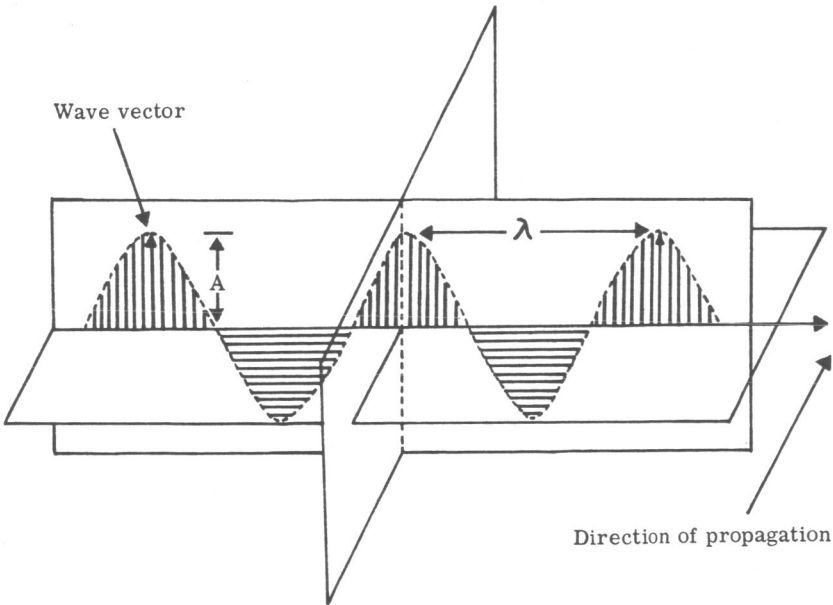When a shear wave is propagated through an isotropic body, it has a velocity which is dependent only on the shear modulus (μ) and the density (ρ) of the body, i.e.,

$$V_s = \left(\frac{\mu}{\rho}\right)^{\frac{1}{2}} \tag{1}$$

If, however, the shear wave is incident on an anisotropic body, birefringence will occur; and, since the wave propagation characteristics of the material along the two paths are different, the two wave components will travel through the material with two different velocities. As a result, a difference in velocity (ΔV) between these components will be produced which is dependent on the degree of anisotropy possessed by the material. If the material is made anisotropic by the application of a stress, this velocity difference is found to vary directly with the magnitude of the stress. By using the nonlinear elasticity theory, theoretical relationships between the wave velocities and stress can be derived. Since the birefringence technique is based on the velocity difference between the wave components with particle motion parallel and perpendicular to the rolling direction, it can be shown that the fractional velocity difference ($\Delta V/V$) is related to the stress (T) by the expression

$$\frac{\Delta V}{V} = -T(4\mu + n)/8\mu V_\rho^2 \tag{2}$$

where μ and n are elastic constants of the material, ρ is the density, and V is the velocity of a shear wave in an isotropic body. Thus, if the $\Delta V/V$ is determined experimentally, the stress may be calculated providing the elastic constants μ and n are known.

EXPERIMENTAL DETERMINATION OF BIREFRINGENCE

To determine the $\Delta V/V$ experimentally, a measuring system is used whose simplified block diagram is shown in figure 4. The system consists of a pulsed oscillator, a switching circuit, a receiver, an oscilloscope, and a piezoelectric transducer. The transducer is a quartz crystal cut so that when an electrical potential is applied, the manner in which it vibrates produces a shear wave which is coupled into the specimen by means of a thin film of grease. The operation of this system consists of the following basic steps:

(a) Generation of an electrical pulse of the desire frequency and pulse length using the pulsed oscillator.

(b) Conversion from electrical to ultrasonic energy by means of the quartz transducer.

(c) Coupling of the ultrasonic energy into the metal specimen.
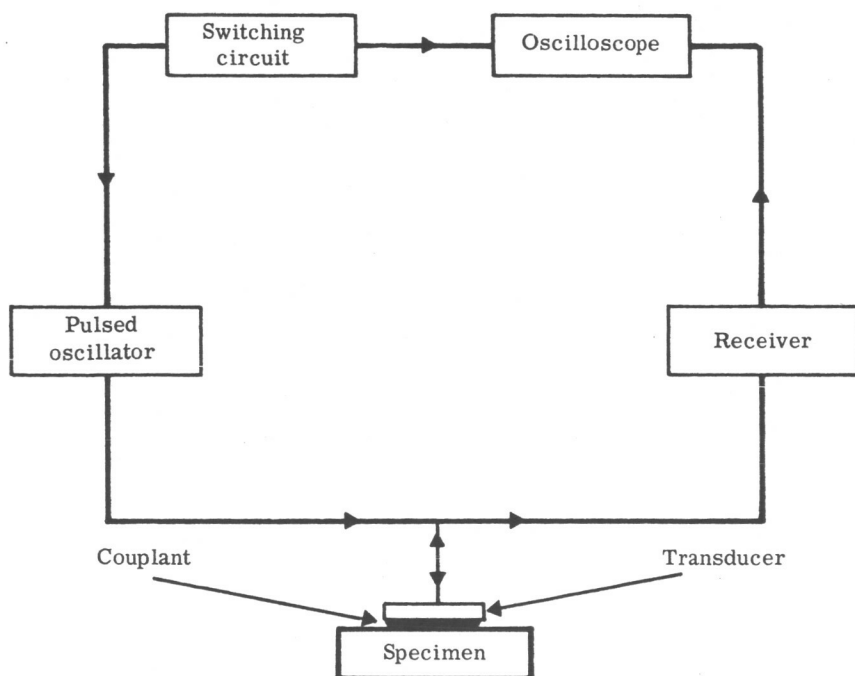
FIGURE 4.—Simplified block diagram of birefringence measuring system.

(d) Transmission of the ultrasonic pulses through the metal specimen.

(e) Reflection and retransmission of the pulses from the opposite face of the specimen.

(f) Coupling of the reflected energy into the transducer.

(g) Conversion of the ultrasonic energy to electrical energy.

(h) Amplification of the electrical energy for display on an oscilloscope.

(i) Interpretation of the electrical pulses to provide a measurement of birefringence.

To be able to interpret the oscilloscope traces, it is necessary to understand what happens to the wave when it propagates through the specimen. If the material is isotropic, a series of exponentially decaying echoes will be observed; however, if the material is anisotropic, such is not the case. It was mentioned previously that the two components produced by the birefringence of the incident shear wave are transmitted through the material with different velocities. Therefore, as they traverse the specimen, their phase difference will increase from the initial in-phase condition at generation. As this phase difference increases, the resultant particle motion will change as shown in figure 5. When the two waves have propagated a distance Z, their phase difference (χ) can be shown to be

$$\chi = \frac{2\pi f}{V} \frac{\Delta V}{V} Z \tag{3}$$
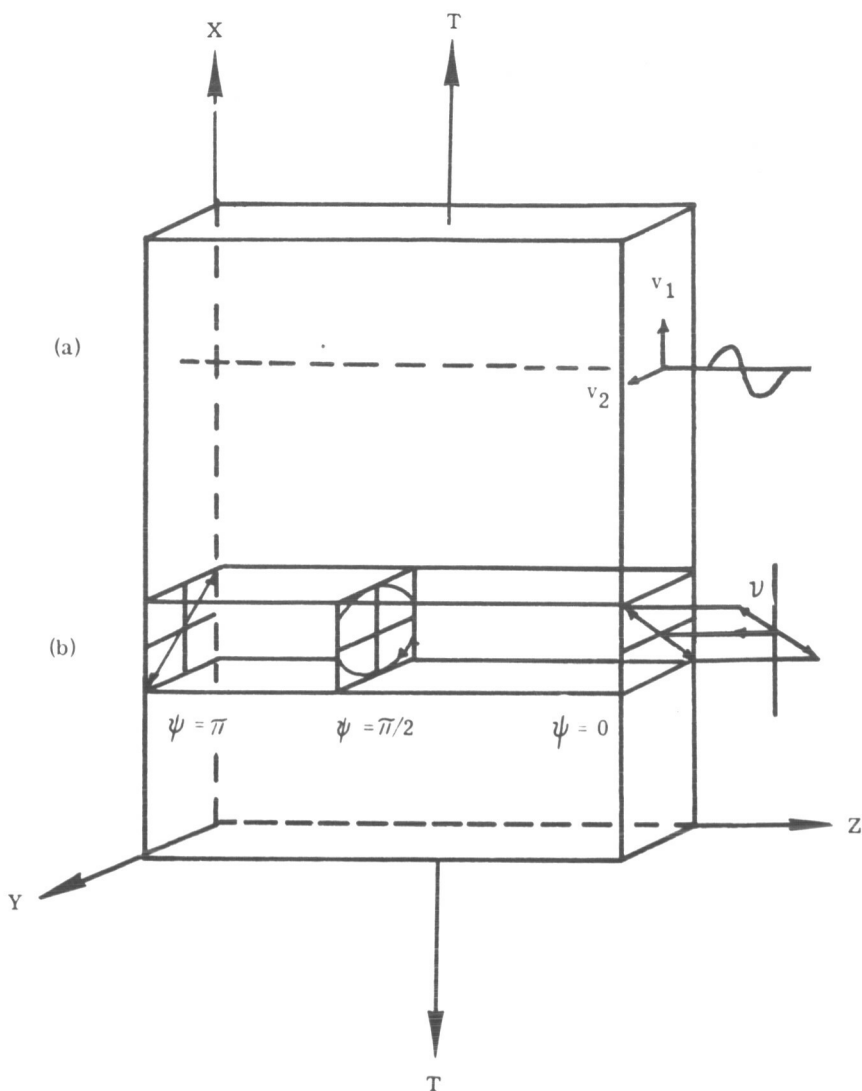
FIGURE 5.—Schematic representation of (a) distortional wave propagation in an anisotropic medium and (b) the resulting particle motion.

where f is the frequency and V again is the shear wave velocity in an isotropic body. When the waves propagate a distance so their phase difference is 180°, the resultant particle motion will be perpendicular to the original motion imparted by the transducer. Since the transducer (which acts as both a transmitter and a receiver) is insensitive to particle motion perpendicular to its axis of polarization, it does not sense the motion and, therefore, does not transmit a signal. Thus, for a phase difference of 180°, a node will occur in the echo pattern observed

on the oscilloscope. Since one echo corresponds to a wave propagation distance of twice the specimen thickness, the relationship between $\Delta V/V$ and the number of echoes (ρ) to the node can be written as

$$\frac{\Delta V}{V} = \frac{V}{4fph} \tag{4}$$

where h is the specimen thickness.

Using the previously shown equipment, birefringence measurements were made on specimens of aluminum which had been cold-rolled by various amounts. The results of these measurements for 6061–T6 aluminum are shown in figure 6. As can be seen, the birefringence increases linearly with applied stress in agreement with the theoretical expression shown previously (equation 2). Notice that the initial birefringence increases with increasing cold-work and that the lines are parallel indicating that the $\Delta V/V$ due to the applied stress adds linearly to the initial birefringence. The question now is whether the initial $\Delta V/V$ is due to residual stress or to some other source of anisotropy. Since the specimens which were investigated were obtained from cold-rolled sheets
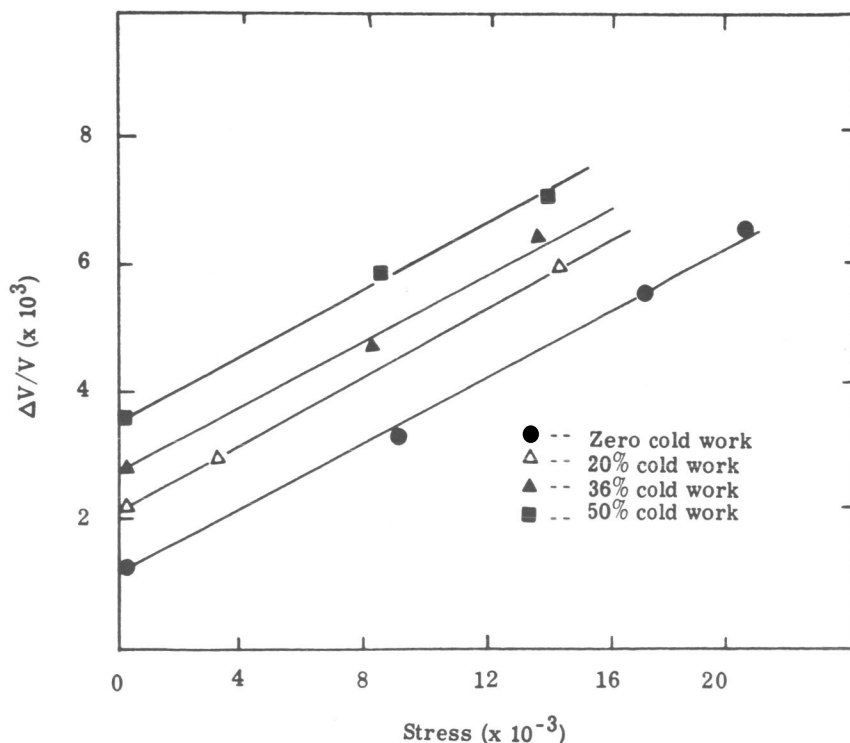
FIGURE 6.—Stress-induced birefringence in cold-worked 6061–T6 aluminum.

of aluminum, two principal sources of anisotropy have to be considered: residual stress and preferred grain orientation.

EFFECTS OF PREFERRED GRAIN ORIENTATION

Figure 7 illustrates preferred grain orientation. When the metal is subjected to rolling forces, the crystallites or grains composing the metal tend to rotate so that a particular crystallographic direction and a specific crystallographic plane are alined parallel to the rolling direction and rolling plane, respectively. If a sufficient number of the grains are oriented in a preferred fashion, the properties of the metal will show, in some measure, directional properties which reflect the inherent anisotropy of the individual crystals.

By considering a specimen as composed of a number of crystallites oriented in the most preferential way embedded in a matrix of crystallites oriented in a completely random fashion (fig. 8), the following expression may be derived:

$$\Delta V/V(P) = VF(V_2 - V_1)/V_1 V_2 \tag{5}$$

where

V shear wave velocity in a random array of crystallites

F fraction of the crystallites which are preferentially oriented

V_1 velocity of a shear wave along the crystallographic axis which is alined parallel to the rolling direction

V_2 velocity of a shear wave along the crystallographic axis which is perpendicular to the rolling direction
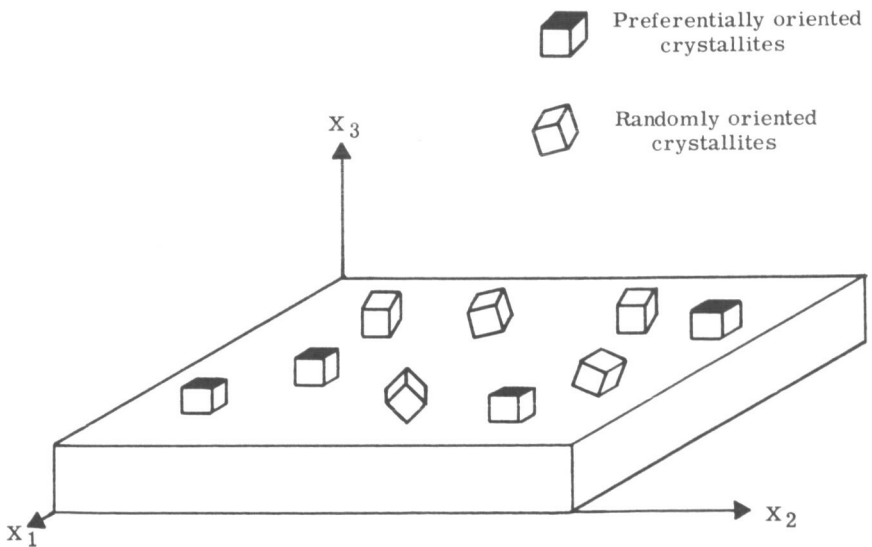
FIGURE 7.—Schematic representation of crystallite preferred orientation in a sheet of rolled metal.
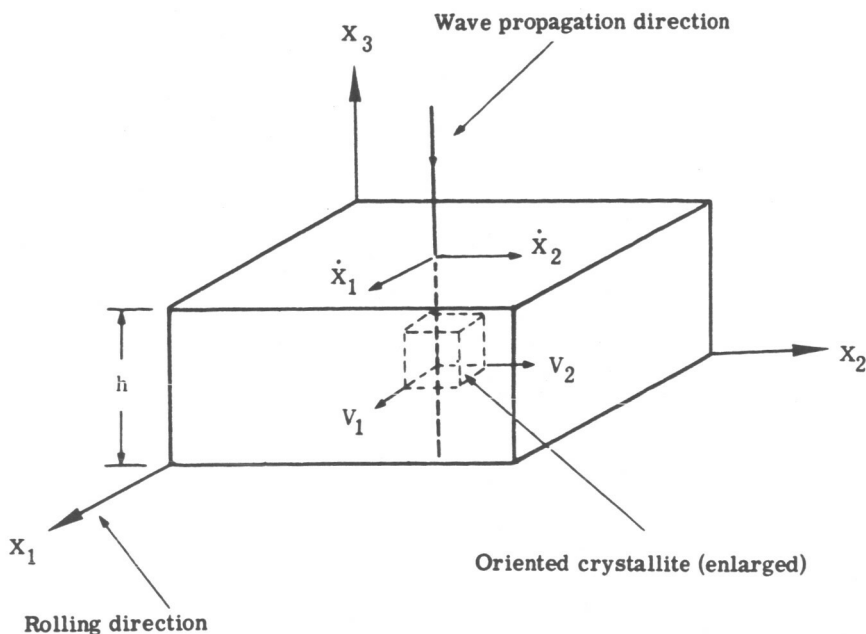
FIGURE 8.—Wave birefringence due to preferred orientation in rolled metal sheet.

In order to use the above expression to calculate the $\triangle V/V$ due to preferred orientation, the specific orientation possessed by the crystallites must be known. This information can be obtained from pole figures, such as the one shown in figure 9, which are generated using X-ray diffraction techniques. Figure 10 shows schematically the information obtained for the crystallite orientation for the 6061–T6 aluminum specimens. As can be seen, the [001] plane is alined parallel to the rolling plane, whereas the [100] direction is alined parallel to the rolling direction. Thus, in order to calculate the $\triangle V/V$ due to preferred orientation in 6061–T6 aluminum, the velocity of shear waves propagating in the [001] direction and polarized along [100] and [010] must be known.

These velocities may be caluated from equations derived using the theory of elasticity. If this is done, it is discovered that, for this particular orientation, the two velocities are identical and equal to

$$V_{1.2.} = \frac{\sqrt{c_{44}}}{\rho} \tag{6}$$

where c_{44} is the shear modulus for an aluminum single crystal and ρ is the density of aluminum.

Thus, since $(V_1 - V_2)$ is zero, theoretically there is no $\triangle V/V$ due to preferred orientation in 6061–T6 aluminum. Since residual stress is the only other major source of anisotropy in cold-rolled aluminum, it is concluded that the observed

Rolling direction
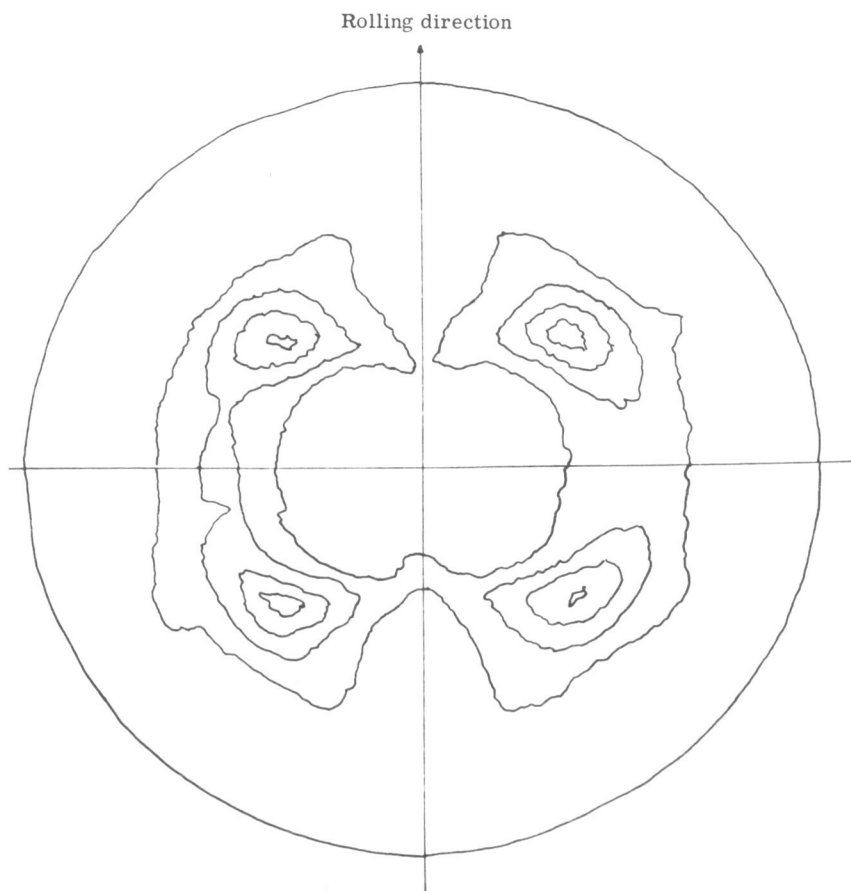
FIGURE 9.—Typical pole figure for cold-rolled 6061–T6 aluminum.

TABLE I.—*Calculated Stresses in Cold-Rolled 6061–T6 Aluminum*

Cold work, percent	Initial birefringence, $(\Delta V / V \times 10^3)$	Calculated stress,* psi
0	1.688 ± 0.062	6 750
20	2.239 ± 0.213	8 960
36	2.544 ± 0.312	10 176
50	3.364 ± 0.408	13 456

*The difference between the residual stress components along the rolling and transverse directions.
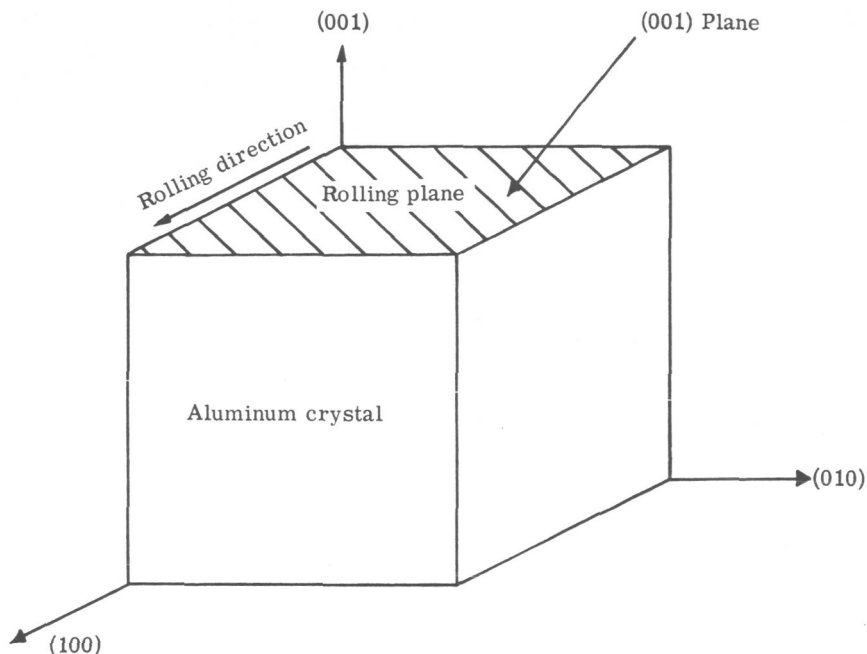
FIGURE 10.—Basic orientation produced in cold-rolled 6061–T6 aluminum.

initial birefringence in the 6061–T6 aluminum is due to residual stresses. Additional work with 1100–0 aluminum reinforced this conclusion.

By using the curves shown in figure 6 to determine the change in $\triangle V/V$ with stress, table I was constructed to illustrate the residual stresses which would exist if the birefringence were only a function of stress. The stresses listed in this table are the differences between the residual stress components along the rolling and transverse directions of the specimens, since the values of $\triangle V/V$ represent the differences between the wave velocities in these directions.

CONCLUSION

A technique which is being investigated for the analysis of residual stresses in engineering materials and structures has been described. To date, the technique has been used only in the laboratory on specimens whose microstructures are well-documented. Before field use becomes practical, several problems which involve transducer coupling and surface preparation must be overcome. In addition, it should be emphasized that at this time the technique is capable of providing information only on the difference between the principal residual stresses, and not on the absolute magnitude of these stresses. However, it is not unreasonable to assume that with further development these problems will be resolved, and the shear wave birefringence technique (or a modification of it)

will emerge in the near future as a powerful tool for the nondestructive measurement of residual stress. The application of such a tool will not only insure greater reliability of space vehicles, but will also contribute to the construction of safer airplanes, cars, bridges, and other structures.

Ultrasonic Measurement of Stress in Aluminum

E. C. McKANNAN

The need to measure the state of stress of a material after basic metal forming, machining, fabrication, assembly, and use is a matter of utmost importance affecting national prestige and safety. This fact is illustrated by two classic examples. During the first mass production of welded cargo ships in 1943, a major problem was experienced with large residual stresses and with stress risers near the hatch corners which combined to cause catastrophic cracking in rough seas. The solution to this problem was of major concern to the safety of our overseas supply lines during that crucial period. The demise of the Comet commercial jet airliner is the second example. Although the Comet was the first of its type to be flown, it experienced several disastrous crashes as a result of fatigue combined with stress risers which were not recognized at the time. By the time the problem was understood and corrected, several American aircraft corporations had many planes in the skies. The Comet lost its position in the world aircraft market, and the nation of Great Britain sorely missed the prestige and revenue. Both of these problems were solved by large research efforts after it was too late to be of any help. Hence, vital issues have rested on the need to measure stress in fabricated materials quickly and easily.

It is possible to measure the applied, or external, stresses in a system by the use of models. It is sometimes possible to estimate the residual stresses by cutting a cross section from a component, allowing that cross section to deform, and calculating the stress which caused that deformation. The latter method, however, is useful only for simple cross sections of components which can be destroyed. A nondestructive X-ray diffraction method is available for materials which produce sharp X-ray diffraction lines. Unfortunately, many aluminum alloys and some highly quenched, tempered steels are not sensitive to this method because they produce broad diffraction lines. In addition, X-ray diffraction techniques are more difficult to make than the ultrasonic techniques which will be described. The measurement of stresses in the bulk of a body by the birefringence of ultrasonic shear waves has been discussed in a related paper by R. L. Gause (ref. 1). However, in this paper, the measurement of residual stresses in the surfaces of materials will be emphasized because many of the effects of fabrication, application of loads, and environment occur at the surfaces of materials.
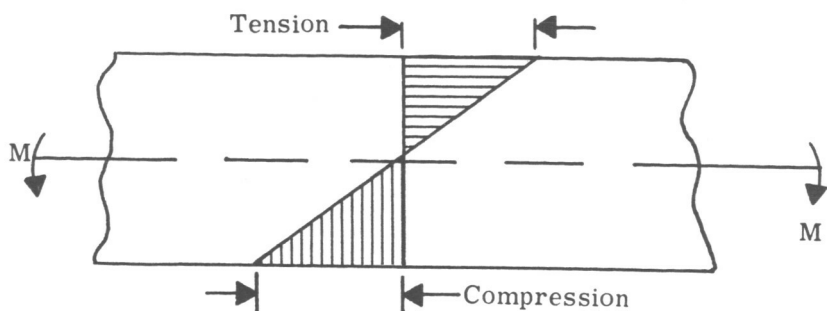
RESIDUAL STRESSES

Residual stresses were defined in the paper by R. L. Gause (ref. 1) as those stresses which exist in a body of material when it is free from external restraints. These stresses arise from uneven changes in shape during basic metal forming processes such as rolling, drawing, forming, and extrusion. A second cause of residual stresses is the machining of materials. Cutting and grinding operations strongly affect the state of stress at the surface, leaving unwanted tensile stresses in the direction of the tool marks even in the smoothest surfaces (ref. 2). Assembly operations which may leave mismatches in joined materials which are forced together and press fits which are often desirable for precision assembly are a third cause. A fourth cause—welding—leads to thermal expansion, contraction, and phase changes in the welded area. These changes leave a condition of stress different from that of surrounding materials, thereby resulting in differential stresses. A fifth cause—heat treatment and subsequent quenching—usually leaves large compressive stresses in the surface of materials. This is primarily a result of the fact that the outside of a component, when rapidly quenched, cools and contracts before the interior. Although these stresses may be desirable, they must be planned for in advance. Finally, stress risers cannot be eliminated in the design of assemblies and systems. Such things as hatches, ports, inlets, and outlets are required in almost every practical shell, tank, or fuselage; however, these stress risers multiply the effects of the local residual stresses. Hence, it can be seen that residual stresses can be placed in a material during normal operations from initial metal forming to the final use of the material.

FATIGUE AND STRESS CORROSION

The environment into which a system is placed interacts strongly with the state of stress at the surface of the material even before external forces are applied. Fatigue and stress corrosion are dependent on environment.

Fatigue, which may generally be defined as the deleterious effect of cyclic stress on a material (ref. 3), is a two-step process. It involves, first, the initiation of cracks on a microscopic scale in crystals or grains of the material in which highly localized stresses have caused large deformations or in which easy slip planes just happen to be alined with the applied stress. For common types of loading, such as bending and torsion, the failure usually starts on the surface with the maximum tensile stress (fig. 1). Second, those microcracks are propagated into surrounding crystals and finally throughout the material by the continued application of cyclic stresses. Both steps of the process are accelerated at higher stresses, and residual stresses in the material merely add to the amplitude of applied stresses on any individual crystal.

It is important to distinguish between macroresidual stresses and microstresses. Macroresidual stresses, which vary throughout the material in a smooth continuum over many grains, can be measured. Microstresses, from which a crack may start, act over dimensions on an atomic scale within one grain or crystal. They

Applied stress
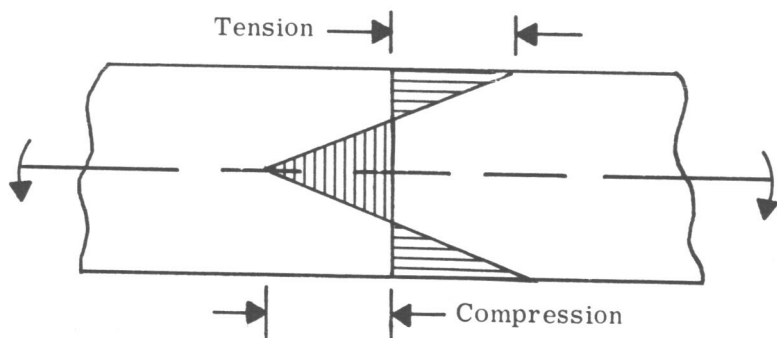
Residual stress
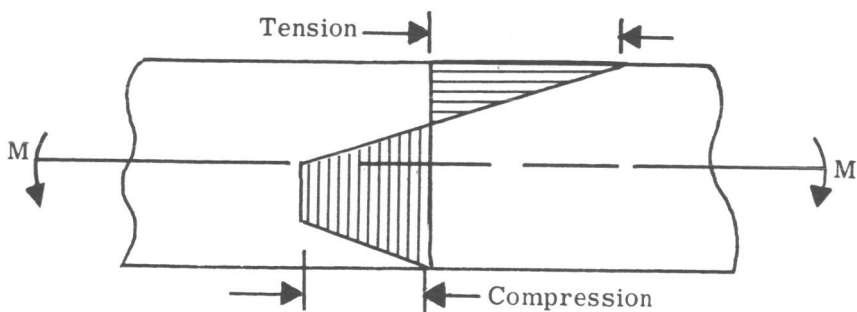
Superimposed stress

FIGURE 1.—Types of stress.

may be caused by the pileup of dislocations or imperfections in the crystal lattice which act in unison to deform the crystal. Treatments such as surface hardening, nitriding, or carburizing, which tend to produce residual compressive
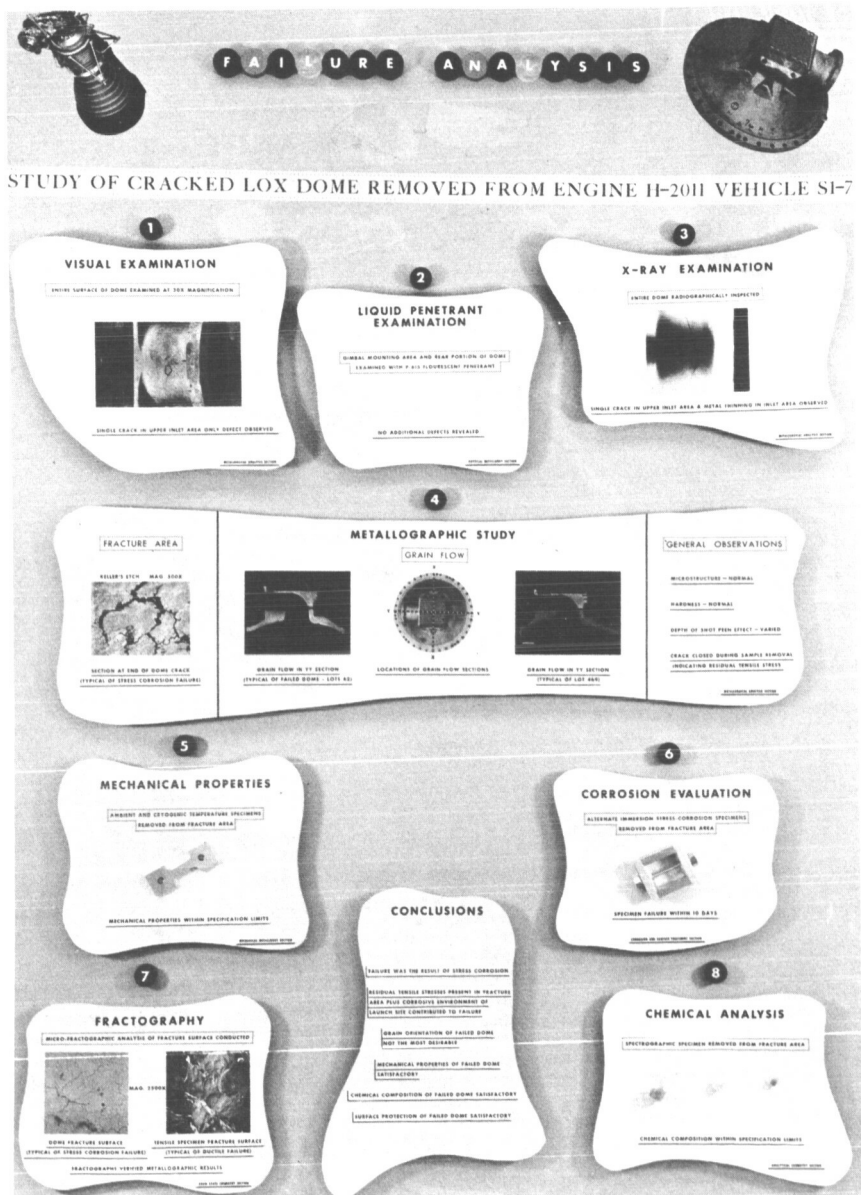
FIGURE 2.—Failure analysis history.

stresses in the surface and to inhibit the formation of microcracks, improve fatigue resistance.

Stress corrosion cracking may be defined as the combined action of corrosion and static surface tensile stresses (ref. 4). It is important to differentiate between stress corrosion cracking and the mere acceleration of corrosion with stress. In the latter case, the effect of stress ruptures the corrosion-weakened crystal boundaries and promotes deeper penetration of the corrosive environment into the material. Stress corrosion cracking is a form of localized failure in which little or no significant attack occurs in the absence of stress and is characterized by brittle fracture in an otherwise ductile material. The cracks propagate in a plane perpendicular to the direction of the stress. Figure 2 illustrates the analysis of a stress corrosion failure in a dome (ref. 5).

Since maximum stresses in a component under bending or torsional conditions are in the surface and since residual stresses from fabrication and environmental effects act at the surface, it is of utmost importance to measure the stresses in the surface of the material.

ULTRASONIC SURFACE WAVES

Following the success of the use of birefringence of ultrasonic waves in measuring the stresses through the bulk of materials, ultrasonic surface waves were applied to measure the stresses in the surface. As shown in figure 3, ultrasonic surface waves may be compared to transverse shear waves as opposed to longitudinal or compression waves which transmit sound through a gas. Transverse waves cause particles in the solid to vibrate perpendicular to the direction of propagation; whereas, in longitudinal waves, the particles of matter vibrate in the direction of the propagation of the wave. Surface waves act very much like

Ultrasonic surface (Rayleigh) wave

Ultrasonic compression longitudinal wave
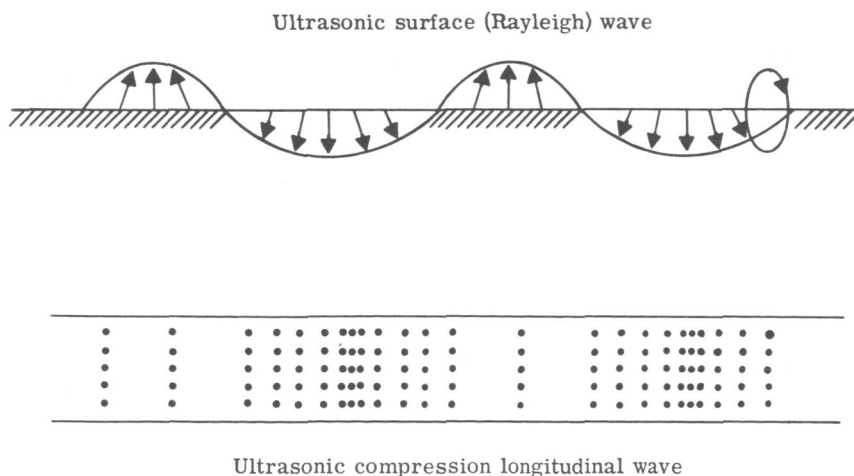
FIGURE 3.—Comparison of transverse and logitudinal waves.

Depth of penetration

Distance below surface (wavelengths)
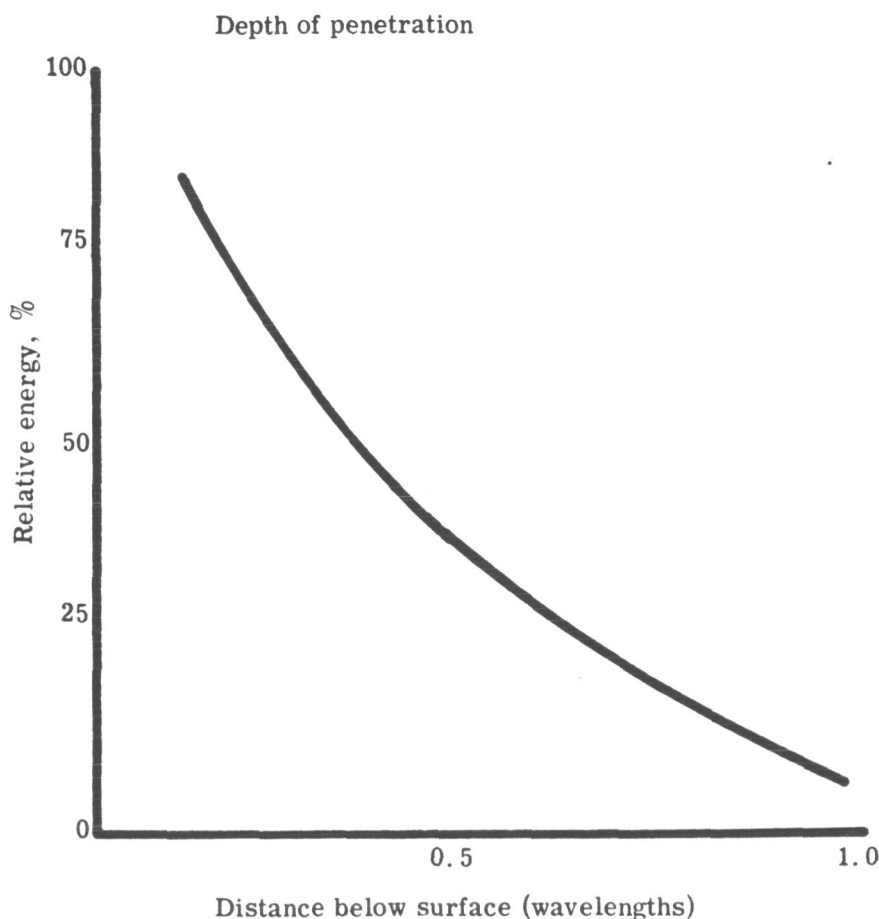
FIGURE 4.—Wave amplitude vs depth.

gravitational waves on water surfaces. The amplitude of vibration decreases exponentially with the depth beneath the surface. Figure 4 shows that at a depth of one wavelength the amplitude is less than one-tenth that on the surface. The velocity of ultrasonic surface waves is independent of the wavelength or applied frequency of the wave; therefore, it is possible to choose the frequency for purposes such as the depth of penetration of the stress to be measured. The velocity of ultrasonic surface waves is dependent only on the properties of the material through which it is passing. The velocity is dependent on the shear modulus of the material and inversely upon the density; hence, it can be directly related to the elastic properties of the material.

This relationship is expressed as

$$V \sim A\sqrt{G/\rho}$$

where

 V velocity
 A a constant
 G shear modulus
 ρ density

Small changes in the velocity of surface waves can be measured with much more precision than the decay of amplitude of the waves; therefore, the most precise measurements are made by comparing velocities. Usually the time to traverse a given path in an unknown material is compared to the time to traverse a similar path in a stress-free material. Hence, any measured velocity change is known to be dependent upon a change (that is, deformation or strain) in the path traversed in addition to the expected dependence on stress. However, these deformations can be measured separately and can be compensated for when measuring stress.

TEST METHODS FOR SURFACE MEASUREMENTS

To measure a stress of about 10 000 psi, the required change in relative velocity is on the order of one-tenth of one percent (ref. 6). Such accurate measurements were first achieved by the use of interferometric techniques borrowed from optics. The physical quantity actually measured with an interferometer is the wavelength. From the value obtained for wavelength in the measurement of frequency, the velocity can be calculated using the relationship $V = wf$ (where V is the velocity, f is the frequency, and w is the wavelength). The interferometric technique can be used with surface measurements because wavelength can be measured directly along a surface.

A surface wave can be generated and detected by several methods, the most efficient of which is the use of an X-cut quartz crystal placed against the surface of a Lucite wedge which is cut at an angle. An X-cut crystal is one which vibra es in the direction of its smallest dimension and which generates longitudinal or compression waves. The wedge is cut at an angle so that the refracted angle of the beam generated by the vibrating quartz transducer will be 90° from the normal of the plastic-aluminum boundary or parallel to the surface. The angle, $\phi 1$, is critical for surface wave generation. The proper angle, shown in figure 5, is calculated from the well-known relationship according to Snell's Law

$$\frac{\sin \phi_1}{\sin \phi_2} = \frac{V_1}{V_2}$$

where

 ϕ_1 incident beam angle
 ϕ_2 refracted beam angle
 V_1 acoustic velocity in the plastic wedge
 V_2 acoustic velocity in the metal surface

Substituting the proper values in Snell's Law gives an angle of incidence close
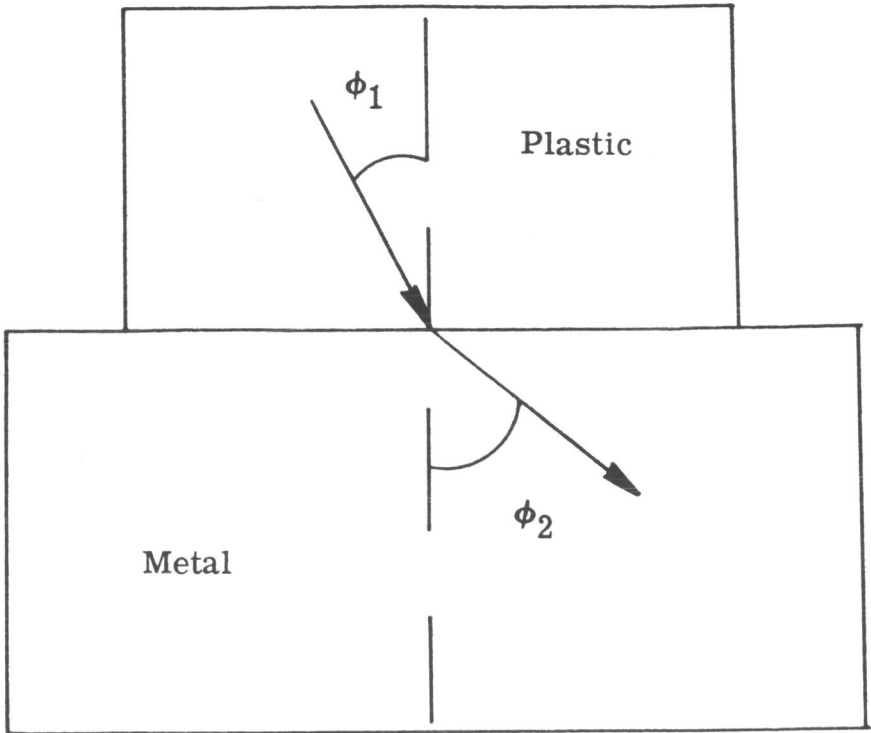
FIGURE 5.—Snell's law.

to 68° for aluminum. An identical wedge is used for the receiver crystal. The Lucite wedges are coupled to the metal surface with a liquid film to improve the contact and match impedance. A lightweight machine oil has been found to be the best couplant. To obtain wavelength measurements, a mechanically stable carriage is employed to change the distance between the transmitting and the receiving transducers, and a micrometer is used to measure the change in distance betwen the transducers (fig. 6). The difference in traverse time obtained from moving the transmitter with respect to the receiver is also measured. Unfortunately, this method is important for basic calibration, but it is restricted to very flat surfaces and is not suitable for practical measurements; therefore, several other methods have been devised.

The delay line method, which is the most practical stress measuring system evaluated to date, has all the requirements for simple, field-type measurements on fabricated materials (ref. 7). It consists of a pulse generator which puts out radio frequency pulses on the order of one per millisecond. As shown in figure 7, the pulse is applied to two different crystal senders. The first sender is on an unstressed specimen called a delay line. The distance between the sending crystal and the receiving crystal on the unstressed delay line is carefully measured. The same pulse is sent, simultaneously, to the sending crystal on the unknown
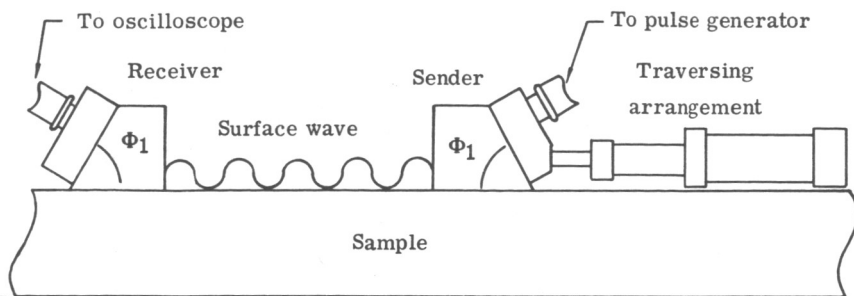
FIGURE 6.—Geometrical arrangement for the determination of surface wave velocity.
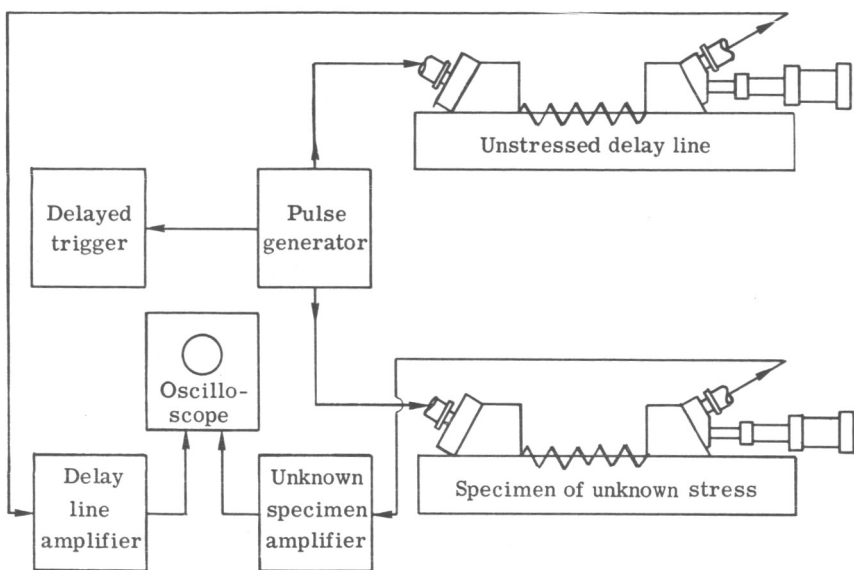
FIGURE 7.—Schematic diagram for determining delay time of ultrasonic surface waves vs stress.
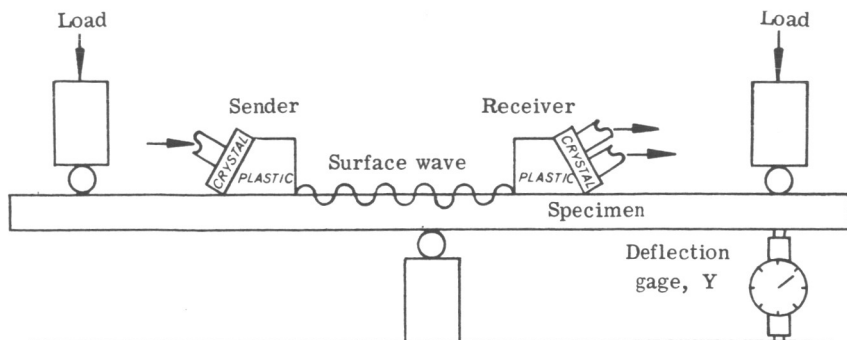
FIGURE 8.—Beam loading for determining surface stresses.

specimen. The distance between the sending and receiving crystals on the surface of the unknown specimen is carefully measured and adjusted to match the distance on the delay line. The received pulses from both the delay line and the unknown specimen are amplified and sent to an oscilloscope where they are displayed, indicating the time delay between the unstressed and stressed specimen. From this time delay and the measure of distance between sending and receiving crystals, the velocity is measured. Once the velocity over a known path on an unstressed specimen has been measured for a given alloy and condition, the delay line may be replaced by an electronically variable delay line.

There is no other method of measuring residual stresses with which to correlate or calibrate this ultrasonic method. To calibrate and to evaluate this simple technique, the unknown specimens were placed under an applied load in bending as a beam (fig. 8). It was assumed that no difference exists between the effects of residual stresses and the effects of applied stresses on a surface. The unknown specimen was bar stock which was one inch by one and one-half inches by forty-eight inches long in the as-received condition from the mill. For calibration purposes the deformation in bending was measured carefully and the maximum outer fiber stress or surface stress was calculated using the well-known beam equation
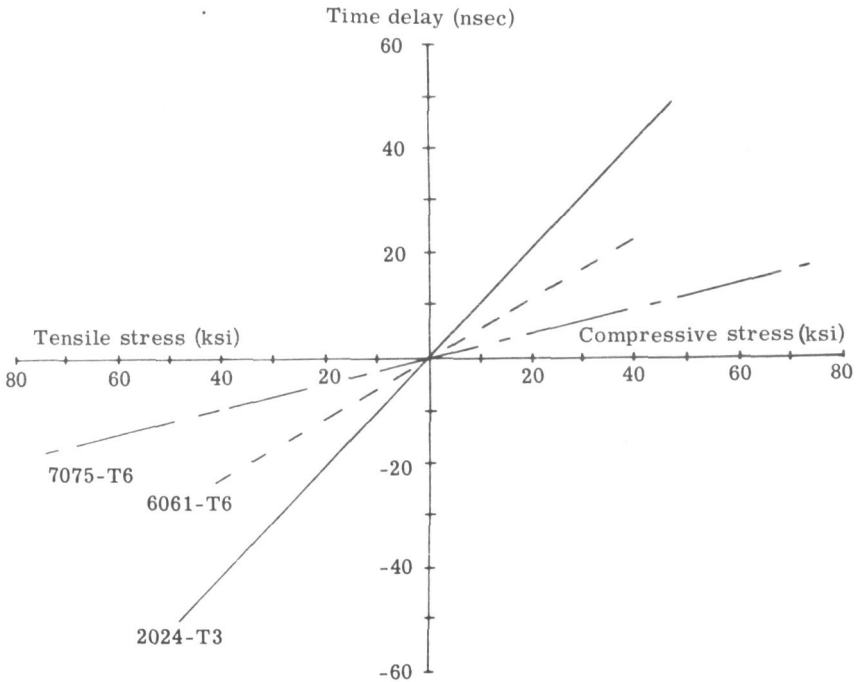
FIGURE 9.—Time delay for ultrasonic surface waves in aluminum with a frequency of 7 megahertz.

$$y = \frac{ML^2}{2EI}$$

where

y deflection
M bending moment
L length
EI flex stiffness

Data were obtained on both the tensile and compressive sides of the beam for three different alloys, 2024–T3, 6061–T6, and 7075–T6. The data (fig. 9), which were corrected for the change in path lengths due to bending, indicate a linear relationship between the time delay and the applied stress. The frequency employed was seven megacycles per second which provided a depth of penetration of approximately one millimeter. It is interesting to observe that the acoustic-stress coefficient of sensitivity of each of these alloys is different by a factor of almost five: 2024–T3 is 1.1 nsec/ksi; 6061–T6 is 0.55 nsec/ksi; and 7075–T6 is 0.24 nsec/ksi. Since it is possible to measure to 0.1 nsec, it is possible to resolve about 400 psi in 7075–T6, 200 psi in 6061–T6, and <100 psi in 2024–T3.

CONCLUSION

It certainly appears that the ultrasonic method is a sensitive and valid technique for measuring surface stresses in aluminum. Although the depth of penetration is sufficient to get far below the oxide layer, the search for any possible effects of varying the mechanical, chemical, crystalline, or electronic surface states continues. The equipment is being miniaturized so that the electronics will fit into a portable package. A small, precise transducer with a fixed distance between sending and receiving crystals (both in one housing) has been made. It is hoped that once this equipment becomes generally available and more widely applied, problems such as those which cracked ships or jet airplanes can be eliminated. Certainly, this method will provide the capability to examine the state of stress of any structures thoroughly, efficiently, and at reasonable cost.

REFERENCES

1. GAUSE, R. L.: Ultrasonic Analysis of Cold-Rolled Aluminum. Nondestructive Testing: Trends and Techniques, Proceedings of the Second Technology Status and Trends Symposium, NASA SP–5082, 1967, pp. 31–42.
2. SCHWARTZBART, H.; and SMITH, E. S.: Development of Nondestructive Testing System for Analysis and Control of Residual Machining Stresses. (Air Force Contract 33(615)–1400), Ill. Inst. Technol. Res. Inst., May 1966.
3. DIETER, G. E., Jr.: Mechanical Metallurgy. McGraw-Hill Book Co., Inc., 1961.
4. JACKSON, J. D.; AND BOYD, W. K.: Stress-Corrosion Cracking in Aluminum Alloys. Defense Metals Information Center Memo. 202, Battelle Memorial Inst., Feb. 15, 1966.

5. CATALDO, C. E.: H–1 Engine LOX Dome Failure.   NASA TM X–53220, 1965.
6. CHAPMAN, J. R.: Velocity-Stress Dependence of Surface Waves in Aluminum Utilizing Ultrasonic Techniques.   Thesis, Vanderbilt Univ., Aug. 1962.
7. BENSON, R. W.: Development of Nondestructive Methods for Determining Residual Stress and Fatigue Damage in Metals.   NASA contract NAS8–20208, R. W. Benson, Assoc., Inc., June 1966.

Automated Ultrasonic Scanning by Triangulation Method

Robert L. Brown

Nondestructive tests have always had two purposes—to accept the good and to reject the bad. Perhaps the oldest test, other than visual examination, is sonic testing, which still remains valuable and valid in noncritical applications. This test, unfortunately, lacks sensitivity.

If a flaw is to be detected by its influence on frequency and resonance, the flaw must be large in relationship to a wavelength of the frequency generated. Middle "C", which is in the midrange of frequencies to which the human ear is most sensitive, has a wavelength greater than seven feet in the common engineering metals. Since rejection limits for flaws in critical applications are normally specified in thousandths of an inch in cross section, it is not possible to detect flaws by sonic testing using audible frequencies.

Progress toward the solution of this problem began with the introduction of ultrasonic testing. Equipment capable of generating and detecting sonic frequencies in the millions of cycles is standard; with these frequencies, wavelengths in the thousandths of an inch make it possible to meet any reasonable limitation on flaw size. It is common practice to operate ultrasonic testers at a level of sensitivity that allows the identification of flaws smaller than the rejectable size. This degree of detection is necessary in establishing confidence that no rejectable flaw will be undetected. This capability has made ultrasonic testing a recognized nondestructive testing method.

The major handicap in ultrasonic testing is scanning speed, since pulse rate must be slow enough to be clearly differentiated by electronic means from shot-type noises, and travel speed must be slow enough to allow interrogation of each flaw by at least three pulses; even so, it takes an almost ideal system to be consistently free of phantom indications. In spite of these handicaps, ultrasonic testing is very rapidly expanding in applications and uses; however, it is felt that this high degree of acceptance of conventional ultrasonic testing methods may lead to a tendency to disregard the possibilities of the unconventional.

ACOUSTIC SPECTROMETER SYSTEM

Recently, it was discovered that a West Coast company was developing an ultrasonic testing system unique in many important concepts.   Although new to ultrasonic inspection devices, these concepts were well-established in other applications and would greatly facilitate inspection of many of the welds in the Saturn V system.   This led to a contract for a system specifically engineered for space vehicle applications.   The system, known as the acoustic spectrometer, is now being evaluated to further determine its capabilities and limitations.

Figure 1 shows the equipment for the acoustic spectrometer system set up in the evaluation laboratory.   A panel, which has a configuration duplicating a section of the 33-foot diameter S–IC fuel tank, is shown in place.   The required tooling is being attached to the test panel.   A horizontal weld extends across the top third of the panel, and a vertical weld is located at the center.   These welds contain flaws which have been precisely located and evaluated by X-ray and conventional ultrasonic methods.   This simulates a test that would normally be performed on the cylindrical tank section.   Prior to being welded to the bulkhead assemblies, all welds in the vertical and circumferential directions would be inspected, repaired if necessary, and accepted, without moving the ultrasonic transducers from their locations.

As a necessary consequence of the new approach taken with respect to data acquisition and analysis, the acoustic spectrometer is much more complex than
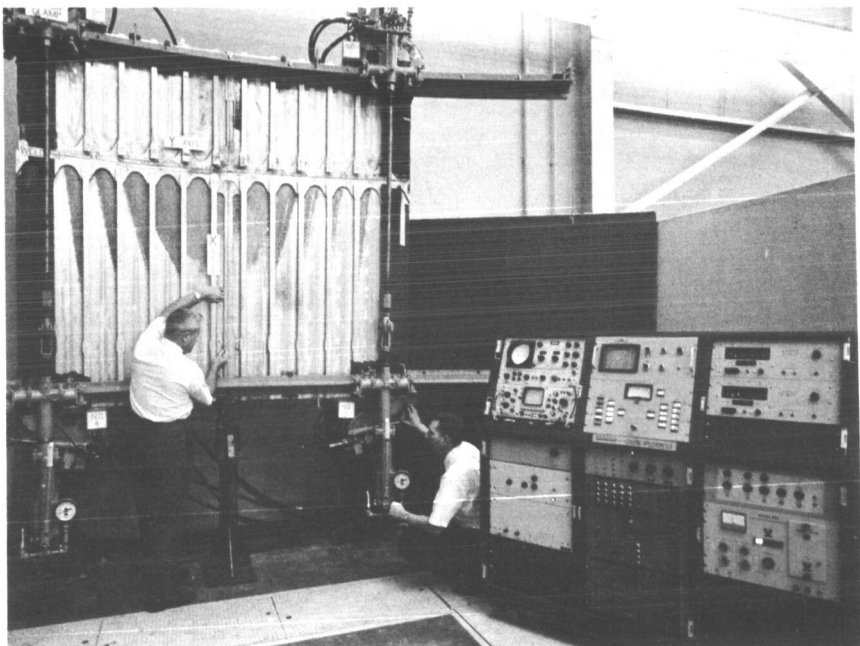
FIGURE 1.—Ultrasonic testing equipment.

the conventional ultrasonic tester. This increased complexity is reflected in the console shown in the right-hand corner of figure 1.

The acoustic spectrometer can be classified as a pulsed system in which one transducer acts as a transmitter and one or more transducers receive information in the form of ultrasonic energy scattered from flaws. All transducers (this system has provision for five) are identical and can be programmed to act interchangeably as transmitters or as receivers. The system does not utilize the "single crystal" mode of operation in which one transducer acts as both transmitter and receiver.

Instead of shock excitation by single pulses, the transducers are driven by widely spaced pulse bursts which are variable in amplitude, duration, and spacing. The burst frequency is independent of pulse spacing. The fact that the duty cycle is low (always under one percent) permits 1500 volt excitation without harm to the titanate transducers. The resultant highly damped wave train of ultrasonics is at the frequency of the burst, which is tunable over a wide range. This ultrasonic energy is fed into a system of acoustical lenses and directors where it is narrowed into a highly columnated beam inside an acoustic waveguide. This unit is coupled to a wave director so that it may be rotated around a quadrant of a circle by a hydraulic servo. The unit then transmits a narrow beam of sound into an attached plate, which acts as a highly directional, rotatable acoustic antenna and which has the same directional pattern in either receive or transmit modes. As an aid to visualization, the terms "transmitted" and "received" beams are used as a convenience in working with this equipment.
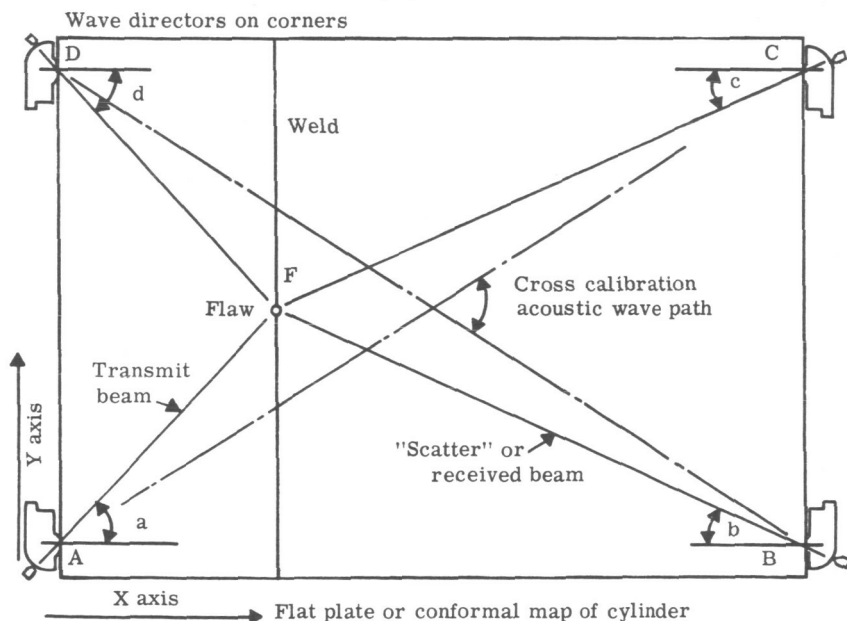
FIGURE 2.—Multiple wave directors.

Figure 2 is a sketch of a typical setup using four transducers. The sonic ray traces are sketched in to illustrate the triangular pattern of distances and angles which the computer solves in locating flaws. Positioning of the transducers is important, because the computer's calculations for locating flaws is based on the accuracy of the base distances from which the locations of the intersections of the transmitted and received beams are computed.

Oscilloscopic studies indicate that the shell is shock excited into compression waves, resonant in the thickness mode—symmetrical Lamb waves—and the conversion is highly efficient if the input ultrasonic excitation frequency approximates the resonant frequency of the plate thickness. The particular shell panel which is presently set up in the acoustic spectrometer responds to the following: Burst frequency, 2.32 megacycles; burst width, 150 microseconds; bursts per second, 150; and peak excitation to the transducers, 1000 volts.

The wave directors are coupled into the shell by soft metal shims under high compression which so effectively bridge the gap between plate edge and waveguide that the acoustic impedance is negligible. This coupling transfers perhaps ten times the sonic energy of a fluid. The clamping force is obtained from hydraulic actuators which are preset to exert the correct pressure.

The control and display functions of the acoustic spectrometer system, as well as a transducer and its functional parts, are shown in a block diagram (fig. 3).

FIGURE 3.—Block diagram of the acoustic spectrometer system.

The heart of the system is a small analog three-channel computer, each channel identical in its circuitry. The transducer-to-transducer distances are manually set into its input as voltages taken from precision potentiometers. The transducer angle positions required to calculate the X and Y coordinates of the intersect point of the transmit and receive beam are controlled by voltage feedback from tangent potentiometers attached to the pivots of the wave directors.
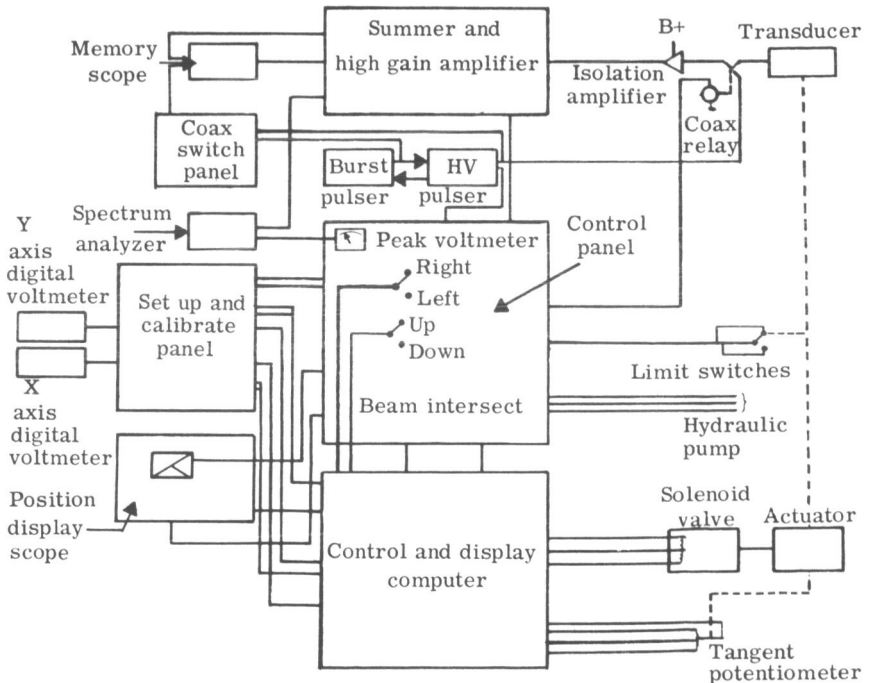
The computer continuously solves the equations of position for all transducers and separately feeds this angular information into the servos on each transducer. Each servo rotates its transducer to an angle which gives an output voltage on the waveguide tangent potentiometer that, fed into the computer, satisfies the equation of position that the computer is continuously solving.

Since all active transducers are positioned by their independent computers, all transmitted and received beams remain pointed at the calculated intersect point. The computer's calculated coordinates of this point are read out by a pair of digital voltmeters as X and Y distances in inches and decimals of an inch. The "scatter" which carries useful information originates at this intersect point. A toggle switch, which has four independently closed positions, switches driving voltages to the appropriate circuit to move the intersect in the direction—$\pm X$ or $\pm Y$—indicated by the position of the handle. The motion is constrained by the computer to move in the X or Y directions only. No combination of these motions is possible; however, combinations of sequences of X and Y motion allow all areas to be covered to any degree of thoroughness required. This constraint is a great advantage when welds, such as the S–IC circumferential welds, lie completely in the X or Y direction. It is possible to steer by sequential moves in X and Y to the correct starting point as shown by the coordinates displayed by the digital position indicators. The switch can then be closed to the required directions; the computer will steer the intersect along the weld until the limit of the scan is reached. Preliminary indications are that error in angle is less than 1° in this directing system.

A second position indicator in the form of a cathode ray oscilloscope is provided at the top of the center panel. The oscilloscope displays the ray paths followed by the ultrasonic beams in the structure as generated by those transducers active at the time of display. This display allows visualization of directions, travel, and position, all of which are difficult to handle without such an aid. A coordinate grid on this readout giving distances in feet is a convenience much used during evaluation. Since the display is, for all practical purposes, a real time readout, it is the preferred means of monitoring the ultrasonic system, while the operator is "steering" by the four-way switch.

Although intersect point is mentioned frequently in this paper, it must be made clear that the word point is a convenience and is not intended to imply that a point can be resolved. A flaw such as a small round pore can be located within a small circular area, which is called a "limit of resolution" for the system, but it is not possible to locate to any tighter limits than the circle. At present, this circle appears to be approximately one inch in diameter at a distance

of ten feet from the transducers. When, as in this case, the acoustic spectrometer is being used solely to evaluate welds which may contain only an occasional rejectable flaw (no located flaw is outside the weld metal), this error is small enough that no corrective action is required to verify the exact location of the flaw. Should this action be required, a conventional portable ultrasonic tester will readily pinpoint such flaws.

An important feature of the system is a time-dependent gate which can be set to receive scatter from the intersect point, but which can also block scatter from other parts of the plate. This helps keep the background noise in the system suppressed and raises the intelligibility of the flaw signal.

Flaw analysis is an integral part of flaw detection, and the acoustic spectrometer is equipped with several devices which aid in this important function.

Since the system is intended for highly automated operation, primary reliance in flaw detection is on a spectrum analyzer. The spectrum analyzer reduces the flaw return information to a voltage which is fed into a peak-reading voltmeter. The peak voltage from the flaw signal return is compared to a reject level which is preset at the smallest rejectable flaw size. The system will indicate each detected flaw which has a cross section larger than acceptable.

In evaluating, the operator analyzes each flaw by consulting a visual display presented on a cathode ray oscilloscope for confirmation of the automatic flaw signal indication. The oscilloscope presents the conventional time base versus amplitude display similar to an A-scan device with the exception that the time gate only allows the first reflection or scatter signal to be displayed. The time gate is opened enough to allow the conditions along the weld to be shown on the oscilloscope. The analysis is a function of the operator's skill and experience in interpreting the changes in the pattern as he swings the intersect point through flaws. This analysis is then applied to evaluation of the reject circuitry and the system as a whole.

The acoustic spectrometer system holds promise as the forerunner of a new type of nondestructive test equipment of wide potential applications. Equipment closely related to the acoustic spectrometer can perform such tasks as routine ultrasonic examination of plate in the rolling mill. Perhaps with tape input and recorder outputs, such equipment could keep watch for hull damage on ships and monitor reactors where severe or dangerous operating conditions exist, and could perform a nondestructive testing task on a routine, repetitive basis which is impossible with conventional ultrasonic testers.

Ultrasonic Emission Detector Evaluation of Strength of Bonded Materials

James B. Beal

The needs of the aerospace industry have rapidly accelerated the use of adhesive bonding in structural applications. Composite structures, particularly those using honeycomb, are largely adhesive bonded. The major problems posed by the use of composite structures have been the variability of bond strengths obtained and the lack of suitable nondestructive equipment for determination of bond strength. The exact causes of strength variations are difficult to establish, since bonding problems can be related to every phase of bonding, i.e., design deficiencies, corrosion, machining errors, improper processing, misuse or handling, fabrication error, and material defects. Proper use of nondestructive testing techniques, however, can effectively reduce these problems.

DEVELOPMENT OF NONDESTRUCTIVE TECHNIQUES FOR DETERMINING BOND STRENGTHS

In June, 1964, a contract was initiated by Marshall Space Flight Center with General American Transportation Corporation to develop a nondestructive method for evaluating adhesion bond strengths in composite adhesive bonded structures. Although acceptable methods for detecting bondline voids, debonds, bondline variations, and porosity were available at that time, there were no nondestructive techniques which would measure adhesion bond strengths in all adhesives specified for this program, i.e., FM–1000, HT–424, Narmco 7343/7139, and Metlbond 329. These adhesives were used to make specimen bonds of aluminum to aluminum, aluminum facesheets to aluminum honeycomb core, and aluminum facesheets to phenolic core. This program, which consisted of three phases, was completed in September, 1965, with a demonstration of ultrasonic emission detection equipment for determining adhesion bond strength in stressed composite structures.

Phase I.—The first phase of this program was a literature survey of the state-of-the-art of nondestructive testing. This survey revealed that the number of papers published on the subject of bond strength evaluation (for the adhesion strength of the bondline) is relatively low. Available papers are concerned with particular equipment for detection of voids, delaminations, porosity, bondline variations, and the cohesive strength of some adhesive systems; however,

this equipment is inadequate for detection of weak bonds in adhesion. It was determined that the need existed not only for a bond strength evaluation system, but also for a method of producing consistently poor adhesion bonds of predictable values in order to adequately evaluate equipment bond strength indications.

Adhesive manufacturers and users agree that very strict controls are necessary in all adhesive bonding processes as well as in the numerous associated fabrication variables. Critical considerations for a good bond include the formation of a strong wettable oxide surface on the metal to be bonded, proper wetting of the surface with the adhesive, elimination of contaminants, and control of the fitting, temperature, and pressure of the bond. The survey indicated that the majority of nondestructive test instruments in use fall within two categories: (1) vibration inputs to structures by the use of resonant, sonic, and ultrasonic frequencies, and (2) structural proof stress tests, which consist of internal pressurization, external tension stress induction, and limited destructive shear.

Phase II.—The second phase of this program was a study into the nature of bonding to determine what properties affect adhesion bond strength and to determine the nondestructive test technique best suited for the measurement of strength properties.

The apparent failure of a bond in adhesion is attributed to such causes as surface contaminants of a low cohesive force or to chemical compositions which weaken the layer of adhesive near the surface. The cause of weak bonds does not appear to be the weakening of the basic bond forces, but rather the failure to form the bond in the first place. Thus, the strength of the surface layer of the adhesive is more important than the nature of its bonding forces. Since small areas of contamination can cause stress risers that propagate cracks parallel with and close to the bondline, any contamination affecting the strength of the first layer of adhesive is very important. If the contamination and discontinuities in the bond layer cause stress risers and contribute to the failure of a bond, it is possible to have complete adhesion over the greater portion of the area being interrogated and still have a weak bond.

It was assumed that detectable sonic and ultrasonic signals would result from stress concentrations in contaminated areas of the samples before the stressed bondline' reached the point of failure. Noise emission from stressed areas would result as the weak bonds failed selectively in the areas of highest stress. The possibility of small contaminated areas affecting the total bond strength indicated that some method of stressing the bondline to fail the weak areas would be necessary. Because the small contaminated areas would be exposed to very high stresses when the bondline was loaded, the areas would emit sonic and ultrasonic signals which could be detected by sensitive listening devices long before the complete bondline reached its ultimate strength. This phenomenon would provide additional data during proof tests of edge-sealed sandwich structures containing perforated honeycomb core and during static load tests of adhesive bonded brackets.

Bond stress methods considered for this program, both theoretically and experimentally, were:

(1) Rapid decompression of samples containing perforated honeycomb core;

(2) High external pressure to a vacuum cup on a bonded structure containing perforated honeycomb core which is placed in a pressure chamber;

(3) Electrical bond stress methods—a theoretical study into forces produced by stationary charges, magnetic fields, and eddy currents;

(4) Force pulses by vibration and energy transfer to the bondline—a theoretical study into forces producible by ultrasonics and shock wave stressing; and

(5) Mechanical methods by static or dynamic loading of bonded brackets or the structure.

Test techniques to be investigated for this program were:

(1) Sonic and ultrasonic emission detection of signals from failing bonds;

(2) Ultrasonic attenuation with applied stress;

(3) Brittle coatings, stresscoat, or equivalents; and

(4) Birefringent photoelastic plastic coatings.

Phase III.—The third phase of this program developed the nondestructive test method for evaluation of adhesion bond strength. In any nondestructive test system, an important consideration is the production of sample flaws. This is particularly difficult in the testing of bond strength because the flaw mechanism relationships are not clearly known. In practice, poor bonds can be caused by a failure in the cohesive strength of the bulk of the adhesive or in an adhesion failure to the faying surface. These failures occur as a result of a multitude of material and structural variations. If it is assumed that the structural materials and adhesives have suitable material properties, the unsatisfactory bonds which cause failures and which must be detected by the inspection system seem to result from:

(1) Improper cleaning and etching, which may result from contaminated cleaning and etching baths or inadequate process controls;

(2) A weak interface in the bondline, which may be present as a result of contamination such as moisture or surface oxides caused by long-time surface exposures before priming or application of the adhesive;

(3) Degradation of the adhesive material cohesive strength, which may occur adjacent to the bondline as a result of contamination of the adhesive with moisture or other chemicals or because of poor cure and fit-up practices; and

(4) Small contaminations which act as stress risers and which can cause the progression of a failure along the bondline. (The various contaminants are introduced at every stage of fabrication until the structure is complete.)

The above conditions must be simulated as closely as possible in order to produce suitable imperfections affecting bond strength.

Attempts to simulate understrength bonds produced a successful method—the photomicroflaw technique—which was used for controlling bondline strength of

test specimens. Other methods of bond contamination which were investigated, but which were found unsuitable because of lack of predictability, were:

(1) Exposure of facesheets to water solutions;

(2) Exposure of facesheets to oils and greases;

(3) Variation of facesheet cleaning methods;

(4) Exposure of cleaned, protected facesheets to long-time storage conditions; and

(5) Partial cure or aging of the adhesives.

PHOTOMICROFLAW TECHNIQUE

The photomicroflaw technique involves coating the surfaces of specimens to be bonded with a photosensitive emulsion and exposing the surface to an intense light source through a grid (fig. 1). At the point at which the light is stopped by the grid, the emulsion is washed away by the developer. Photographer's "screen-tints," which are size- and density-controlled dots on a polyester film base, are used for the grid. This satisfies the need for simulating poor bond strengths through controlled surface contamination.

The importance of proper process control during bonding operations and the effects of bondline contamination on bond strength are illustrated in figure 2. The fact that adhesive bond strength drops of 25 to 38 percent occur when a surface to be bonded is uniformly degraded by 10 percent contamination indicates, as expected, that the higher the bondline stress, the more effect a small defect, debond, or weak bond can have as a stress riser. This fact significantly illustrates the need for contamination control in the process of fabrication; therefore, components should be assembled as soon as possible after the completion of the cleaning operation. A 30 to 40 percent reduction in the bond strength of cleaned facesheets, which were protected against surface contamination and stored for one month prior to test sample preparation with FM–1000
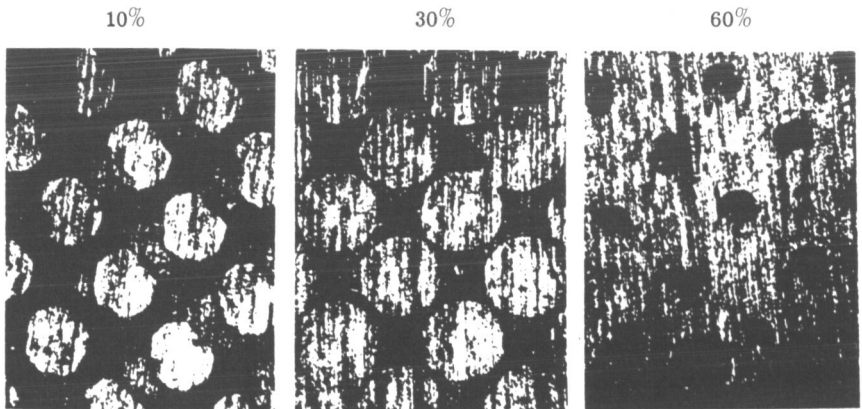
10%   30%   60%
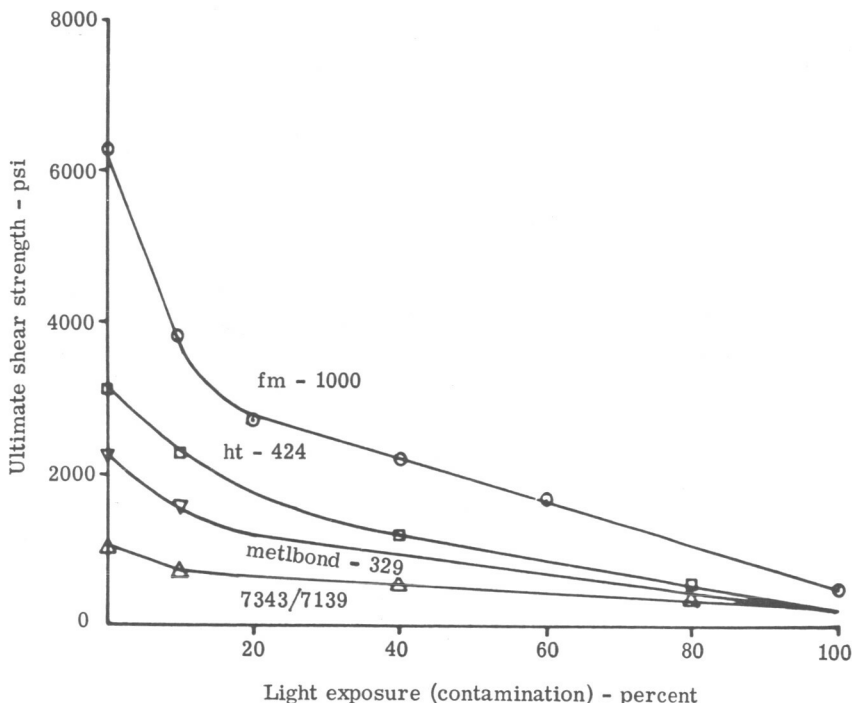

FIGURE 1.—Contaminated surfaces.

FIGURE 2.—Photomicroflaw control of bond strength with lap shear samples.

adhesive, was noted. This further emphasized the rigid holding time and handling requirements necessary for cleaned parts prior to adhesive application, assembly, and cure.

EQUIPMENT EVALUATION TESTS

Specimens with bonds of known strength were required for suitable evaluation of nondestructive test equipment developed for this program. Confidence in the production of specimens with controlled bond strengths required destructive tests in accordance with established specifications. All specimens for this program, including lap shear, drum peel, and flatwise ring tension for metal-to-metal tests, were prepared in accordance with military specifications for bonded structures. Adhesion bond strength degradation was attempted by environmental exposures of samples to a temperature of 500° F for two hours, a temperature of −308° F for two hours, and vacuum exposure to 8.0×10^{-7} torr. No degradation of bond strength was discernible by either nondestructive or destructive testing.

Fabrication of Samples.—No problems were encountered in the preparation of test samples with the exception of Narmco 7343/7139. This is a two-component adhesive which requires mixing before use and which is very sensitive
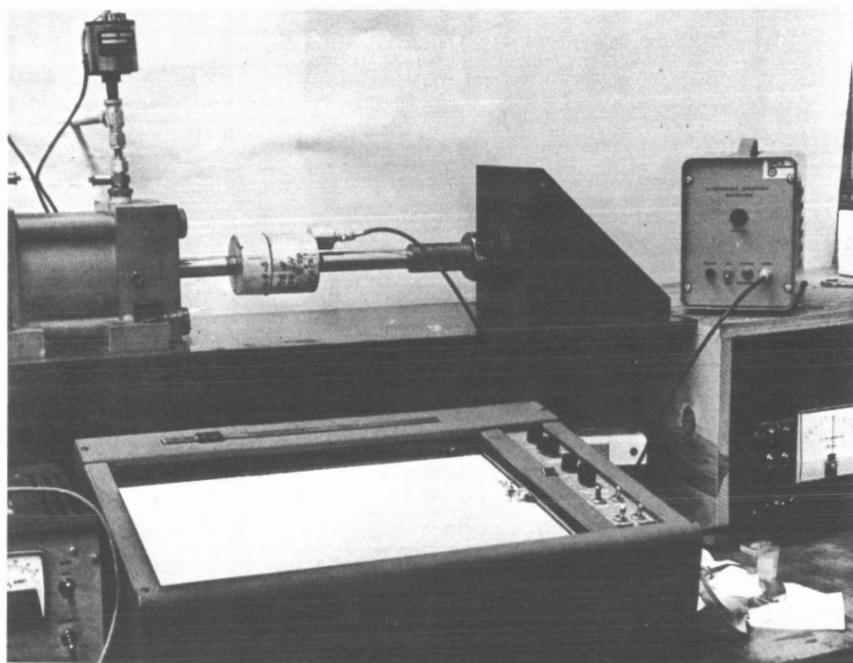
FIGURE 3.—Flatwise ring tension test setup.

to ambient environmental conditions.   Although it is the best cryogenic adhesive available, the difficulty in preparing samples with this adhesive prevented its use in the equipment evaluation tests.   The elasticity of this adhesive at room temperature also precluded testing by the developed ultrasonic emission detector. Possibly, further tests, conducted at the cryogenic operating temperatures normally associated with this adhesive, would produce useful data.

The flatwise ring tension test specimens (fig. 3), which were prepared in order to represent metal-to-metal bonded laminate construction and bonded brackets, were made from cylindrical aluminum blocks measuring three inches in diameter.   Two blocks, one of which would contain a central machined recess, were required for each test specimen.

To evaluate metal-to-metal adhesive bonds, test samples were fabricated utilizing cylindrical aluminum blocks with annular recesses for ring tension flatwise tests.   A transducer was attached to the cylindrical block by threaded stud.   The first few samples were broken to allow the operator, listening with the headphones, to become familiar with the sounds preceding bond breakage. The bond force on the remaining samples was increased to the point just prior to bond breakage, as judged by the operator.   The maximum force applied to the bond was then increased by 10 percent, and this value was considered the predicted bond failure point.

To achieve the large bond stresses required for the evaluation of the strength of sandwich bonds, a suction cup with a spring-mounted ultrasonic transducer in its center was fabricated for use in a pressure chamber. With the inside of the vacuum cup vented to atmosphere, the force on the bond is equivalent to the pressure in the chamber. The transducer in the vacuum cup transmits the ultrasonic bond stress noise emissions to the equipment. The signals are monitored, and the predicted bond failure point is judged by the operator. This type of testing is impractical for evaluating large sandwich structures. The same results may be obtained by edge-sealing the structure and installing removable pressure valves.

Application of the Equipment.—The ultrasonic emission detection equipment constructed for this program may be applied as shown in figure 4. A transducer (or microphone) capable of detecting or measuring ultrasonic vibrations is mounted on the metal surface of the test specimen in the vicinity of the bond. For a large complex structure, several transducers may be required. The transducer output is amplified and selectively filtered so that only vibrations in a particular frequency band are transmitted to the data translation system. The data translation system converts these signals to frequencies in the audio spectrum, permitting the signals from the specimen to be heard via a set of earphones or a loudspeaker. If desired, the data can be suitably processed for display on an oscilloscope or a recorder through the accessory equipment outlet on the back of the chassis.
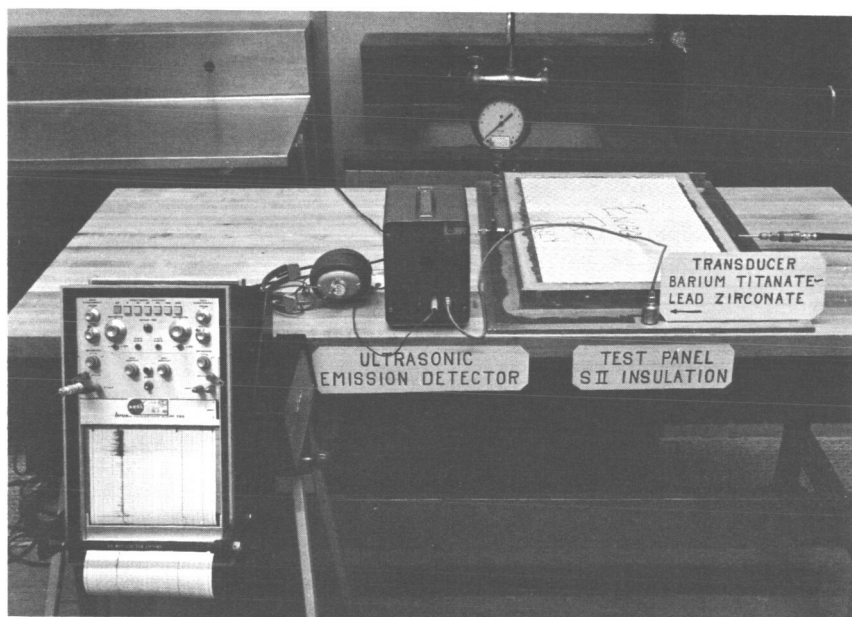

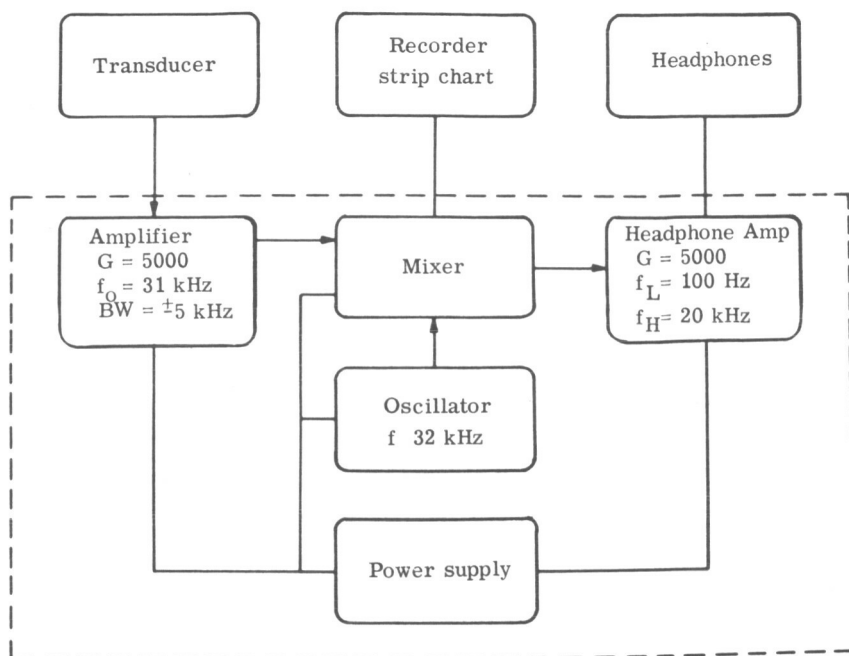FIGURE 4.—Ultrasonic emission detection equipment application.

FIGURE 5.—Block diagram of ultrasonic emission detector.

Figure 5 is a block diagram of the ultrasonic emission detector. The output of the transducer is amplified with a gain of 5000 and a restricted usable bandwidth of 5 kHz on either side of a 31 kHz center frequency; this allows energy in a frequency band of 26 kHz through 36 kHz to be amplified and processed. The input of this amplifier can handle large signals below 26 kHz without distortion so that the noise pulses, either from the test fixture or from a shop environment, which are below 26 kHz are attenuated and do not disturb the system. The amplifier output and a signal from a 32 kHz oscillator are fed to a mixer. The mixer produces both the sum and difference frequencies of the two inputs, but, only the difference frequencies are used. Since these difference frequencies are in the audible range (approximately 0 to 6 kHz), one output of the mixer is connected to a set of headphones so that the operator can monitor the noise generated by the adhesive under stress. The other output of the mixer is used to drive a recorder or other accessory, allowing the data from this equipment to be interpreted while the sample or structure is being stressed.

Acoustical Energy.—Acoustical energy in the sonic and ultrasonic region is generated when stresses are applied to materials. This effect is presently being used to detect evidences of plastic deformation in metal structures and to determine how boron filaments break up. Results indicate that adhesive ultrasonic emission above 16 kHz can be used to predict bond failure points. Acoustic

emission also occurs at lower frequencies; however, below 16 kHz, considerable noise is generated by the test fixture (fig. 6). For each adhesive tested, i.e., FM–1000, HT–424, and Metlbond 329, there was a large increase in noise above 16 kHz as the ultimate strength of the bond was approached. Thus, if a method of stressing a bond were available, this technique would provide a means of determining bond strength.
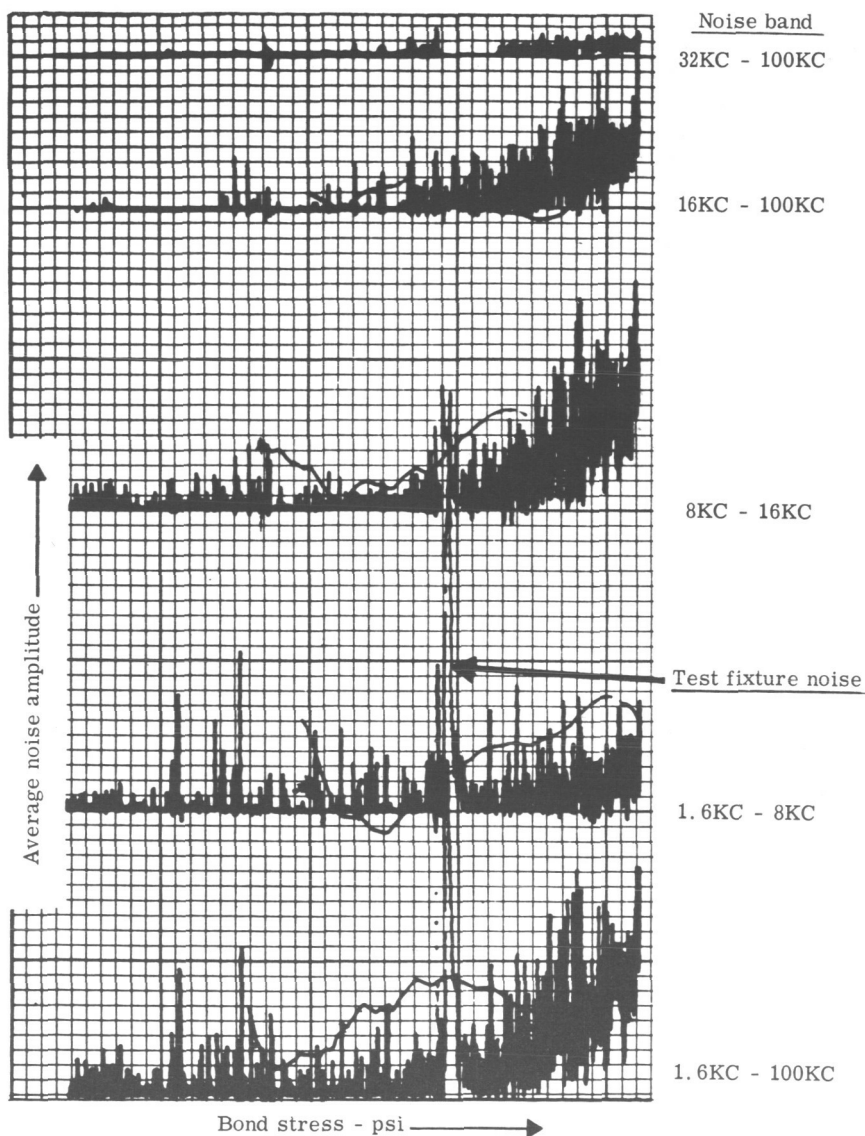
FIGURE 6.—Typical stress noise emission spectrum for HT–424 adhesive in flatwise tension and 40% bondline contamination (failure at 2260 psi).

The acoustical energy generated from sandwich or metal-to-metal bonded specimens under stress can easily be distinguished from the sounds of the test stand or environment. The adhesive produces many bursts of energy of short duration which sound like a high-pitched crackling noise. The amplitude of the emitted signals becomes significantly stronger as the yield stress is approached; therefore, the amplitude can be used to predict the yield point and ultimate strength without damage to the structure. The test results for metal-to-metal bonds presented in table I are for Metlbond 329 and HT–424 adhesives only. Strength limitations of the test fixture prevented evaluation of FM–1000, but other investigations of this adhesive verify that it has similar acoustic emission response characteristics. The prediction errors (i.e., deviation of predicted breaking point from actual failure) ranged from three to thirty percent. This range was influenced by the simultaneous evaluation of the ultrasonic emission method and the ultrasonic attenuation method on the same specimen. The predicted value of breaking point was determined initially by stressing the sample at a constantly increasing rate to the maximum bond pressure determined by the operator. From this point upward to the actual failure point, the specimens were subjected to alternate tension-compression cycling due to the dynamics required for the

TABLE I.—*Bond Strength Prediction Results* [a]

Adhesive	Contamination, %	Estimated 90% ultimate strength, psi [b]	Predicted ultimate strength, psi	Actual ultimate strength, psi [c]	Percent deviation of predicted breaking point from actual breaking point
MB–329	none	2500	2750	3750	−27
	20	2100	2310	2520	−8
	20	2100	2310	2180*	+6
	30	1600	1760	1900*	−7
	40	1400	1540	1500	+3
	40	1000	1100	1150	−4
HT–424	none	5800	6380	5400*	+18
	20	3550	3900	3200*	+22
	20	2180	2400	2075	+16
	40	2360	2600	2670*	−3
	40	3700	4070	3120*	+30

*±5% accuracy; all other ±1%.

NOTES

[a] Tests performed in flatwise ring tension between cylindrical blocks. One block recessed to form outer annulus of five square inches bond area.

[b] The point from which, based on hearing judgment, a 10% increase would fail the test sample.

[c] In alternate tension-compression cycling.

ultrasonic attenuation test; this varying stress rate influenced the actual breaking point and thereby produced large errors. The incorporation of an electronic gating circuit at the output of the detector would decrease the possibility of operator judgment error. The electronic gating circuit can be set to energize a warning lamp or buzzer when the amplitude of the average peak-to-peak noise level (determined from previous tests) reaches the point at which ultimate strength may be predicted.

Methods of Bondline Stressing.—When employing internal pressure to stress the facesheets of sandwich panels with a perforated honeycomb core, the porosity of the adhesive must be considered if the integrity of the bond between the adhesive and the facesheet is to be verified. The problem with this method of bondline stressing is that the portion of the force which is absorbed in the facesheet and the portion of the force which stresses the bond is determined by the thickness of the facesheet. With a thicker facesheet, the samples fail at a substantially higher value. Tests of sandwich panels with phenolic honeycomb core revealed that more ultrasonic energy is generated by the phenolic core than by the adhesive. Since the phenolic core was not perforated to relieve internal pressure as was the aluminum honeycomb core, the high pressure vacuum cup and other internal stress induction methods could not be used; however, external compression or tension can be used to determine when core failure begins for unperforated phenolic core sandwich panels. Further evaluation of perforated nonmetalic core sandwich structures, based upon cryogenic insulation used on the S–II stage of the Saturn V vehicle, is advised. Time and funding precluded further investigations into production results for perforated core or laminate samples. Noise emission spectrum graphs supplied by the contractor were essentially the same for both types of bonded structures. Well-bonded samples emitted little or no noise below 90 percent ultimate strength; whereas, poorly bonded samples began emitting noise at lower levels, depending on the adhesive used. Further in-house work on equipment applications will more fully develop prediction results based on structures and adhesive systems used in Saturn and subsequent programs.

ULTRASONIC EMISSION DETECTOR

The ultrasonic emission detector is applicable, nondestructively, to metal-to-metal and metal-to-nonmetal bonds in laminate and sandwich core structures. Although it is limited to some extent by configuration, materials, and stress induction methods used, this equipment does have merit.

Merits.—The ultrasonic emission detector is portable, requires no couplants, and may be used on both metal and nonmetal composites if the transducer can be mounted on the bonded metal surface. The equipment, exclusive of accessory recording equipment which is standard laboratory supply, costs only approximately one thousand dollars per unit and requires nominal skill for operation. The unit is capable of detecting low bond strength. When concentrated

stresses sufficient to cause limited failure occur in defective areas, the noise emission in most adhesives is large enough for determination of the ultimate bond strength or bond quality. Because tiny areas fail in the weak bond locations, the weaker the bond, the more noise emitted for a given stress. The total amount of noise emitted may, therefore, be equated to an indication of bond quality. Some examples of the multitude of material and structural variations which affect bond strength and which may produce noise are voids and porosities, inadequate cleaning, debonds, residual stresses, and inadequate cure.

The ultrasonic emission detector is, for the most part, independent of configuration. Since the sound is transmitted along the facesheet material to the stationary transducer, configuration size may influence sound level; however, this possibility has not yet been evaluated. In addition, the unit is capable of simultaneous evaluation of a large area. Noise emitted by highly stressed areas is radiated in all directions through the facesheet to the stationary transducer or transducers; however, the maximum area of coverage by one transducer has not been determined.

Another merit of the ultrasonic emission detector is the fact that it can be readily adapted for automatic test evaluation. With attachment of an electronic gating circuit to the equipment output, a go-no-go system based on the level of noise emission detected can be devised. Location of noise-emitting areas could be established by three or more transducers and the use of triangulation techniques. Scanning of the structure is not required since the transducer or transducers are stationary. The bonded structures which are rejected can be submitted to more thorough tests with other types of equipment to determine the cause of excessive noise emission.

Limitations.—As is the case with all nondestructive test methods, the readout of the ultrasonic emission detector is affected by density, material, and thickness combinations. For a given stress, the noise level emitted by stresed structures will decrease with increased facesheet thickness and core density; and, because of their different densities, variation in metals used will also affect readout.

Both structural bondline stressing and surface contact are required. Not only must the transducer be securely attached to the structure, it must also be applied to a metal surface. Nonmetal surfaces rapidly attentuate the noise signals from distant areas. Further applications studies will be made to determine exact distance limitations in all types of bonded structures and their component materials. Bonded honeycomb sandwich structures may require access to both sides for transducer attachment; however, no evaluations were performed on sandwich structures to determine whether or not the stress noise emission level of the opposite side is high enough for use of only one transducer.

The ultrasonic emission detector does not define defects; only noise signal levels, as emitted from areas of high stress concentration, are discerned and interpreted from noise level standards. However, an instrument with a three-channel capability and three transducers could be used—with triangulation techniques and a real-time computer—to locate defective areas.

The ultrasonic emission detector is further limited by the fact that structural test specimen evaluation is required prior to equipment production applications. Noise level standards must be determined, and values for panel reject–accept conditions based on noise emission ranges from satisfactory panels must be established. The basic equipment requires interpretation of audio signal intensity by the operator. Since the operator's sense of hearing may vary at times and produce inconsistent results, minimum backup equipment, such as an electronic gating circuit and a strip chart recorder, is essential for optimum evaluation.

Recommended Development.—The following are specific areas in which further development of the ultrasonic emission detector is recommended for adhesion bond strength analysis. It is desirable that the equipment be used to obtain data on the dual-seal and the 1.6-inch foam and plastic laminate panels during proof-pressure tests of panel integrity on the cryogenic insulation of the S–II. It is also desirable to perform a check of each individual edge-sealed section of the instrument unit structure by pressurization. Data may be obtained from the points at which the common bulkheads of the S–II and S–IV stages can be internally pressurized or externally stressed. It may also be possible to monitor bulkhead bond-line noise emissions over periods of storage or installation time where built-in residual stresses may cause gradual debonds, and payload shrouds and nosecones may be evaluated by proof pressure or static loading.

Nondestructive and destructive test data may be obtained during the strength tests to be performed on the 120- and 260-inch diameter metal honeycomb sandwich shrouds at Marshall Space Flight Center. In this instance, a check of each individual edge-sealed section by pressurization would be required.

Data may be obtained from structural destructive tests of any bonded structure which is bonded with the adhesives (or equivalent) evaluated by this program. Information from these tests will indicate when the adhesive bonds start to yield and will give the bondline stress noise emission characteristics from stress induction until complete structural failure. Yield points and allowable noise levels may then be established for the particular structure and used on future nondestructive test evaluations. Structural static or dynamic load tests of bonded brackets or other bonded structural attachments will give information on the bond integrity. Possibly, a static test would start a bond failure; however, failure would not occur in creep before completion of the test period. Noise emission from the bondline during static stress would indicate the quality of the bond and perhaps prevent embarrassment later should the bracket fall off during a vibration test.

In order to extend applications of the ultrasonic emission detector, test programs are underway to establish maximum evaluation range of the transducer as well as the effect of other adhesives, metals, and nonmetals which are used in bonded structures. Evaluation of defective bonds and associated noise emission characteristics will be initiated.

RESULTS

The completion of the three-phase program produced the following results. For bondline strength control, the development of the photomicroflaw technique satisfied the need for simulation of poor bond strengths through controlled surface contamination. Rigid cleaning, holding time limits, and handling requirements for cleaned parts prior to bonding (contained in all satisfactory specifications and required by military specification MIL–A–9067C, "Process and Inspection Requirements for Adhesive Bonding") were verified. The ultrasonic emission detector and the methods of equating noise signal level of stressed bonded structures to an indication of bond strength quality were developed and furnished in accordance with the majority of contractual requirements and objectives. The equipment supplied may be used for evaluation of destructive tests used on specimens and structures. Data obtained will indicate when the adhesive bond starts to yield and will give the bondline stress noise emission characteristics from stress induction until complete structural failure; this will permit allowable noise level standards to be established for nondestructive evaluation. Nondestructive evaluation may be made on structures containing perforated cores which can be edge-sealed and internally pressurized as well as on structures in which stresses can be induced externally by mechanical fasteners or fixtures. One of the most immediate applications for the equipment developed during this program is the evaluation of brackets and associated attachments which are bonded to structures.

APPENDIX

Operation of the Ultrasonic Emission Detector

The ultrasonic emission detector (fig. A–1) is a heterodyne ultrasonic receiver designed to operate in the 26 to 36 kHz frequency region for use in the ultrasonic NDT procedures previously described in this report. (A block diagram is shown in figure 6.) Construction of the ultrasonic emission detector was undertaken with a high regard for portability and field use. Removable modular design was used to facilitate repairs. The four basic modules are: (1) amplifier (fig. A–2), (2) oscillator (fig. A–3), (3) mixer and pulse detector (fig. A–4), and (4) headphone amplifier (fig. A–5). In addition, a spare module receptacle was provided for easy storage of a replacement module.
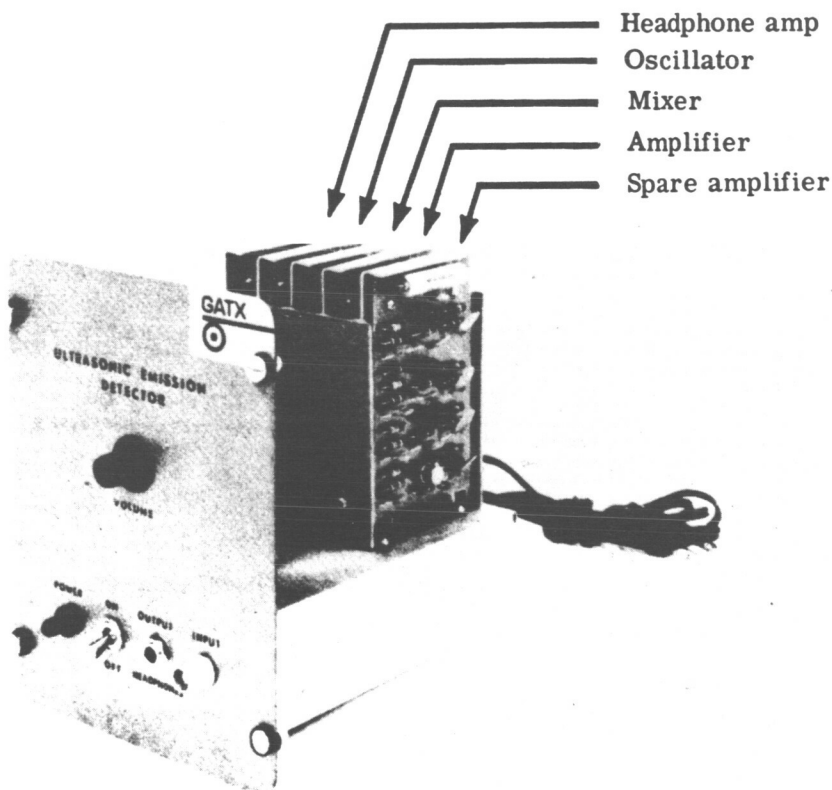

FIGURE A–1.—Ultrasonic emission detector.

FIGURE A–2.—Amplifier.

FIGURE A–3.—Phase shift oscillator.

Ultrasonic energy impinging upon the transducer will result in the transmission of an electrical signal to the ultrasonic emission detector. The first stage of signal processing consists of an amplifier with a voltage gain of 5000 around a center frequency of 31 kHz with a usable range of 5 kHz on either side of the center frequency. This restricted bandwidth effectively filters out noise and spurious signals.

The next stage of signal processing converts the 26 to 36 kHz signals to signals within the range of human hearing (under 6 kHz). This is accomplished by heterodyning the output of the first amplifier with a local oscillator of 32 kHz. Of the sum and difference frequencies produced, the difference will be within
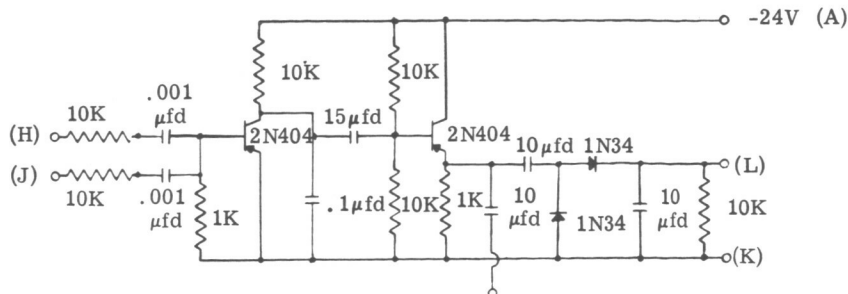
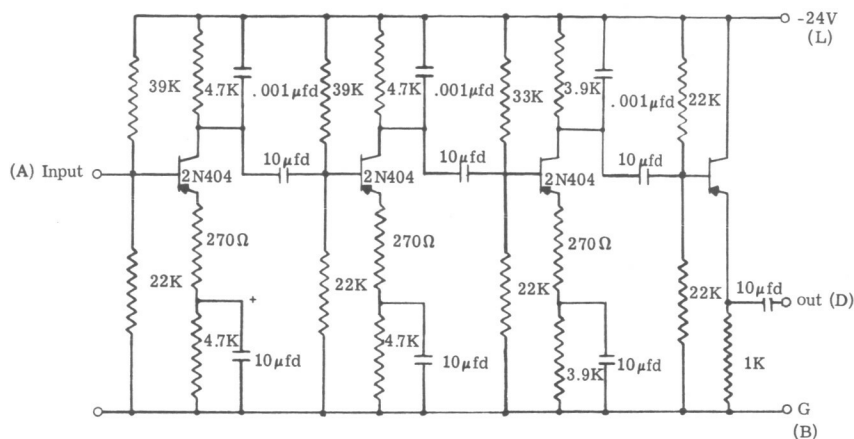FIGURE A-4.—Mixer and pulse detector.

FIGURE A-5.—Headphone amplifier.

the desired audio range. A potentiometer is provided on the rear panel to adjust the amplitude of the local oscillator for maximum mixing efficiency. This control is adjusted to the point at which background noise is just audible with maximum headphone volume.

The final stage of signal processing consists of signal presentation. The signal from the mixer is made available for meter or chart recorder presentation by a pulse detector with an integration time of about 0.1 second; this output is available on the rear panel. In addition, signals from the mixer are amplified for headphone use by an audio amplifier with a gain of 5000; this output is available on the front panel. A potentiometer adjustment of headphone volume is also located on the front panel.

REFERENCES

1. SCHMITZ, GERALD; AND FRANK, LOUIS: Nondestructive Testing for Evaluation of Strength of Bonded Material. Prepared under Contract NAS8–11456, Gen. Am. Res. Div., Gen. Am. Trans. Corp., Sept. 1966.

NONDESTRUCTIVE TESTING: TRENDS AND TECHNIQUES

2. MIL–A–005090E (Wep): Mil. Spec., Adhesives, Heat Resistant, Airframe Structural, Metal-to-Metal, Apr. 22, 1963.
3. MIL–A–25463 (ASG): Mil. Spec., Adhesive, Metallic Structural Sandwich Construction, Jan. 14, 1958.
4. MIL–A–9067C: Mil. Spec., Adhesive Bonding, Process and Inspection Requirements for,
5. BRADDOCK, P. H.: New Method for NDT Uses Ultrasonic Waves from Loads. Metalworking News, Oct. 5, 1964.

BIBLIOGRAPHY

JUDGE, JOHN F.: Nondestructive Testing Fundamental to Advanced Materials Development. Missiles and Rockets Publ., vol. 16, no. 8, Feb. 22, 1965, pp. 27–32.
SCHMITZ, G. L.: Nondestructive Testing of Adhesive Bonds. Design News Publ., Sept. 15, 1966, pp. 182–185.
SIMPKINS, ALAN B.: Silent Sounds of Industry. Design News Publ., Mar. 16, 1966, pp. 50–53.
ANON.: New NDT Method Probe: The Look, Sound and Smell of Quality. Steel, vol. 158, no. 7, Feb. 14, 1966, pp. 79–88.

X-Ray Television Techniques for Nondestructive Testing

Michael F. Nowakowski

Today's fast-growing technology has produced a vast array of complicated machinery and equipment made up of thousands—even millions—of parts, making the task of the quality and reliability engineer increasingly complex. He has in recent years devised ingenious equipment to meet the need for more efficient methods of testing and inspecting parts. Automated testing of parts and materials has replaced crude and time-consuming manual testing, and automated equipment is the everyday occurrence rather than the exception. This trend toward complexity and sophistication in test and inspection equipment is continuing. The ultimate goal is to be able to monitor and assess the quality and reliability of parts and materials by using the most economical and reliable means while maintaining the capability of handling large volumes.

Since the discovery of X-rays, radiographic examinations and tests have been used primarily for medical and industrial applications. One industrial application is the inspection of castings and welds. Until a few years ago, X-ray technology advanced very slowly, especially as related to quality control; however, when the space age came into being, the need arose for new inspection techniques, and the use of radiographic inspection spread to this new field. Gradually, this inspection technique moved into the area of electronics. Resistors, capacitors, diodes, and transistors were being radiographed with startling results, and this encouraged even wider use of radiographic inspection, especially in critical space applications. There is no question that radiographic examination is still a time-consuming and costly method of inspection to determine the integrity of an electrical or mechanical part. Resistors, for example, are produced in extremely large volumes (millions). To radiograph such large quantities would involve enormous expenditures for equipment, material, and personnel, and the cost would be prohibitive to both the manufacturer and the user. Even when sampling plans are used, the operation can be very costly if it is desired to use this technique to observe manufacturing process control.

X-RAY TELEVISION SYSTEM

Means are now available by which radiographic techniques can be at least semiautomated, and large quantities of radiographic film can be eliminated.

79

This equipment, an X-Ray Television System, utilizes a conventional X-ray generator in conjunction with an X-ray-sensitive vidicon tube to produce a picture on a television screen (fig. 1). The closed-circuit television system is entirely electronic and does not employ energy transformations, such as an image intensifier. The X-ray beam is converted to electrical impulses in the vidicon tube and transmitted through cables to a conventional television monitor where the object under inspection can be directly viewed, normally with ten to thirty times magnification. Handling equipment may be used in conjunction with the system to achieve motion in the X and Y axes (horizontal plane); rotational motion can also be achieved. When automatic loading devices are used, the operation of the system is highly automated. The operator may not be replaced in all applications, but the number of personnel can be significantly reduced. In many applications, the final decision to accept or reject a specimen may depend on a subjective evaluation, and an operator must therefore be present.
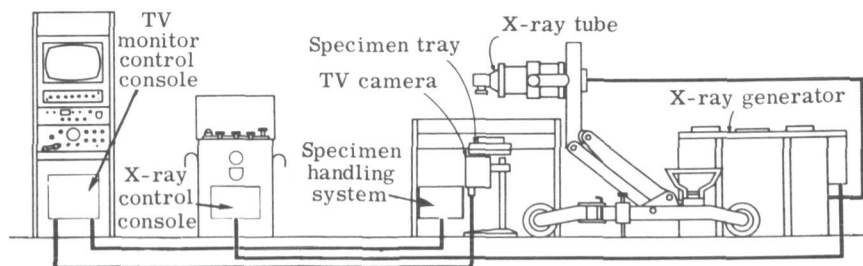

FIGURE 1.—Schematic illustrating subsystems of vidicon closed-circuit television X-ray system.

The X-Ray Television System eliminates most of the disadvantages of conventional radiographic inspection systems. Disregarding the initial, relatively high investment, the cost of performing radiographic examinations is significantly reduced because it takes less time, fewer materials, and less manpower to perform the examination. An additional advantage is that inspection can be performed on a real-time basis, thereby expediting decision-making and reducing the paperwork involved. A third major advantage is that the system is dynamic, that is, the parts undergoing inspection can be observed while they are in motion (in rotation, translation, or possibly vibration). Not only does the X-Ray Television System have economic advantages, but with the capability of motion and real-time radiography, a broad new field has also been opened to the quality and reliability engineer. When using conventional radiographic techniques, a separate film is made for each position of a specimen if a record is needed. With the X-Ray Television System, the part can be viewed in a sequence of positions and the best position for photographing selected if a record is required. If no record of inspection is required, the system can be used on a go-no-go basis.
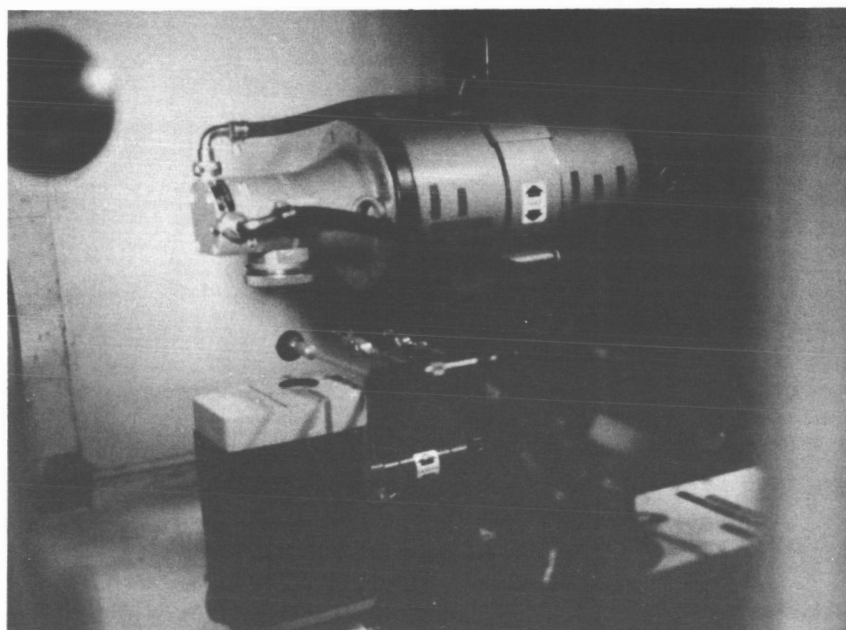
FIGURE 2.—X-ray television system.

FIGURE 3.—Constant potential dc X-ray source.

THE MSFC SYSTEM

The MSFC system (fig. 2) was purchased by Marshall Space Flight Center under a development contract with Philips Electronics and Pharmaceutical Industries Corporation. The system is in operation at the MSFC receiving inspection facility where it is used to visually inspect electronic parts (such as resistors,

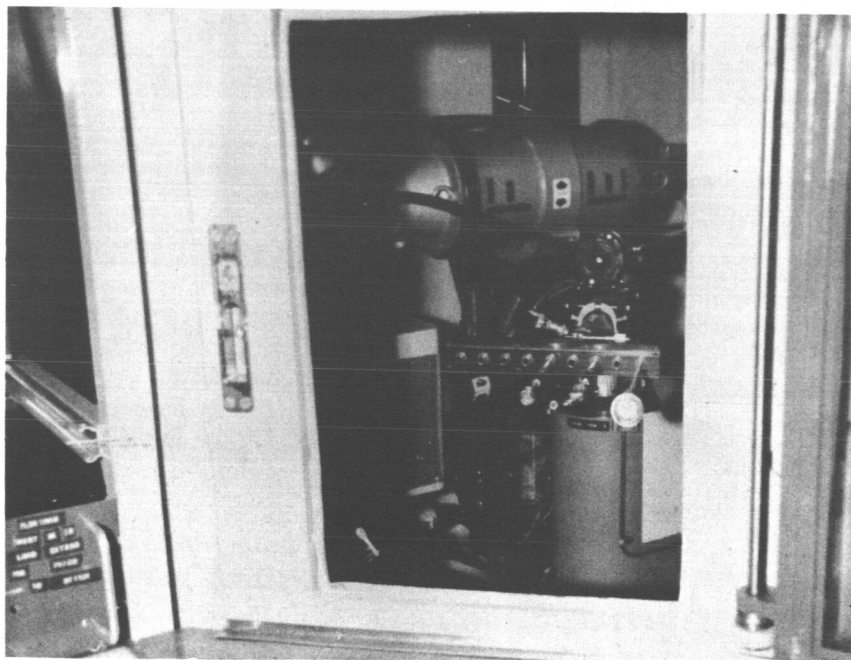FIGURE 4.—Television and automatic handling controls.

FIGURE 5.—Parts handling system controls.

FIGURE 6.—Parts handling system.

FIGURE 7.—1-mil diameter copper wire.
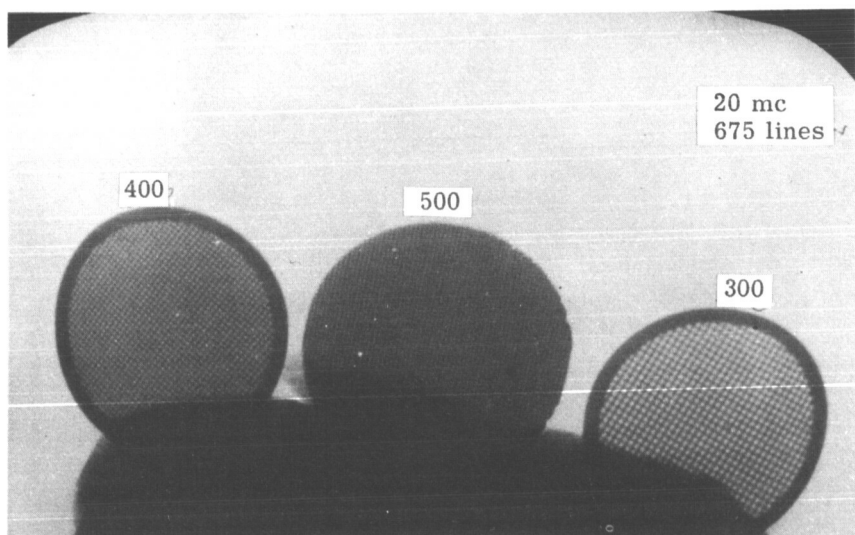
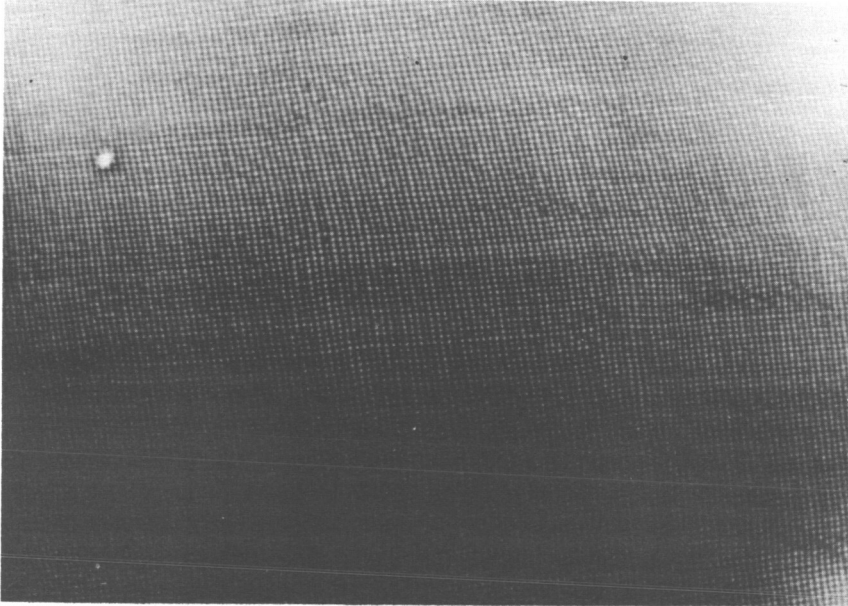FIGURE 8.—Resolution capabilities of X-ray television system.

FIGURE 9.—370 mesh screen with maximum magnification moving at the rate of 7 inches per minute.

capacitors, diodes, transistors, and relays) and small mechanical parts and components. The main objective of this inspection is to look for internal defects, such as particle contamination, misalinement, mechanical damage, or anomalies. The system has the capability of rotational and translational motion in all three axes simultaneously while the specimen is in the X-ray beam. The part can be seen on the television monitor or, if desired and especially if any defects are found that should be permanently recorded, the screen may be photographed.

The X-ray subsystem includes a constant-potential source (DC) (fig. 3), a stationary anode with a focal point 0.7 × 0.7 mm, a beryllium-window X-ray tube with an inherent filtration value of 3 mm beryllium, and a self-contained cooling system. The television subsystem includes a camera with an X-ray sensitive vidicon tube, sync generator, high voltage power supply, and television monitor (fig. 4). The system has a horizontal resolution of 650–800 lines as measured by EIA standards.

For parts handling, the system (figs. 5 and 6) has a positioning mechanism to hold the objects and move them into the line of sight of the television camera and the X-ray source. The system provides for separate (or combined) X-axis and Y-axis travel by means of a "joy-stick" control, as well as variable-speed rotation around one of these two axes. The specimen under test can be rotated at varying speeds up to a maximum of 30 rpm.

The system will detect wires as small as 0.5-mil diameter (fig. 7) and drilled holes as small as 1-mil diameter in materials 1-mil thick. It is believed that the system is capable of revealing holes as small as 0.5-mil diameter in thin materials. The resolution capabilities (fig. 8) are such that the system will resolve 300 mesh ASA phosphor-bronze screen, when motionless at the camera surface, without additional absorbers in the X-ray beam. For direct viewing, the system will resolve 100 mesh ASA phosphor-bronze screen, free from image lag or blurring, at rates of travel up to 15 inches per minute (fig. 9). The system shows penetrameter sensitivity of 1.4 percent through 0.25-inch aluminum and 0.12-inch steel per ASTM E142–59T, using penetrameters per MIL–STD–271.

In compliance with Marshall Space Flight Center requirements, every shipment of high reliability semiconductor devices received must be accompanied by

MG-150 B$_E$ window x-ray tube 0.7 mm focal spot

1 150 kv, 4 ma
2 100 kv, 6 ma
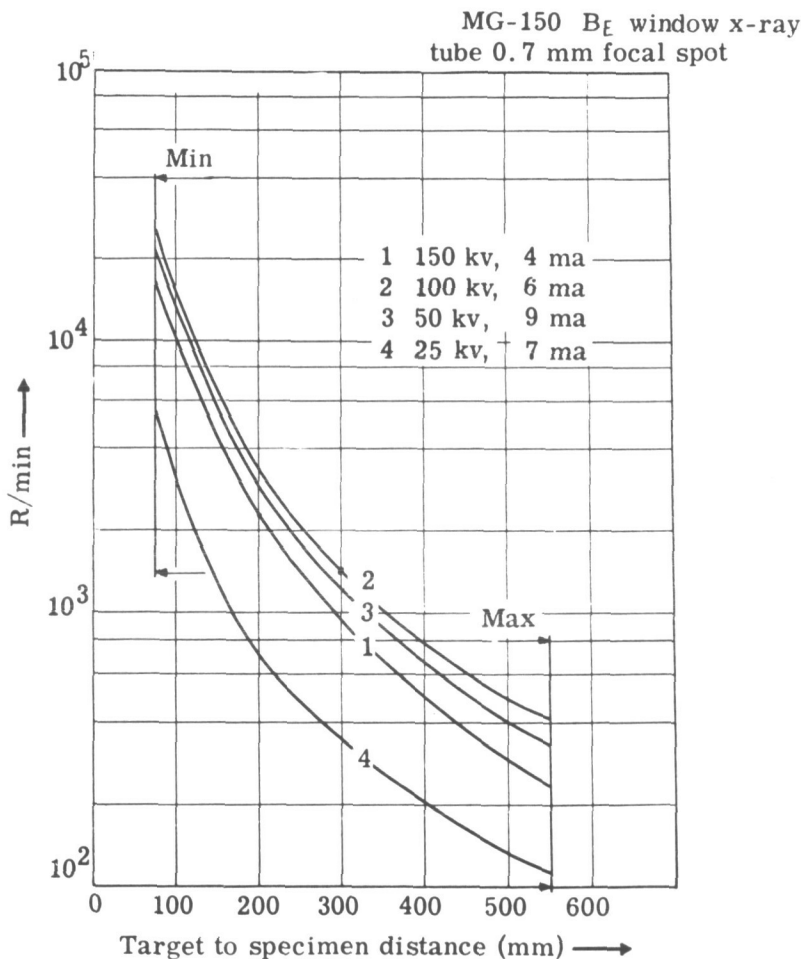3 50 kv, 9 ma
4 25 kv, 7 ma

FIGURE 10.—Approximate free air dose rate as a function of target to specimen distance (mm).

radiographs of the parts in the shipment. These requirements are also being extended to relays and capacitors. The films are reviewed by receiving inspection personnel at the Center. If any discrepancies or problems are noted, the doubtful devices are immediately subjected to inspection in the X-Ray Television System. The acceptability of the parts can be determined easily since the parts can be viewed from many different angles in order to assess their integrity. Procedures are being established whereby a sample of all semiconductor devices and relays purchased will undergo inspection on a lot-by-lot basis.

Much effort is still needed to establish a formal procedure and define the AQL levels for inspection of electronic parts by this system. One variable that must be evaluated is total X-ray dosage, since it is known that if the cumulative dosage becomes too high, sensitive devices such as transistors, integrated circuits, and capacitors can be seriously degraded. The dosage increases very rapidly as the X-ray source-to-specimen distance decreases (fig. 10). Tests have been run using relatively sensitive semiconductor devices to determine the maximum allowable exposure. In one test involving a single diffused Mesa transistor, approximately fifty minutes of exposure at 150KV, 4MA, and approximately 150-mm target-to-specimen distance resulted in a degradation of only ten percent in collector-base leakage current (ICBO). The normal exposure time based on these tests of semiconductors has been limited to a maximum of one minute.

To date, many anomalies have been found in various electronic parts received at Marshall Space Flight Center for use in Saturn flight hardware (figs. 11–20);
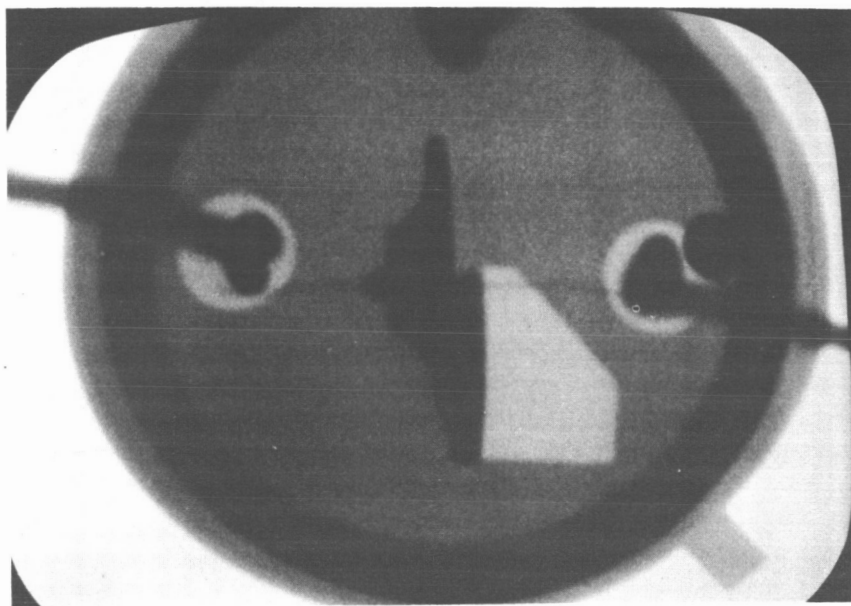

FIGURE 11.—Transistor viewed using conventional negative polarity X-ray mode.
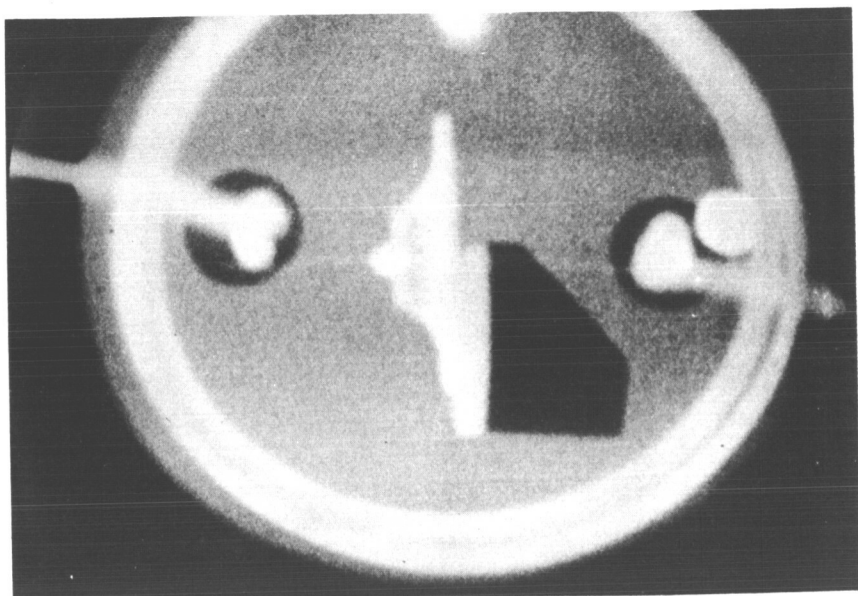
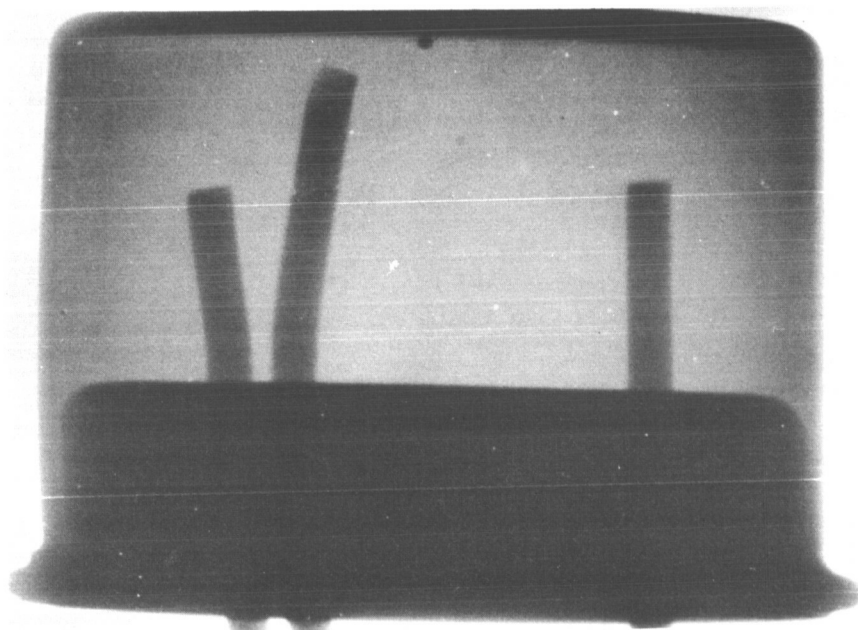FIGURE 12.—Transistor viewed using positive polarity X-ray mode.

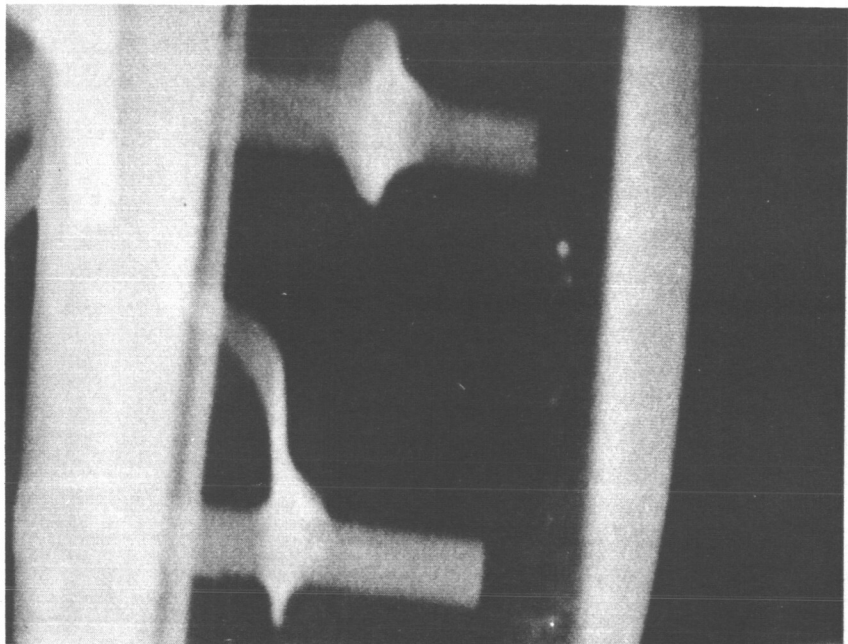FIGURE 13.—"Loose" solder ball located in TO–5 transistor.

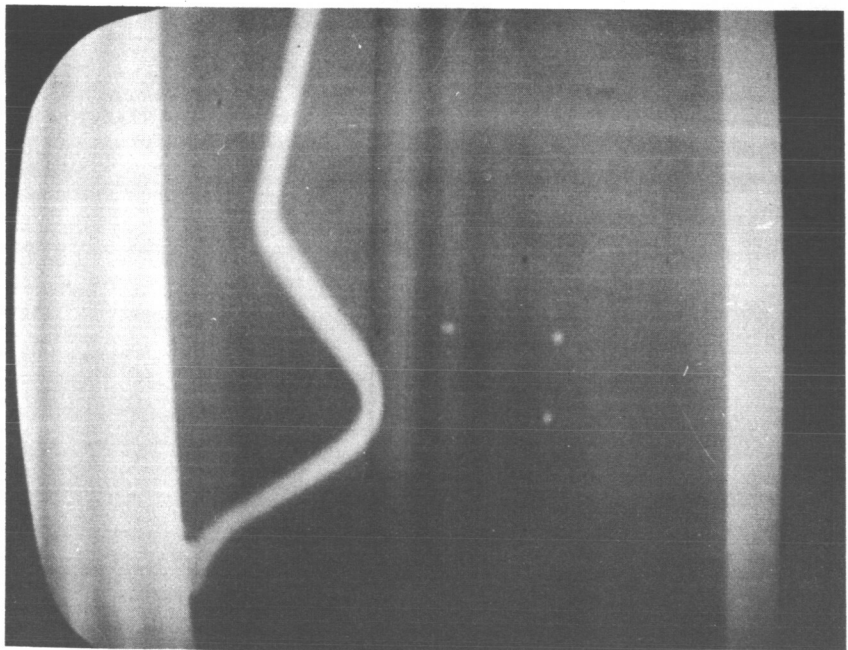FIGURE 14.—"Loose" weld splash located in TO–5 transistor.

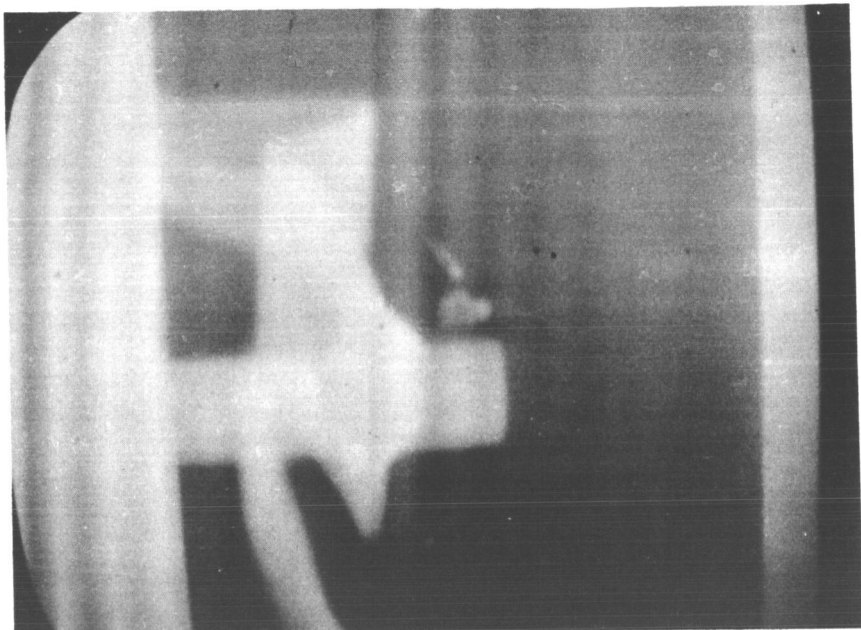FIGURE 15.—Magnified view of weld splash in TO–5 transistor.

FIGURE 16.—Verification of "loose" particles (same transistor as shown in fig. 15).
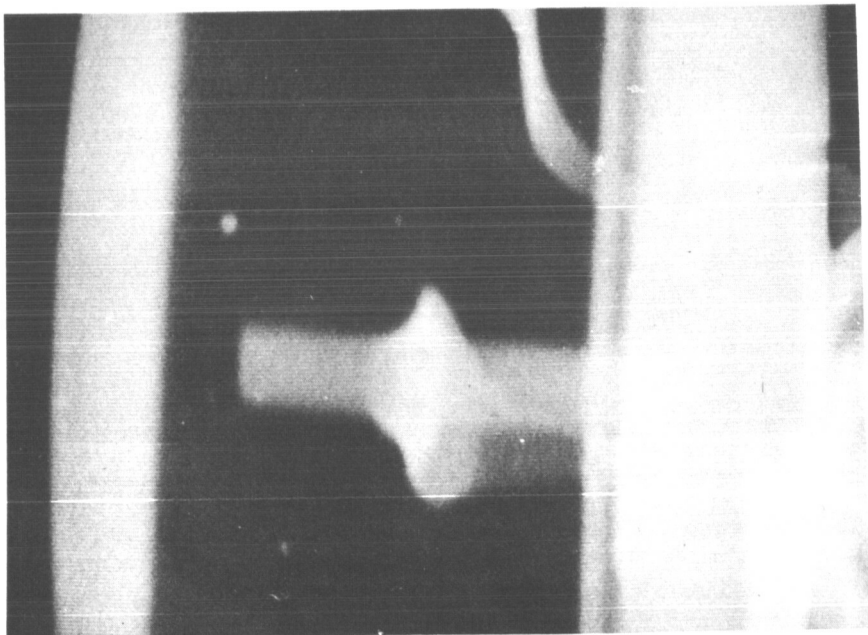

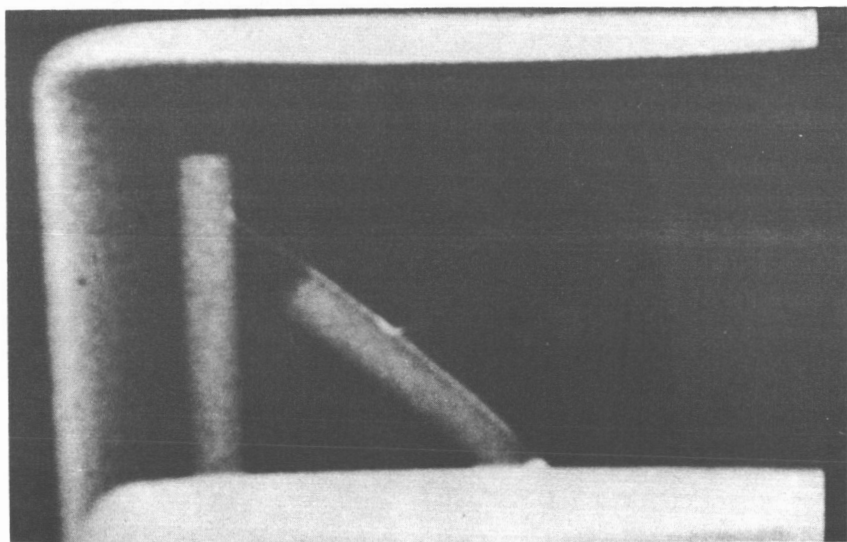FIGURE 17.—Combination of "loose" solder balls and weld splash.

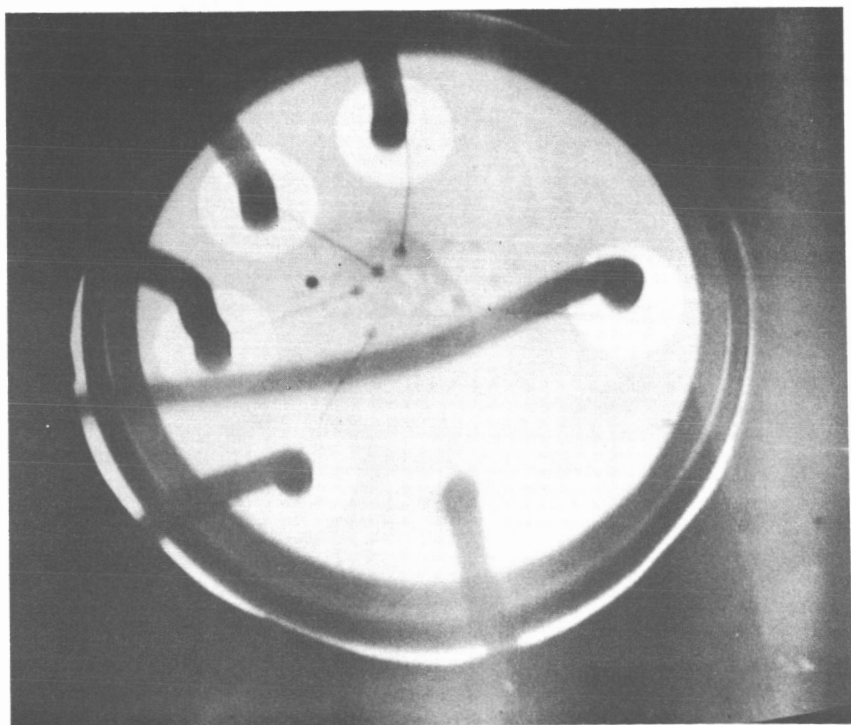FIGURE 18.—"Bent post" in TO–5 transistor.

FIGURE 19.—Integrated circuit showing additional gold bond and large voids under the circuit.
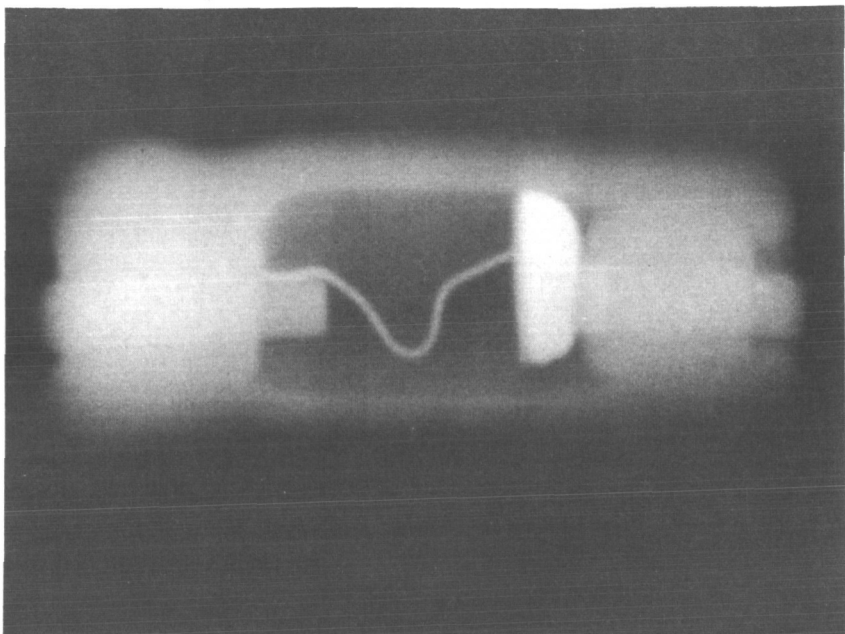
FIGURE 20.—X-ray of a glass diode.

some of these may not have been detected using conventional radiographic tech-niques. In each case, the part was rotated until the best view was obtained, and then the screen was photographed for a permanent record. The presence of particles inside the devices was easily detected. These particles may not have been detected using conventional radiographic techniques since they could have been hidden by the posts or other structures inside. If any of these parts had been used in a flight-critical application, a serious failure could have resulted.

COMPARISON WITH CONVENTIONAL SYSTEM

A study has been performed to compare the capaiblities of the X-Ray Tele-vision System with the capabilities of the "conventional" radiographic system (ref. 1). The results of this study are summarized in table I. It is apparent from this table that each method has definite advantages. Resolution is com-parable; both systems can resolve a 0.0005-inch gold wire so that it is discernible but not inspectable. The filmless method, with capability of rotation of the specimen, is much more effective in inspecting for internal clearances, cracked elements, misalinement, and other defects which may be detectable only over a 5° to 10° span when viewing. The rotational feature is also a distinct ad-vantage when loose particles are present. Their movement within the case while the specimen is being viewed makes detection much more probable.

TABLE I.—*Comparison of Conventional Film versus X-Ray Television Techniques*

Defect category	Conventional X-ray method	X-ray television method	Preferred method
Solder	Good results	Good results and ability to easily determine whether loose or attached, internal or external	Filmless
Weld splatter	Good results	Not quite as good as film when splatter is attached because of less contrast	Film
Foreign material, loose	Good on particles ≥ 0.003-inch Fair on particles ≤ 0.002-inch Poor on particles ≤ 0.001-inch	Good on particles ≥ 0.002-inch Poor on particles < 0.002-inch	Filmless
Foreign material, attached	Good on particles ≥ 0.002-inch Fair on particles 0.001-inch	Good on particles ≥ 0.003-inch Fair on particles 0.002-inch	Film
Extended whisker or lead	Dependent on view(s) taken	Very good with full rotation, limited to wire size ≥ 0.0005-inch	Filmless unless wire < 0.0005-inch
Internal leads	Satisfactory resolution for inspection of 0.0007-inch Au leads in 0.007-inch Kovar wall can and 0.020-inch Al leads in 0.014-inch Kovar wall can	Satisfactory resolution for inspection of 0.001-inch Au leads in 0.007-inch Kovar wall can and 0.020-inch Al leads in 0.014-inch Kovar wall can	Filmless unless wire < 0.0005-inch
Mounting paste build-up	Satisfactory	Satisfactory	Either
Internal clearances	Dependent on view(s) taken	Very good with full rotation as worst case can be presented	Filmless
Undercutting	Dependent on view(s) taken	Very good with full rotation	Filmless
Misalinement	Dependent on view(s) taken	Very good with full rotation	Filmless
Voids or glass striations in diodes	Dependent on view(s) taken	Very good with full rotation	Filmless

FAILURE ANALYSIS

The X-Ray Television System is an especially useful tool when performing failure analysis. Since the system has motion capabilities, the component can be completely area-scanned and rotated. The image seen on the television monitor is enlarged approximately thirty times, and many of the internal details can therefore be examined in great depth for defects. When cross sectioning molded or potted components or parts, the area of interest is often inadvertently sectioned through, and valuable information thereby lost. With the X-Ray Television System, the area of interest can be accurately determined and, if a cross section is necessary, the probability of destroying the area of interest is greatly reduced (figs. 21–23).

When it becomes necessary to determine if a part failed as a result of particle contamination, the X-Ray Television System can be used to determine whether or not particles are present inside the device and whether or not they are loose. This determination is made without opening the device, thereby eliminating the speculation that the particles were introduced when opening the specimen. The only analysis remaining then is to determine the composition of the particle
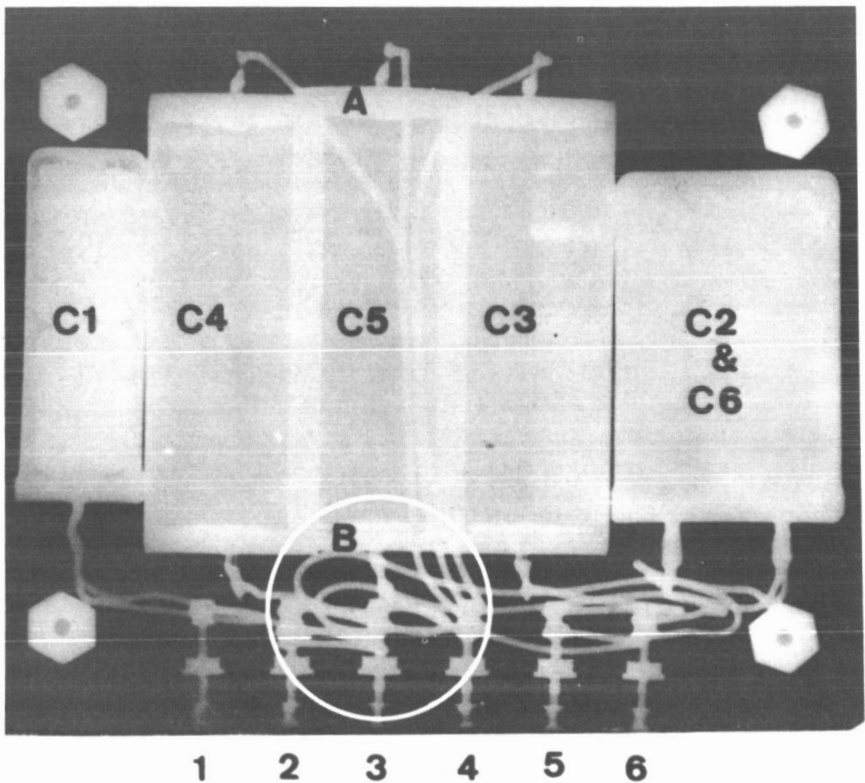

FIGURE 21.—X-ray of capacitor module that failed during checkout of Saturn vehicle systems.
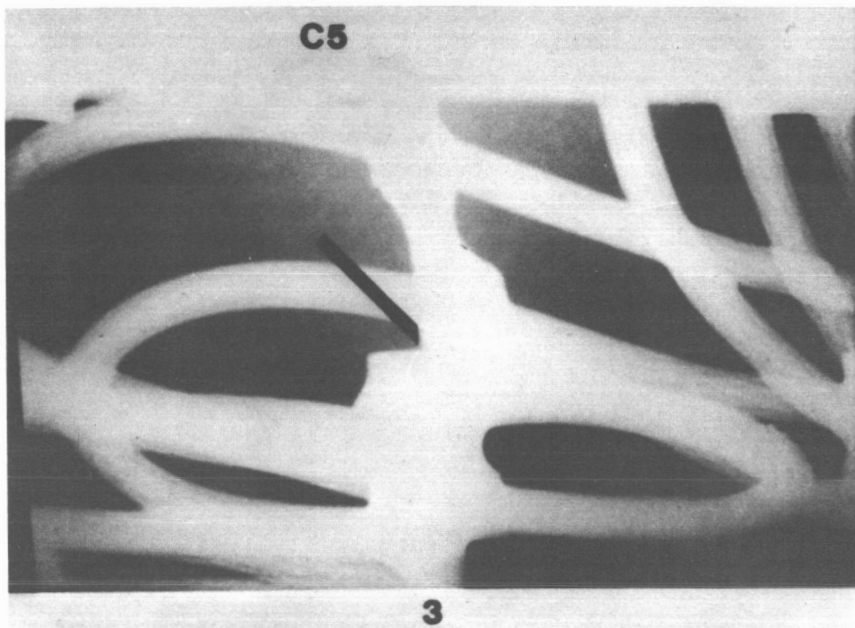
FIGURE 22.—Magnified view of circled area Ⓑ in figure 21.

contamination.   Since the system is used on a real-time basis, a timely failure analysis can be performed, i.e., certain failure mechanisms can be determined almost immediately and corrective action may be implemented in a timely manner.   It is not always necessary to know the cause of a failure immediately after it occurs; however, on certain occasions, such as when a space vehicle is standing on the pad ready for launch, timely knowledge can be advantageous.   Also, in a "tin can" factory where the weld or solder seams are being monitored on a high volume production line and where the volume may be on the order of tens of thousands per hour, a timely failure analysis has economic advantages since a delay in the analysis could result in a loss of production for an extended period of time.

OTHER APPLICATIONS OF X-RAY TELEVISION

Other uses for the X-Ray Television System will include such applications as monitoring the welding of bulkhead seams for space vehicles, ships, or submarines to determine their integrity.   Real-time X-ray television may prove to be an invaluable asset since a determination can be made of the integrity of the weld or joint almost before the weld is completed.   The operation of many types of intricate components, such as wrist watches or other timing mechanisms, can be observed to insure proper operation and alinement.   Relay contacts and valves may be observed while operating to detect binding or misalinement.   Where
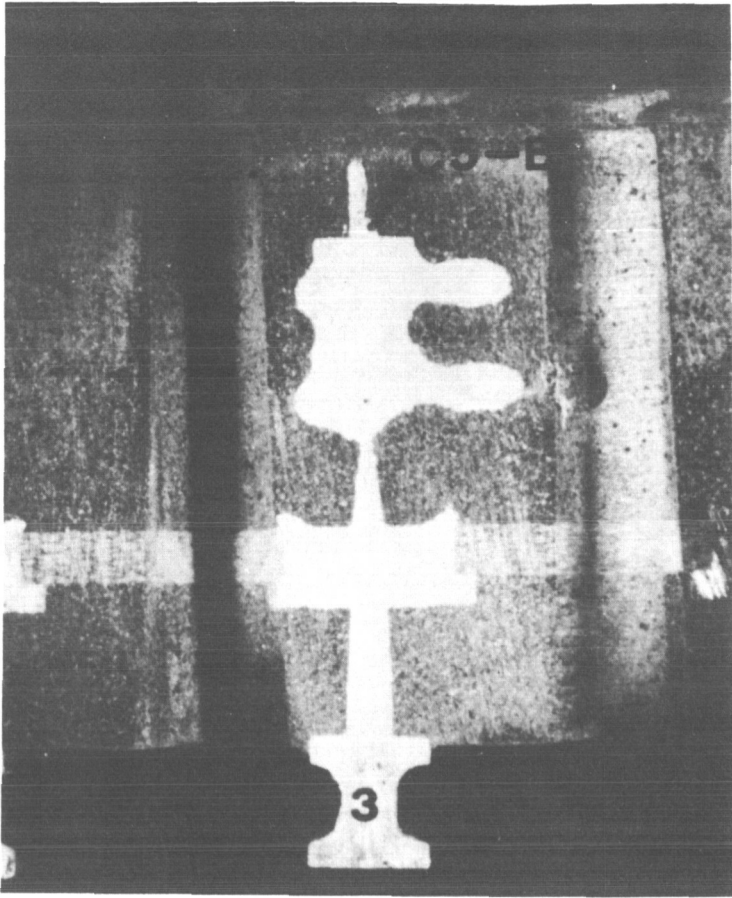
FIGURE 23.—Cross section of circled area Ⓑ (fig. 21) verifying shortened condition of capacitor module.

high reliability is needed, it is possible that all items may go through a one hundred percent production inspection to observe and remove any defective items. One advantage is purely economical in that an item which does not meet specified criteria can be rejected in the very early manufacturing stages. Another advantage is the improvement of reliability on a lot-by-lot basis. The X-ray television system of the future will undoubtedly grow in complexity and be used in countless industrial applications.

REFERENCES

1. McCULLOUGH, R.: Correlation of Film and Filmless Radiography. Tex. Instruments, Inc. Paper presented to ASTME–7 Sub-II Task Group G, Soc. Nondestructive Testing, July 1966.

BIBLIOGRAPHY

BAKER, J. M.: Evaluation of Film and Filmless Radiographic Systems for the Nondestructive Testing of Thin Materials and Electronics Assemblies.   The Boeing Co., Jan. 1964.

McMASTER, R. C.: New Developments in Nondestructive Testing of Small Components and Thin Materials.   Nondestructive Test Res. Lab., Dept. Welding Eng., Ohio State Univ., June 1962.

McMASTER, R. C.; and Mitchell, Jay P.: Process Control with an X-Ray Television System. Nondestructive Test Res. Lab., Ohio State Univ., Mar. 1966.

Fast Scan Infared Microscope for Improving Microelectronic Device Reliability

Leon C. Hamiter, Jr.

Traditionally, technological progress occurs in two phases. First, a new device is created; second, better and more consistent means of manufacturing it are sought.

The field of microelectronics is now in the second phase, and progress is being made toward better manufacturing methods and processes. In the test area, a new approach—infrared testing—is being developed as a promising technique capable of yielding large amounts of information on thermal and electromechanical parameters affecting reliability that conventional test equipment and methods are incapable of measuring.

The cause of the difficulty lies in the physical size of the elements to be tested and accessibility to them. Semiconductor chips have an area in the order of magnitude of 1 mm², and in this area some integrated circuits pack dozens of transistors, diodes, and resistors. Since the electrical interconnections are often only a few microns in width, physical contact with them for test purposes is not only difficult, but is also dangerous to their mechanical and electrical integrity. Probe measurements can only be made, on a practical basis, prior to dicing and encapsulation. Consequently, in most instances, only input and output measurements are obtainable through the use of conventional test equipment. In the case of complex integrated circuitry, this is inadequate, because it does not give information about the performance of the individual elements of the network. For instance, the poor performance of one element could go undetected because of the compensating effect of another element. Furthermore, several design or manufacturing defects that may eventually cause a failure are not detectable by conventional testing. Table I shows some of the failure mechanisms and defective conditions in this class.

Infrared radiation is an electromagnetic oscillation of the same type as the electromagnetic waves that are called "visible light" and may be thought of as "invisible light." The electromagnetic radiation band, as it is presently known, goes from the very low frequencies of the ac oscillations to the extremely high frequencies of the gamma rays and cosmic rays produced by variations in energy of subatomic particles. All these radiations are of the same nature and

TABLE I. *List of Semiconductor Defects*

Semiconductor bulk material	Resistivity irregularities
	Dislocations
	Lattice anomalies
	Secondary breakdown
Design	Junction proximity
	Thermal interaction
Surface	Pinholes
	Contamination
	Ion migration
	Channeling
Mechanical	Uneven metal deposition
	Poor bonding of deposited elements
	Poor bonding of lead wires
	Poor die bonding
	Cracks, voids, and scratches

have the same characteristics of traveling at the same speed (the speed of light) and of transporting energy.

The infrared radiation is contained in the area between the visible light and the radio waves. There is even an overlap in the microwave radio wave region. The difference is that the radio waves are usually of the coherent type, whereas the infrared radiation is normally of the incoherent type. This fact can be easily understood when we consider that the infrared radiation is generated by the vibrational and rotational movements of the atoms and the molecules of which physical matter is composed. Consequently, the spectrum of the infrared radiation emitted by physical matter is extremely broad and peaks at a frequency which varies with temperature.

A physical body containing atomic and subatomic particles of all possible sizes would emit at all infrared frequencies on an uninterrupted spectral band. Such a physical body is called a blackbody. Although it does not exist in nature, very close approximations to it can be made, and infrared radiation laws are formulated upon it. No physical body has the perfect spectrum of the theoretical blackbody, but the shape of its radiation band will depend upon its temperature and surface condition called emissivity. Emissivity can be thought of as the quality which in the visible range is called color.

In addition to the infrared radiation emitted by physical matter as a result of thermal agitation, infrared radiation is also being emitted by semiconductors independently from the thermal status. This is called recombination radiation and is the result of the energy liberated by the current carriers when they step down from the higher energy level of the carrier band to the lower energy level of the valence band. This liberated energy manifests itself as infrared radiation and is called recombination radiation because it occurs when the electron hole pairs recombine. It is of the coherent type and is directly proportional to the amount of current flowing through the semiconductor and its variations of the

current flow. Consequently, detection and measurement of the recombination radiation should make it possible to read, without time delay, modulated operation and even pulse operation of semiconductors. Since the recombination radiation occurs in a different wavelength from the radiation resulting from thermal effects, it can be read, with the use of adequate filters, independently from the thermal variations.

Wherever electrical current flows, a fraction of it turns into heat. This is generally called power dissipation and results in a temperature rise of the element through which the current flows. This thermal rise increases the power of the infrared radiation emitted by the surface of the element, and in turn this variation can be measured by an adequate infrared detector. Thus, a direct correlation can be established between the electrical power dissipation of an electronic part of a given design and the infrared radiation emitted by it. This correlation is the key to the infrared evaluation of electrically energized microelectronic circuits.

Passive elements can be evaluated by plotting the temperature variation through them when they are subjected to a thermal gradient. This can be achieved by mapping the infrared radiation emitted by each surface point of the target. In this way, physical anomalies, such as material discontinuities, lack of proper bonding, and cross section variations, can be detected and evaluated.

When the target is a semiconductor chip, the infrared test equipment requirements are set by its physical size, the temperature gradients to be observed, and the speed at which thermal flooding of the target takes place.

MICROSCOPE DESIGN

Figure 1 is a photograph of the fast scan infrared microscope that has been developed by Raytheon Company under contract for Marshall Space Flight Center. On the left is a pedestal for mounting the device to be examined; the microscope is for alinement and visual observation of the sample. The upper right area contains the drive mechanism for the helix and polygon scanning system. A functional block diagram of the instrument is shown in figure 2. Basically, the unit can be divided into five major sections: optics, scanning system, detector with cryogenic cooling, signal processing, and display system.

Optics.—Larger than normal optics with several unique properties were deliberately chosen for the infrared microscope. The detector aperture requirements dictated the use of a magnifying system; a 7.6 to 1 system was used. A diameter of 8 inches was chosen for the primary, and the focal ratio was set at F1.1. This long focal length permits the object to be away from the primary optics in a space of its own; it further permits the use of an off-axis system. The only aberrations from this system occur because the field is spherical rather than flat; however, under the conditions in which this device will be used, the aberrations are of no major importance. Optical resolution of a diffraction-limited characteristic is achieved in a lens system which has a concentric, spherically round, germanium corrector and a spherical primary lens.
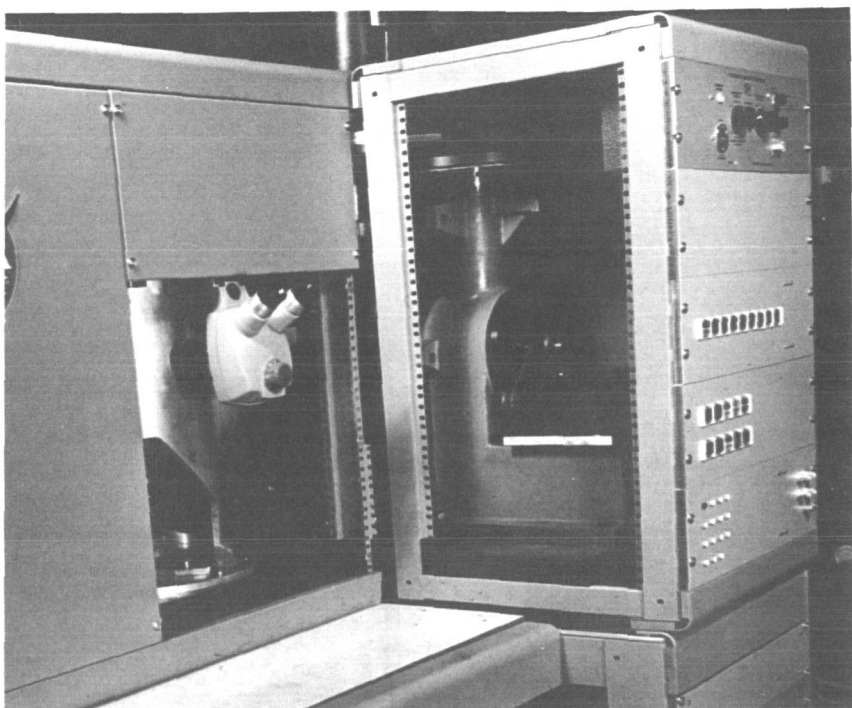
FIGURE 1.—Fast scan infrared microscope.

Scanning system.—The high-speed infrared microscope required a unique scanning system. This requirement was met by the development of a polygon helix scanner in which a polygon, having 64 internal facets and 64 spaces, is rotated for the aperture mask of the detector at a speed of 1000 lines per second. This scanned beam is relayed to a pair of flat annuli oriented to fold the beam 180°. Only a small segment of each annuli is used. The main effect is to provide the system with a corner reflector. This would be the effect if the annuli were perfect doughnut-shaped flat surfaces of glass; however, they are split with one end raised 0.15 inch to form a helix. When rotated together, these helixes transversely move the optical image as far as necessary to permit scanning a 1½-millimeter surface at 10 cps with linear speed and 90 percent efficiency.

Detector with Cryogenic Cooling.—The detector and the cooling system were chosen to be compatible with the rest of the microscope. The detector has a 0.0003-inch diameter aperture with an aperture-limiting mask of 13° in one axis and 6° in the other axis; this aperture permits the detector to see all areas in the target plane. The detector is mercury-doped germanium with a normal operating temperature of 30° K. Cooling is provided by a Malaker Mark 7 closed-cycle cryogenic cooler. The closed-cycle system offers significant convenience advantages over the alternate manually filled helium system.

Signal Processing.—Signal processing for the infrared microscope was made as simple as possible. The detector amplifier and log postamplifier have variable gains and a variable bandwidth. To provide x and y drives for the cathode-ray oscilloscope or magnetic tape, sync pulses come from both the polygon wheel and the helix wheels. The net result is an ability to provide a single frame image of the target to be scanned, as well as radiation or amplitudes versus time data on a continuous basis.

Display System.—The output of the instrument is an analog signal having a maximum frequency of 100 Hz and the indexing of a video signal. Due to these characteristics, it can best be fed to a conventional video tape recorder. The device has framing rates consistent with those held in the microscope and can record one frame of infrared data on each diagonal line sweep of the rotating head. Information from the video tape recorder can then be reproduced sequentially as video images on an oscilloscope, and line scans can be recorded directly on a strip chart recorder. In addition, information from the video recorder can be used as the input to an A to D converter, whose output proceeds into a buffer unit for storage and future computer processing.

Since the smallest elements of an integrated circuit are the junctions which can be only a few microns wide, the area resolution of an adequate infrared system should be able to view them. An even finer resolution capability might be useful, but the wavelength of the radiation emitted by the target is the limiting factor.

The instrument was designed to have the following capabilities:

Area resolution	20 microns
Temperature resolution	1° C at 25° C ambient
Frame composition	100 lines/frame
Scan speed	1000 lines/second
Optical magnification	7.6
Depth of field	±20 microns
System efficiency	40 percent
IR wavelength	6 to 12 microns

Once a microelectronic device engineering prototype has been built and is operating, a thermal map of it will enable the design engineer to verify that the thermoelectric stress is as calculated at every point of the unit. Electrical overstress, resulting in excessive power dissipation and thermal interaction which cause unwanted heating of sensitive elements, will be apparent. Once these conditions have been pinpointed, design changes can be implemented and their effects verified on a modified prototype. A comparison of thermal maps of production units with standards established for each basic device will immediately disclose any significant variations of the production process. From this information, either suitable process changes can be made to correct the defects or anomalous devices can be discarded.
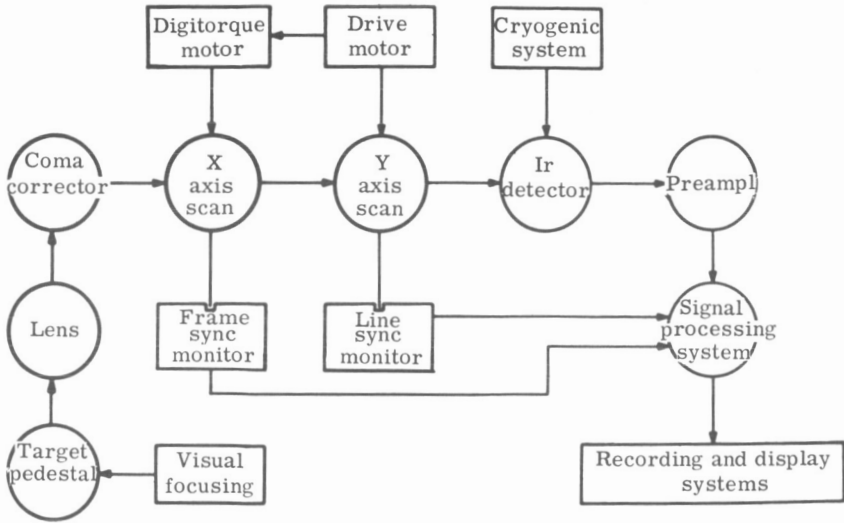
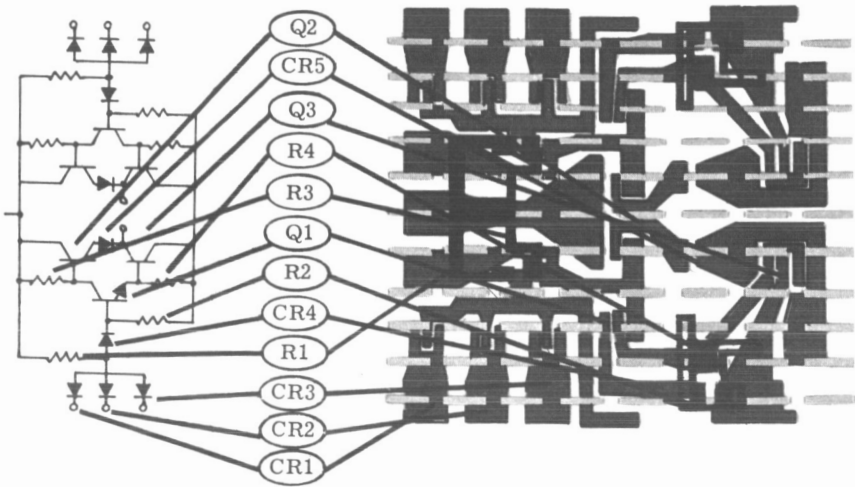FIGURE 2.—Block diagram of fast scan infrared microscope.

FIGURE 3.—Schematic diagram and physical layout of dual gate.

Figure 3 shows the circuit diagram and physical layout of a diode transistor logic dual 3 input gate that was evaluated for its thermal design characteristics. The location of every fifth line of scan of the fifty made is shown by the dotted lines. The size of this chip is 50 mil by 50 mil.

Figure 4 is a collection of scope displays of each scan line of the fifty scans that were made. A cutout was made of each line of scan and assembled into an IR profile of the circuit, as shown in figure 5. By correlating figures 3 and 5,
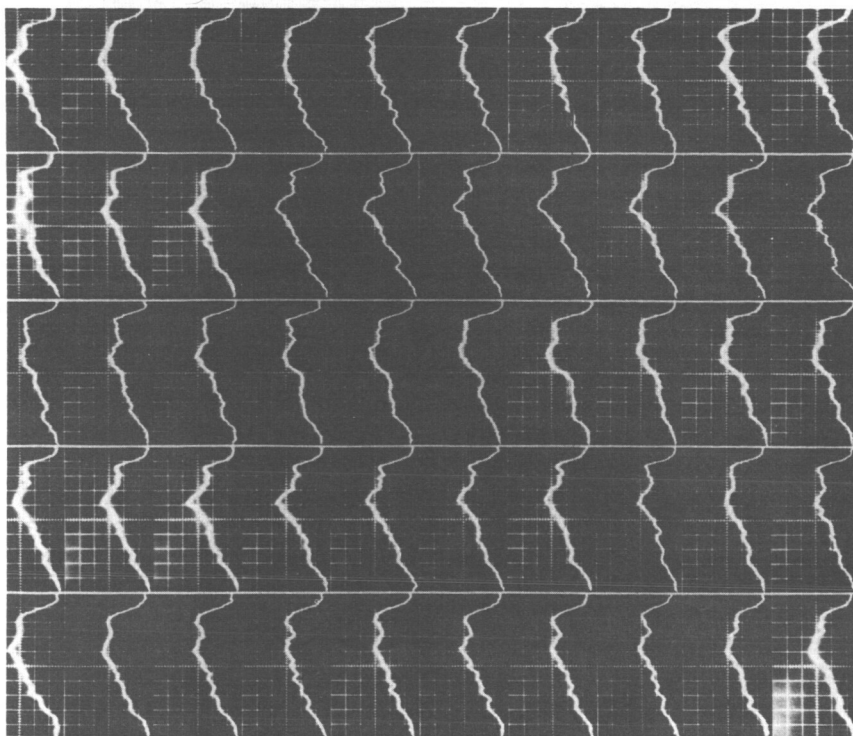
FIGURE 4.—Fifty infrared scan lines of microcircuit.

the peak infrared emission can be related to resistors and transistors within the chip. This analysis shows a maximum temperature rise of 120° C in the circuit with no major concentrations of heat. The evaluation indicates this circuit design has a relative uniform thermal gradient. Figure 6 shows a single line of scan superimposed over layout of the circuit. The infrared radiation profile shows the location and temperature of the diode and transistor junctions and buried resistors in the chip.

Figure 7 shows a single line scan of a good circuit and a circuit with poor bond to header that was measured at 1, 6, 16, and 46 seconds during warmup. It can be seen that in the good unit, warmup is rather slow; at the end of 46 seconds, the temperature has reached approximately 90° C. At the end of the same time, the temperature of the bad unit has reached approximately 115° C. Under the infrared scan is an X-ray of the units that shows the void causing the evaluated temperature. No voids are seen under the good circuit.

Figure 8 depicts the scans made of a circuit containing a crack in the silicon. The scan line labeled "initial warmup" was made about 10 seconds after power was applied and shows a large drop in IR in the area of the crack. The scan
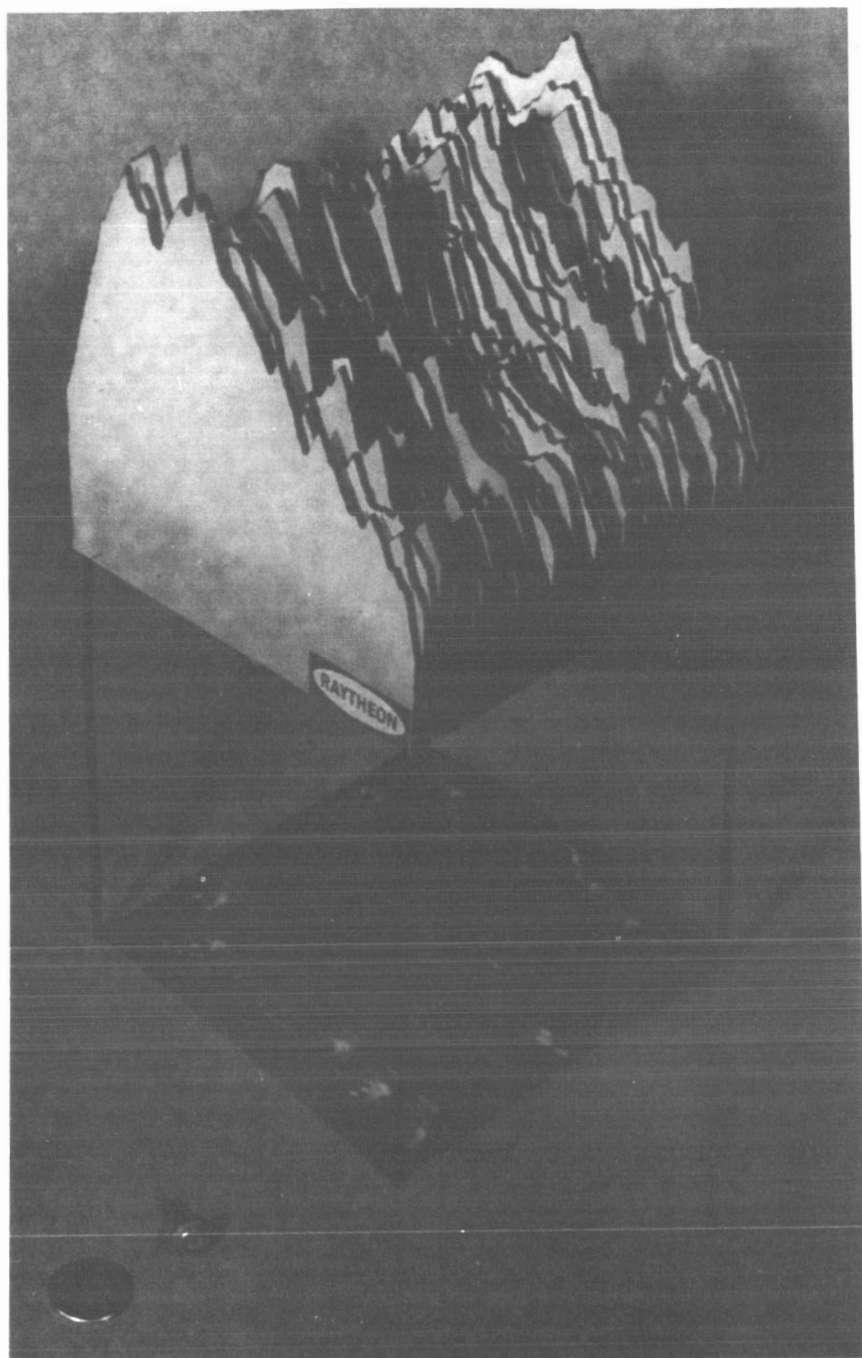
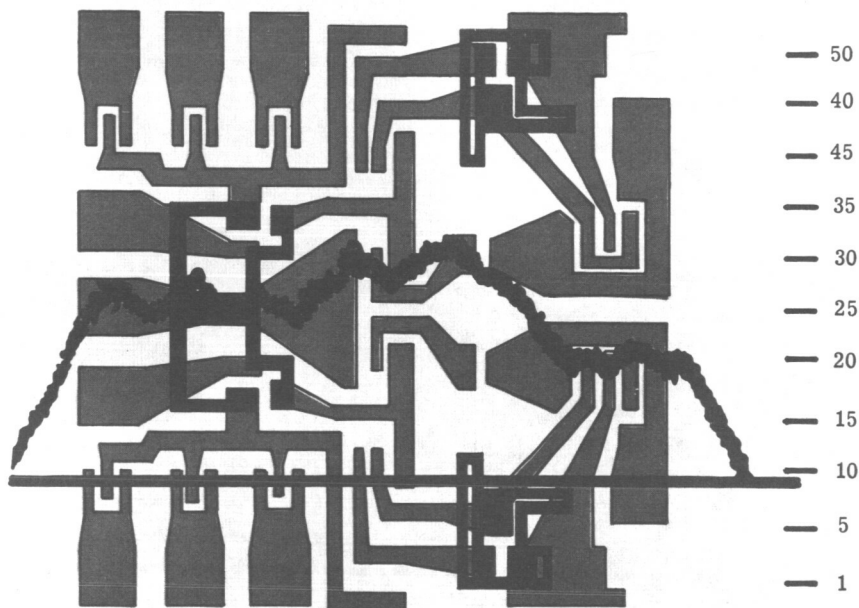FIGURE 5.—Infrared profile and photograph of microcircuit.

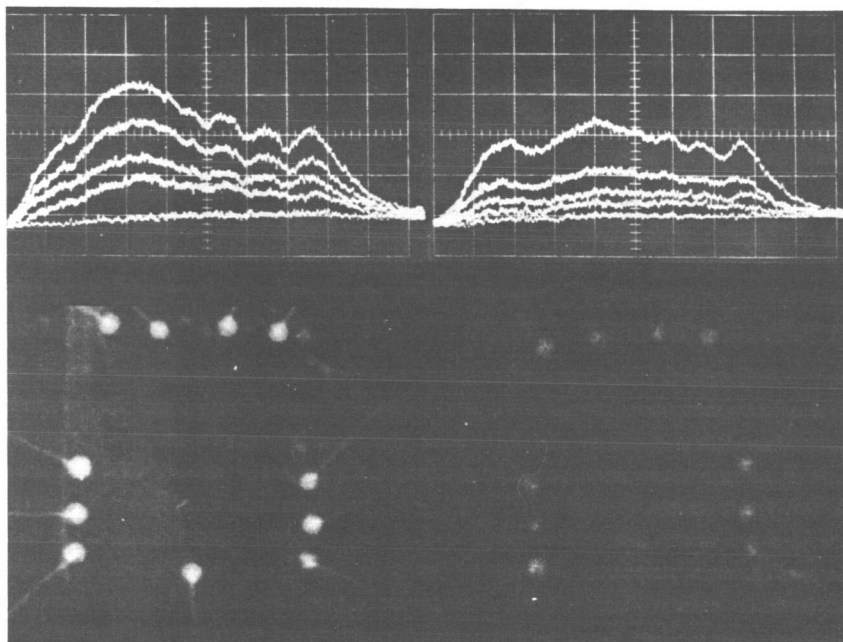FIGURE 6.—Single scan IR superimposed on circuit schematic.

FIGURE 7.—IR scan of circuit 0, 1, 6, 16, 46 seconds during warmup related to X-ray of unit.

line made after thermal stabilization shows the same condition, but less pronounced. Although the defect is readily detectable when initial power is applied, it is less easily detected after thermal equilibrium is reached. This illustrates the need for an instrument which can scan at a fast speed and which has a fast response detector.
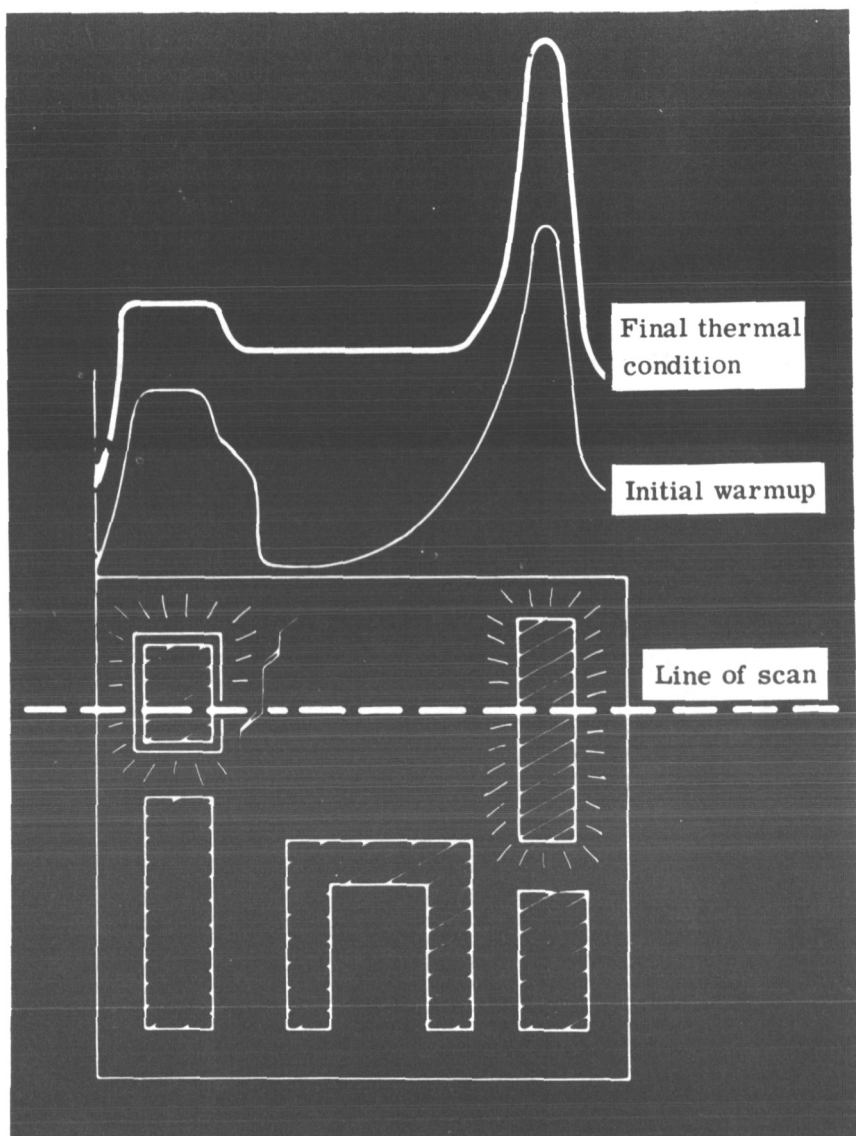

FIGURE 8.—IR scan of circuit with a crack.

CURRENT STUDIES AND FUTURE PLANS

A study is in progress to determine the possibility of using infrared to predict which transistors are likely to fail as a result of secondary breakdown as well as the area in which the breakdown will occur. The 2N1722 power transistor used for this study is shown in figure 9. The chip of this transistor is 250 mils square. The infrared profile of the transistor was measured just prior to driving it into breakdown and was found to be uniform and normal throughout the chip. The device was then driven into secondary breakdown and measured with the infrared microscope. The infrared spike shown in figure 10 was found at the point of secondary breakdown which occurred at a small point within the 50 mil square as shown in figure 11. There was deterioration around this point. This IR peak represents a spot temperature of more than 800° C.
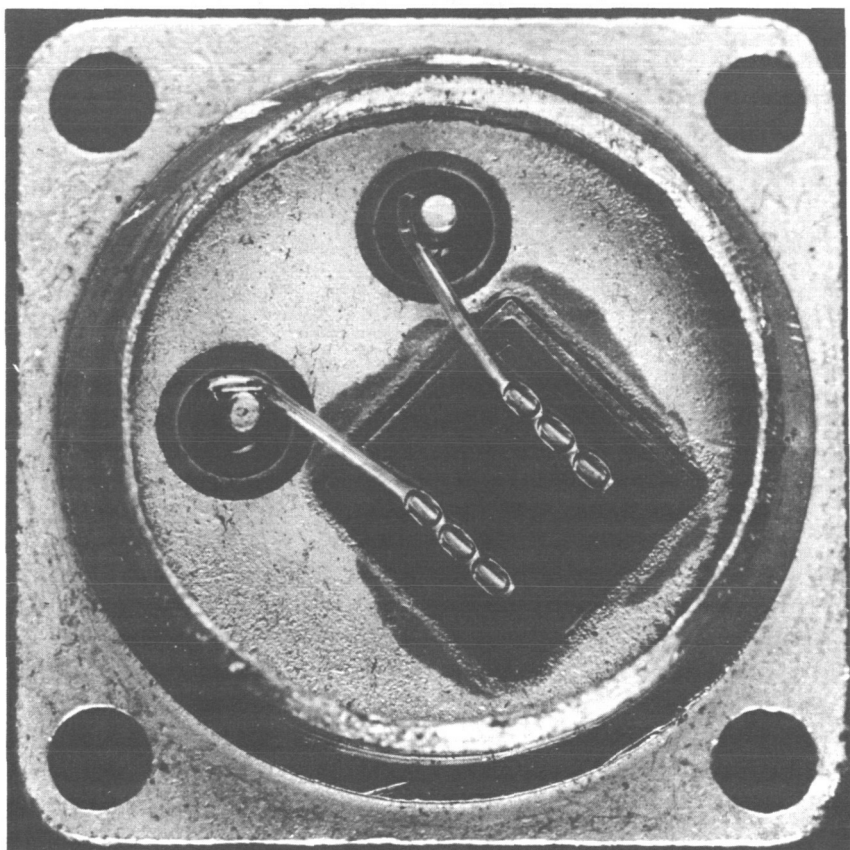

FIGURE 9.—Power transistor used for secondary breakdown study.

Several investigations using the infrared microscope are being planned over the next 12 months. Detail studies of devices which contain thermal related failure mechanisms will be conducted in order to establish a more exact relationship between the infrared emission of these units and good units. From this
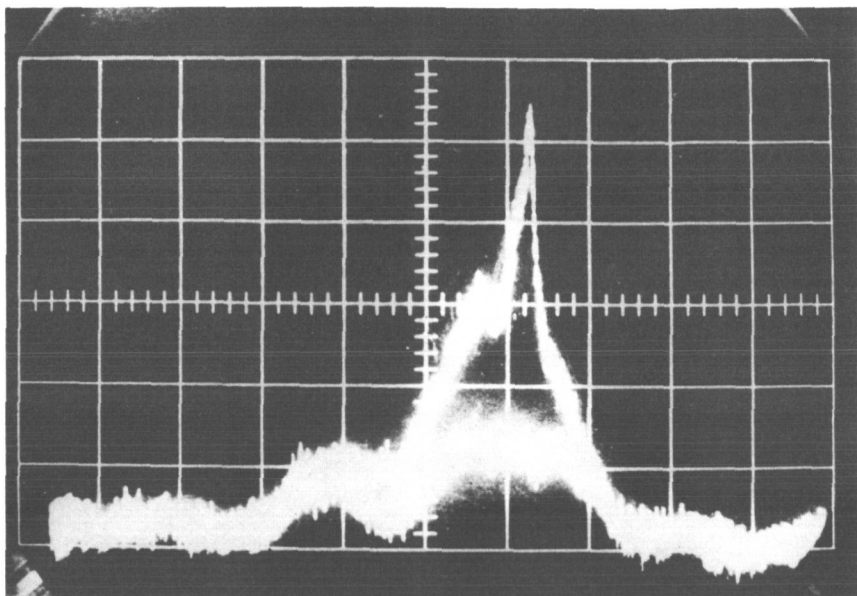

FIGURE 10.—Normal and secondary breakdown infrared emission.
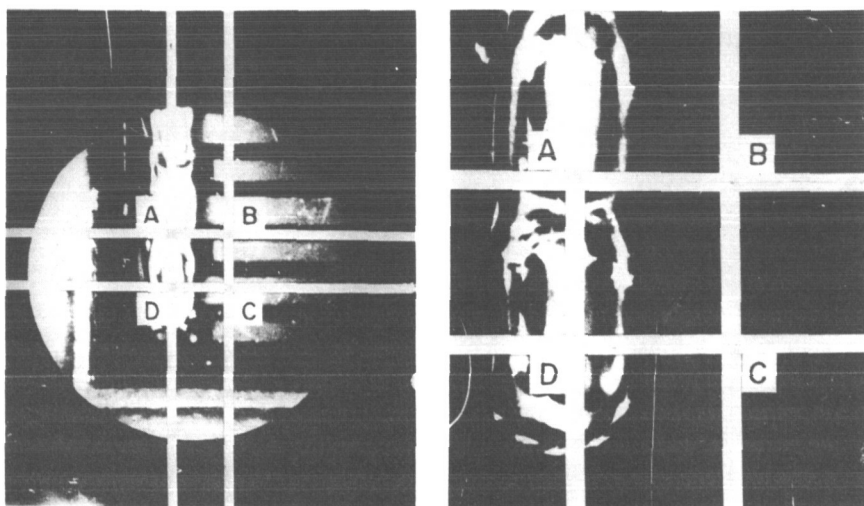
FIGURE 11.—Area where secondary breakdown occurred.

information, detailed test procedures and acceptance criteria can be developed for microcircuits. In addition, standards for the thermal and infrared design of microcircuits and detailed procedures for IR evaluation of circuits will be established as a part of qualification and lot acceptance tests. The infrared microscope will be located in a microcircuit manufacturing plant for approximately three months of testing in order to establish the relationship between the effectiveness and efficiency of infrared testing of microcircuits in accomplishing the functions of the other investigations.

Nondestructive Testing—Predictions of the Future

Robert W. Neuschaefer

The state-of-the-art for nondestructive testing (NDT) has been forced to advance rapidly during the last 10 years to keep pace with the demands of industry and the government. This advance has been spurred largely by the stringent quality requirements imposed on the fields of atomic energy and aerospace technology. More rigorous requirements in these and new fields will provide the impetus for future advances in such testing.

Through various studies at Marshall Space Flight Center, attempts have been made to predict future developments in nondestructive testing in relation to anticipated requirements. For instance, pressure vessels will be made from new structural materials, such as the fiber-reinforced metals and nonmetals, and from the new higher-strength aluminum and steel alloys. Materials will be joined to form structural components by advanced techniques, such as electron beam welding and diffusion bonding, as well as by improved conventional techniques. The major goals regarding new developments and applications of nondestructive testing include: (1) the achievement of complete assurance of hardware interrogation to the desired quality levels and (2) the development of faster testing methods.

ASSURANCE OF HARDWARE INTERROGATION TO THE DESIRED QUALITY LEVELS

It is vitally necessary that complete assurance of hardware interrogation to the required quality levels be provided and maintained, or catastrophes, such as the loss of the space vehicle propellant tank as shown in figure 1, will continue to occur. This particular failure resulted from a defective weld repair area which ruptured during hydrostatic testing.

The capability of resolving discontinuities in material that would have been undetectable a few years ago is now available. A great deal of improvement remains to be achieved, and it will be accomplished with advancements in physics and engineering design. New ultrasonic transducer designs will permit the interrogation of material immediately beneath the transducer which previously had been lost due to the near field effect.
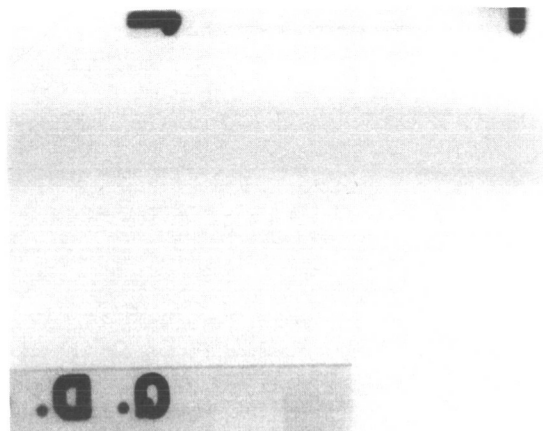
113

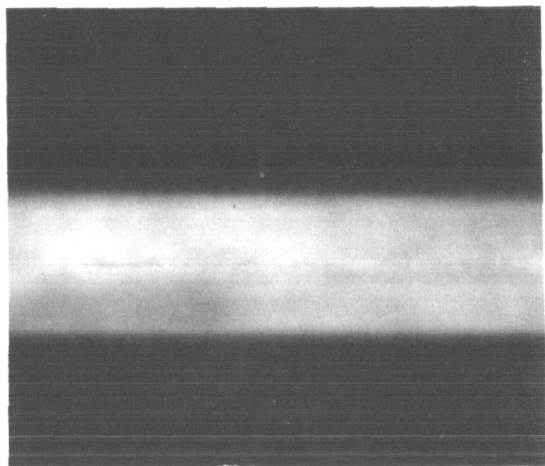FIGURE 4.—Radiograph of weld shown in figure 3.

FIGURE 5.—Fusion zone of weld.

obviously fails to disclose the discontinuity. It has been determined by investigators within the government and industry that the welding process can be modified by incorporating a metallurgically compatible material that is opaque to X-radiation between the abutting surfaces of the material to be welded. After being welded, all of the material will go into solution in the fusion zones; however, the opaque material will remain undisturbed. There will be slight porosity at the edges of the fusion zone; therefore, a line of high contrast remains (fig. 5). The copper plating which was used in the weld shown in figure 5 is significantly more opaque to X-rays than the copper aluminum alloy used in the weld with incomplete penetration. Through the use of a radiographically opaque material,

incomplete penetration can be detected. It should be noted that any such modification to manufacturing processes requires extensive testing prior to implementation.

DEVELOPMENT OF FASTER NONDESTRUCTIVE TESTING METHODS

There is an urgent need for faster nondestructive testing. For example, the evaluation of one girth S–IC tank weld by semiautomatic radiographic, conventional penetrant, and ultrasonic inspection of questionable areas requires approximatel eight hours and delays work on the rest of the tank for two hours. Since ther re four girth welds on the S–IC lox tank and two on the fuel tank, this amounts to a total delay of approximately twelve hours. Miniaturization of equipment, and the resulting compactness, will permit several complementary testing methods to be grouped together as an integrated system for attachment to a single tooling head such as a welding fixture. This will shorten the total time required for quality assurance while still permitting adequate interrogation of the part.

In the future, computers will be commonly used to control automated data acquisition systems where the data are of a relatively uncomplicated nature, such as that obtained from a weld. Computers will analyze nondestructive testing data in light of previously programmed quality criteria and print out the results. The use of automated film readers and analyzers as part of a computerized system has already been instituted at Lockheed Missiles and Space Company.

Computers will be required to aid quality assurance personnel in selecting the optimum inspection technique or group of techniques. For example, at least 11 testing methods presently exist for the interrogation of bonded honeycomb structures, and more are anticipated in the future. Obviously, not all of these techniques will be required for the analysis of a particular structure; however, a computer programmed with a description of the material and specification requirements could provide valuable assistance in method or methods selection.

OTHER AREAS OF INVESTIGATION

It is important to note that the development of new nondestructive testing equipment and techniques has proceeded rapidly; yet, progress in adapting this equipment and these laboratory techniques to rapidly and reliably solve floor inspection problems is somewhat lacking. This is due in part to the sophistication of much of the new equipment which practically dictates that an engineer operate the equipment and interpret the data. Improvements in data display systems, inspection fixtures, and tooling will help to alleviate this condition.

As the inspection of new materials and structures with advanced instrumentation becomes mandatory, the development of uniform and comprehensive nondestructive testing specifications is urgently required. It is anticipated that these requirements will be met by future aerospace specifications. There is also an

urgent need for the development of improved display systems. The *A* scan ultrasonic display systems leave a lot to be desired regarding ease of interpretation. Although the *C* scan method is an improvement, it is still a far cry from the radiographic image type of penetration. New developments, such as the ultrasonic imaging system developed by James Electronics Inc. are of interest (fig. 6).

In this ultrasonic testing system, sound waves travel from the transmitting crystal through the part being tested to be picked up by crystal target. Variations imparted in the target crystal by changes in the broadcast beam of ultrasound are detected by the traversing beam of the electron gun. The image is displayed on the television screen (ref. 3).

Techniques which will permit the instantaneous conversion of ultrasonic images to visible displays are under development. One such method is discussed in reference 3.

This can be done by using a solid-state display panel such as already successfully developed for x-ray image conversion. To apply this technique to ultrasound visualization, a piezoelectric plate would have to be mounted on the display panel, which consists of a luminescent screen sandwiched between special electrodes. The device must be constructed to amplify electrical potentials (developed by the piezoelectric effect) enough to excite the luminescent substances. Solid-state panels such as these do not require evacuated tubes; this should make it easier to construct ultrasonic image converters of larger dimensions.

The development of solid-state image intensification systems for radiography offers the promise of rapid, enhanced displays over the old film systems which require development prior to interpretation. The ultimate requirement for the production of three-dimensional imaging systems for both ultrasonic and radiographic inspection methods may be accomplished by applications of solid-state imaging, video tape, and computer technology. Wavefront reconstruction techniques (fig. 7), as developed at the University of Michigan by E. N. Leith and Juris Upatnieks, offer promise in this area (ref. 4).

In the recording stage of wavefront reconstruction photography (top) no lens or other image-forming device is used and consequently, no image is formed. Instead each point on the object reflects light to the entire hologram; conversely, each point of the hologram receives light from the entire object. The reference beam produces, by means of interference effects, a visible display of the wave pattern of the light impinging on the hologram from the object. In the reproduction stage (bottom) the hologram is illuminated with a collimated beam of monochromatic light and two images are produced by the "first order" diffracted waves emerging from the hologram interference grating. One diffracted order consists of waves that, when projected back toward the illuminating source, seem to emanate from an apparent object located at the position where the original object was located. These waves are said to produce a virtual image. The other first-order diffracted waves have conjugate, or reversed, curvature. These waves produce a real image, which can be photographed directly, without the need for a lens, by simply placing a photographic plate at the position of the image. The hologram can be made with radiation of one wavelength and the reconstruction with another. El-Sum and Baez have made holograms with an x-ray microscope and the reconstructions in visible light. This application holds much promise, because x-rays can be focused only crudely and with extreme difficulty. The resolution achieved in x-ray microscopy falls several orders of magnitude short of what is theoretically possible by wavefront reconstruction methods.
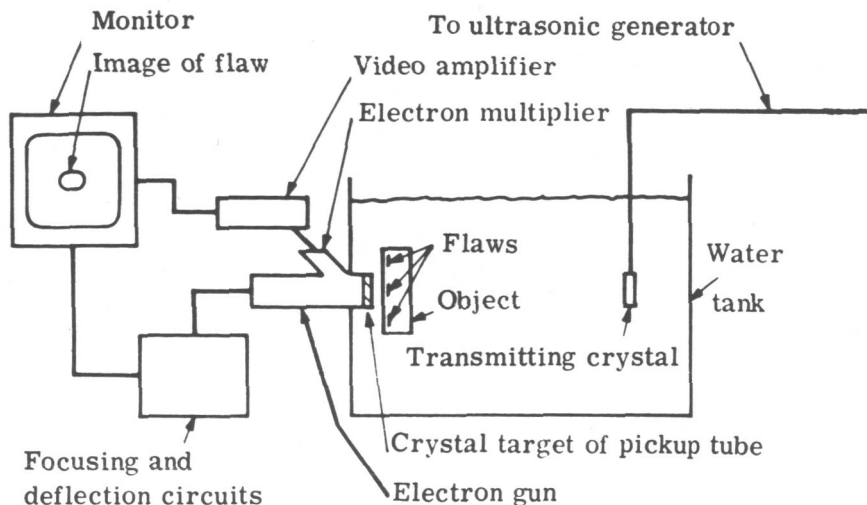
FIGURE 6.—Ultrasonic imaging system.

The wider applications of color radiography to the interrogation of composite materials and components will result in more readily interpretable data than that obtained by conventional radiographic techniques. A means of producing color radiographs has been devised by Argonne National Laboratories.

The x-ray beam passes through the specimen, is intensified by the fluorescent screen, and impinges on conventional color film. The film is developed by conventional technique to a point where the image is brought out on the top-emulsion layer. Then the film is exposed to a flash of monochromatic light, usually red or green, in order to print the partially developed image on the bottom of two layers. The resultant radiograph is then the combination of hue, brightness, and saturation wrought in each layer by the screen fluorescence, the x-rays, and the colored light (ref. 5).

There is a definite need for an improvement in inspection record keeping. Adequate means for recording A scan ultrasonic or liquid penetrant indications are not available. As a result of shop lighting conditions and inspection inter-ruptions, photography is not adequate. Video tape may be applied to store ultra-sonic and radiographic data in the future, and it is believed that lox insensitive strippable penetrants, which have defect sensitivities comparable to presently used liquid penetrants, will find wide application.

The trend to miniaturize nondestructive testing equipment to permit ease of handling will continue. It has been estimated that within the near future 100-kv X-ray machines will weigh less than 20 pounds including power source. Further significant weight reductions are anticipated as integrated circuits are utilized. In the future, the only component of significant size remaining will be the data display system.
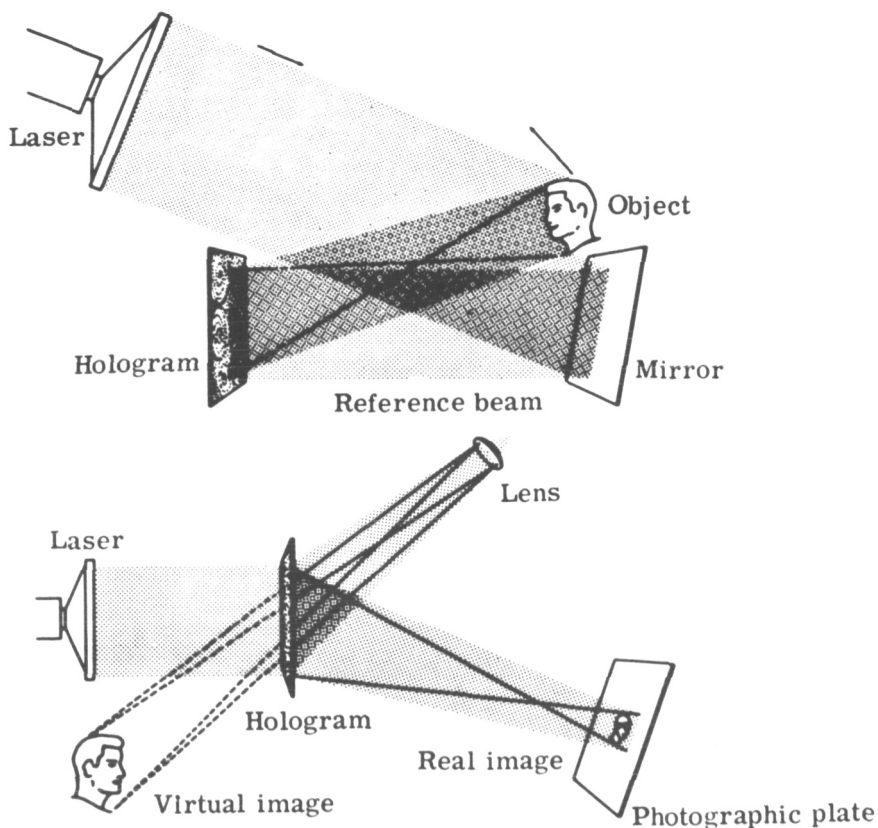
FIGURE 7.—Wavefront reconstruction photography showing recording stage (top) and reproduction stage (bottom).

Applications of energy sources not previously utilized are also being investigated. A few years ago the application of thermal energy to nondestructive testing was not considered. However, infrared techniques are now finding applications in the location of solid rocket motor second interface unbond, and the use of cholesteric liquid crystals to detect defects in bonded honeycomb structures is under development.

G. H. Brown has recently reported:

Liquid crystals are intermediate in many of their properties between the liquid and solid states. They have the mobility of liquids and the optical properties of solids. The liquid crystalline state has more order in arrangement of its molecules than the liquid state, but less than the solid state.

The cholesteric structure is found primarily in derivatives of cholesterol, especially the esters. When the isotropic melt of a cholesteric material is cooled, a confocal texture of the cholesteric structure is produced. The material consists of layers which are about 2,000 angstroms thick

(contrast this with the smectic structure where the layers are about the length of the molecule, that is, about 20 angstroms). The layers are parallel. While the major portion of the individual molecules in the cholesteric state are essentially flat, side chains project upward from the plane of each molecule while some hydrogen atoms extend below. Thus, the direction of the long axis of the molecule in a chosen layer is slightly displaced from the direction of this axis in adjacent layers. The resultant displacement produces a helical design (ref. 6).

J. I. Fergason earlier observed:

The molecular structure of a cholesteric liquid-crystal substance is very delicately balanced and can be easily upset. Thus any small disturbance that interferes with the weak forces between the molecules can produce marked changes in such optical properties as reflection, transmission, birefringence, circular dichroism, optical activity, and color.

Perhaps the most striking optical transformation that occurs in a cholesteric substance in response to subtle changes in the enviroment is the variation of color with temperature. Although most cholesteric substances are colorless as liquids, they pass through a series of bright colors when they are cooled through their liquid-crystal phase. In this phase they may first appear to be violet, then blue, then green, then yellow, then red, and finally colorless again as the reflection maximum enters the infrared region (ref. 7).

New gamma ray sources with low energy levels suitable for radiographing thin materials, such as ytterbium 169, have recently been introduced. It is anticipated that more new sources will be introduced in the future, thus facilitating radiography in the field. Neutron radiography will find wide application in the future.

The neutrons penetrate materials much like x-rays and gamma rays. However, materials absorb the neutrons much differently than they do x-rays. The mass absorption coefficient for tungsten tube x-rays for all elements ranges only from 0.10 to 5, whereas the mass absorption coefficient for thermal neutrons ranges from about 0.03 to 48.5. The figure illustrates how the absorption coefficient of neutrons and tungsten tube x-rays varies with atomic number (fig. 8).

Note how the mass absorption coefficient of x-rays increase regularly with increasing atomic number, while the variation for neutron absorption is irregular. In fact, if a pattern exists, the relationship seems to be opposite to that of x-ray absorption. Note also how the light elements absorb neutrons more strongly than the heavier elements. This can be advantageous when inspecting large thicknesses of heavy metals. At present, nuclear reactors and accelerators are the chief source of neutrons used in neutron radiography. In addition, isotopes such as radium-beryllium and polonium-beryllium are under investigation.

Neutron radiographs are produced on conventional x-ray film. Exposure techniques differ from normal x-ray procedures only in that an intensifying screen is placed over the film during exposure. Neutrons bombarding the screen cause it to emit alpha, beta, and gamma radiation which exposes the film. An alternate technique, which eliminates loss of resolution due to scattered radiation, is to expose only the screen to neutrons and subsequently expose a piece of x-ray film to the irradiated screen (ref. 8).

Lasers will probably find applications in nondestructive testing as heat sources for both the infrared testing of small components and for wavefront reconstruction three-dimensional displays.

There are presently 25 to 30 colleges and universities offering semester length and short courses in nondestructive testing; it is anticipated that most of the technical schools in the country will offer such courses within the next 10 years.
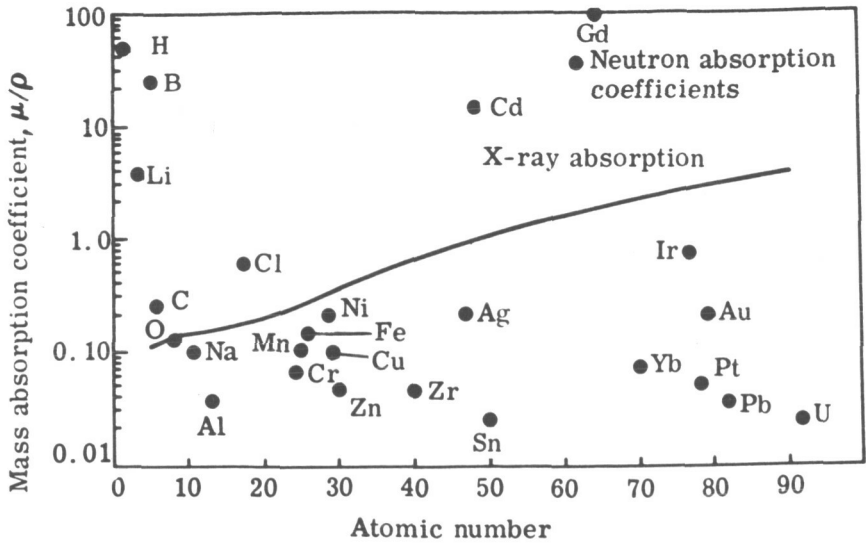
FIGURE 8.—Absorption of neutrons and X-radiation.

NEW APPLICATIONS FOR NONDESTRUCTIVE TESTING

Many new applications, such as the continuous monitoring of critical aircraft structures for fatigue cracking by the use of pattern placed transducers, are envisioned for nondestructive testing. Means will have to be developed for the analysis of forthcoming structural materials such as the fiber reinforced materials. Ideally, the development of testing techniques will occur simultaneously with the material development program; however, this is not always the case.

Most of us are familiar with medical applications of radiography and with the fact that medical X-ray technology was well-developed before significant industrial applications were available. The medical field is now making use of ultrasonic technology which was initially developed for industry.

Ultrasonic visualization systems which have been used to outline various internal structures of the human body have been described in the literature. Although these visualization systems or echoscopes differ in constructional detail, they are identical in principle. The transducer is electrically coupled to the transmitter and the receiver; it is mechanically coupled to the scanner and, via the ultrasonic path, to the patient. The visualized anatomy is also considered as part of the basic echoscope as it determines the frequency of operation. The position of the transducer is monitored and used by the deflection system to position the trace on the screen of the main display unit. On the main display unit the returned echoes are represented by an illumination of the trace, and the main design criterion for all echoscopes is the spot size of the display unit, which, for high quality display tubes, is 0.1 cm in diameter (ref. 9).

The manufacturing, repair, and damage assessment of structures and other hardware in the space and lunar environment will require the development of a whole new family of nondestructive test instruments and procedures.

As the assurance of hardware interrogation is improved, along with materials and processes, safety factors can be reduced, thus permitting higher payloads. Virtually every space vehicle component and assembly which is subjected to nondestructive testing is undergoing evaluation to determine how faster and more thorough quality assurance techniques can be applied as they are conceived and developed. This is a continuous process which requires the close cooperation of NASA and industry. It should be obvious that improvements will be equally beneficial to the pipeline contractor or tank car manufacturer as to the manufacturer of space vehicle propellant tanks.

Efforts to improve discontinuity location and identification should have the highest priority. The development of faster testing systems is also urgently required. Improvement in applications, specification improvement, improved display systems, and miniaturization are also of significant importance and deserve major development efforts.

There is an unlimited future for nondestructive testing, and only a sampling of new and predicted developments has been covered in this paper. It is obvious that to derive the maximum benefit from nondestructive testing, not only technology, but also communications between management, the physicist, the materials engineer, the design engineer, and the floor inspector must be improved.

REFERENCES

1. Kossoff, G.: Design of Narrow-Beamwidth Transducers. J. Acous. Soc. Am., vol. 35, no. 6, June 1963, pp. 905–912.
2. Anon.: Ultrasonic Imaging. Steel, vol. 58, no. 7, Feb. 14, 1966.
3. Klinker, Louis G.; Jacobs, John E.; and Gericke, Otto: Inspecting Metals by Ultrasonic Visualization. Metal Progress, vol. 88, no. 1, July 1965, pp. 82–84.
4. Leith, Emmett N.; and Upatnieks, Juries: Photography by Laser. Scien. Am., vol. 212, no. 6, June 1965, pp. 24–36.
5. McGonnagle, Warren; and Park, Ford: Nondestructive Testing. Inter. Sci. Tech., no. 31, July 1964, pp. 14–27.
6. Brown, Glenn H.: Liquid Crystals. Indus. Res., May 1966, pp. 53–58.
7. Fergason, James L.: Liquid Crystals. Scien. Am., vol. 211, no. 2, Aug. 1964, pp. 76–85.
8. Clark, W. G., Jr.: New Nondestructive Tests Improve Quality and Safety. Materials in Design Eng.
9. Kossoff, A.; Robinson, E. E.; Liu, C. N.; and Garrett, W. J.: Design Criteria for Ultrasonic Visualization Systems. Ultrasonics, Jan.–Mar. 1964.

NASA TECHNOLOGY UTILIZATION PUBLICATIONS

These describe science or technology derived from NASA's activities that may be of particular interest in commercial and other non-aerospace applications. Publications include:

TECH BRIEFS: Single-page descriptions of individual innovations, devices, methods, or concepts.

TECHNOLOGY SURVEYS: Selected surveys of NASA contributions to entire areas of technology.

OTHER TU PUBLICATIONS: These include handbooks, reports, notes, conference proceedings, special studies, and selected bibliographies.

Details on the availability of these publications may be obtained from:

National Aeronautics and Space Administration
Code UT
Washington, D.C. 20546

Technology Utilization publications are part of NASA's formal series of scientific and technical publications. Others include Technical Reports, Technical Notes, Technical Memorandums, Contractor Reports, Technical Translations, and Special Publications.

Details on their availability may be obtained from:

National Aeronautics and Space Administration
Code US
Washington, D.C. 20546

NATIONAL AERONAUTICS AND SPACE ADMINISTRATION
Washington, D.C. 20546